Vol. 62 • No. 11

November 2019

Microwave Journal®

Keeping It Cool

horizon house®

Founded in 1958

mwjournal.com

We are making high performance microwave and millimeter wave filter and antenna products for 4G and 5G applications.

- Diplexers with Built in Coupler and OMT: Low insertion loss (< 1.0 dB); high isolation (> 35 dB); compact design.
- Tunable Filter: Large tunning range (> 10%); low VSWR; high out of band rejection; low insertion loss; constant bandwidth; compact design; high reliability.
- Dielectric TE Mode Filter: Ultra low insertion loss (Q > 10000); ultra small temperature drift; small size.
- 5G Millimeter Wave Patch Array Antenna: Different array configuration; dual polarization; high gain; beam scanning.
- 5G Millimeter Wave Filter: Designed for 28 GHz system; low insertion loss (< 2.5 dB); high out of band rejection (> 50 dB); ultra small size; light weight (< 1g).

Dielectric Microwave TE Mode Filter

Diplexer with Built in Coupler

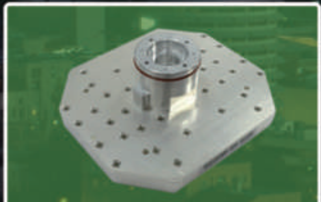

Diplexer with Built in OMT

5G Millimeter Wave Patch Antenna

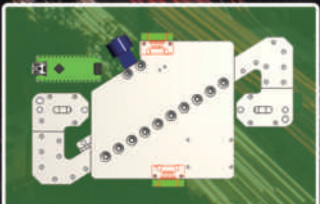

Tunable Filter

5G Millimeter Wave Filter

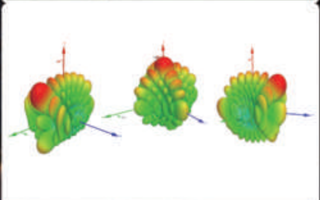

Pattern of 5G Millimeter Wave Patch Antenna

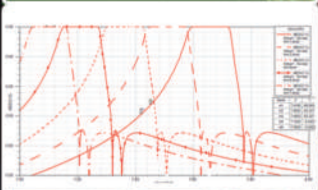

Test Curve of Tunable Filter

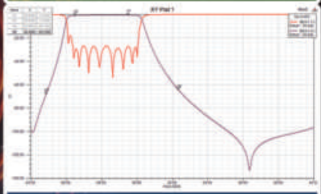

Simulation Curve of 5G Millimeter Wave Filter

PIVOTONE

One Dream One World

www.pivotone.com


RUGGED & RELIABLE
MADE IN THE USA FOR OVER 57 YEARS!
M*E*C*A* - MICROWAVE EQUIPMENT COMPONENTS OF AMERICA
Airborne Radar & Communications
Satellite Communications
Test & Measurement
L, S, C, X, Ka & Ku
Missile Guidance
Military Electronic Countermeasures
Research & Development
ML-SERIES PRODUCTS
(COMMERCIAL OFF THE SHELF)
Power Dividers/Combiners
20 MHz - 40 GHz
SMA, 2.92, QMA, N, TNC, BNC,
RPTNC 4.1/9.5 & 7/16 Up to 120 watts
MIL-DT-23971 Available.
Attenuators
Up to 40 GHz
SMA, 2.92, QMA, N,
TNC, BNC, RPTNC & 7/16
Up to 150 watts.
Directional Couplers/Hybrids
0.4 - 40 GHz
SMA, 2.92, QMA, N, TNC, BNC,
RPTNC & 7/16 Up to 500 watts
MIL-DTL-15370 Available.
Bias Tees
Up to 6 & 18 GHz
SMA, 2.92mm, QMA,
N,TNC, RP-TNC & 7/16 DIN.
Terminations
Hz-18 GHz
N, SMA & 7/16 Up to 250 watts
MIL-DTL-3903E
Circulators/Isolators
Up to 40 GHz
SMA, 2.92, N, & 7/16
Up to 250 watts.
MECA
MECA Electronics, Inc.
Microwave Equipment & Components of America
e-MECA.com
Since 1961
Tel. 973-625-0661 • Fax: 973-625-9277 • sales@e-MECA.com

Now up to 40 GHz!

TEST

MODUL[redacted]

PROGRAMMABLE ATTENUATORS

NxM SWITCH MATRICES

PATCH PANELS

SOLUTIONS

Flexible, Reliable, Affordable & Fast

MECHANICAL SWITCH MATRICES

SOLID STATE SWITCH MATRICES

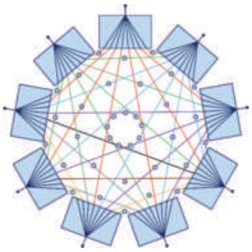

MESH NETWORK TEST SYSTEMS

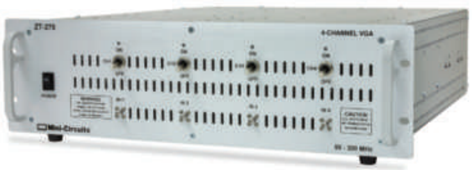

INSTRUMENTATION AMPLIFIERS

SIGNAL GENERATION,
MEASUREMENT & CONTROL

HIGH POWER TEST SYSTEMS

SIGNAL DISTRIBUTION

CUSTOM SYSTEMS

Mini-Circuits®

www.minicircuits.com P.O. Box 350166, Brooklyn, NY 11235-0003 (718) 934-4500 sales@minicircuits.com 616 Rev Orig_P

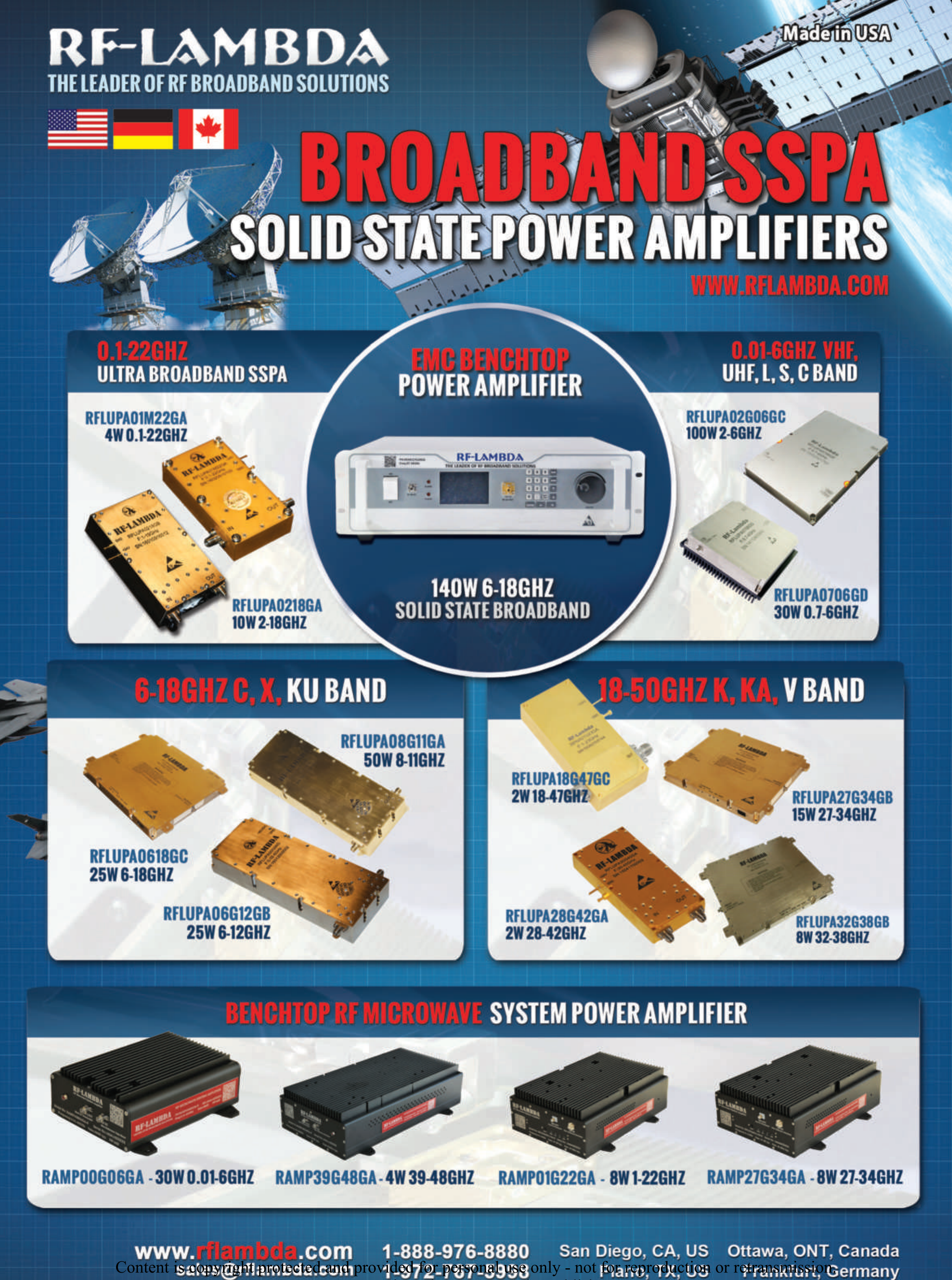
RF-LAMBDA
THE LEADER OF RF BROADBAND SOLUTIONS
Made in USA
BROADBAND SSPA
SOLID STATE POWER AMPLIFIERS
WWW.RFLAMBDA.COM
0.1-22GHZ
ULTRA BROADBAND SSPA
RFLUPA01M22GA
4W 0.1-22GHZ
RFLUPA0218GA
10W 2-18GHZ
EMC BENCHTOP
POWER AMPLIFIER
140W 6-18GHZ
SOLID STATE BROADBAND
0.01-6GHZ VHF,
UHF, L, S, C BAND
RFLUPA02G06GC
100W 2-6GHZ
RFLUPA0706GD
30W 0.7-6GHZ
6-18GHZ C, X, KU BAND
RFLUPA08G11GA
50W 8-11GHZ
RFLUPA0618GC
25W 6-18GHZ
RFLUPA06G12GB
25W 6-12GHZ
18-50GHZ K, KA, V BAND
RFLUPA18G47GC
2W 18-47GHZ
RFLUPA27G34GB
15W 27-34GHZ
RFLUPA28G42GA
2W 28-42GHZ
RFLUPA32G38GB
8W 32-38GHZ
BENCHTOP RF MICROWAVE SYSTEM POWER AMPLIFIER
RAMP00G06GA - 30W 0.01-6GHZ
RAMP39G48GA - 4W 39-48GHZ
RAMP01G22GA - 8W 1-22GHZ
RAMP27G34GA - 8W 27-34GHZ
www.rflambda.com
1-888-976-8880
San Diego, CA, US
Ottawa, ONT, Canada

K&L MICROWAVE
a DOVER company
SUPPORTING OUR WARFIGHTERS SINCE 1971
Phase Matched Filters
High-Power Lowpass Filters
PIN Diode Switches
Multiplexers
• Filters DC to 94 GHz
• Bandpass
• Bandreject
• Lowpass
• Highpass
• Switched Filter Banks
• Tunable Filters
• Filter/LNA Assemblies
• Rugged Designs for Harsh Military Environments
• In-House MIL-SPEC Environmental Testing
• Multiplexers
• Non-Contiguous
• Contiguous
• Overlapping Bands
Microwave Products Group
a DOVER company
K&L MICROWAVE
BSC
POLE ZERO
Dow-Key Microwave
ENABLING COMMUNICATION AND SIGNAL CONTROL
www.klmicrowave.com • www.klfilterwizard.com • 410-749-2424 • sales@klmicrowave.com


AMPLICAL
Let Amplical
Jump Those Hurdles for You
with our Complete In-House Design, Manufacturing and Test Capabilities
Customers can depend on us for quick order fulfillment, competitive pricing and dedicated service.
Let us prove our commitment to you today.
High performance standard and custom Control Components and Amplifiers to 40GHz.
• EW Systems
• Communications Systems
• Radar
• Test
• Simulation
Products:
• Switches
• Attenuators
• Phase Shifters
• Limiters
• Switch Matrices
• Broadband Amplifiers
• Low Noise Amplifiers
• High Power Amplifiers
• Custom Components and Sub-assemblies
Phone: 973-386-1119
Fax: 973-386-1131
E-mail: info@amplical.com
web: www.amplical.com
AMPLICAL
SW4A004

Microwave Journal

CONTENTS

November 2019
Vol. 62 • No. 11
Government & Military Electronics
mwjournal.com

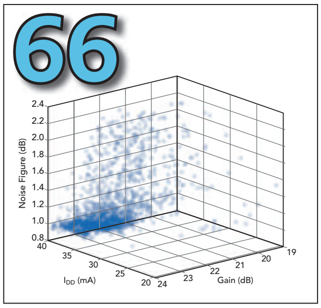

Look for this month's exclusive article online at mwjournal.com

First-Pass Design of Ultra-Wideband Microwave and mmWave Filters for Multi-Stage Frequency Multiplication

H. M. Talasila, F. R. Morales, J. Paden, Center for Remote Sensing of Ice Sheets (CReSIS), The University of Kansas; N. D. Orloff, D. Gu, National Institute of Standards and Technology (NIST); M. Conte, University of Massachusetts Amherst; C. Oakley, Michigan State University; and M. McKeown, Hesse-Mechatronics Inc.

Cover Feature

Technical Features

Application Notes

62 YEARS OF PUBLISHING EXCELLENCE


NATIONAL INSTRUMENTS
TOMORROW'S DESIGNS REQUIRE
SMARTER
SOFTWARE TODAY
AWR
NI AWR Design Environment software provides a seamless platform for developing next-generation wireless electronics and communications systems, from concept to product. Its powerful interface, integrated system, circuit, and electromagnetic simulation technologies, and design flow automation ensures your design success.
Visit awr.com/smarterdesign to learn more.
©2019 National Instruments Corporation. All rights reserved. AWR, AWR Design Environment, National Instruments, and NI are trademarks of National Instruments. Other product and company names listed are trademarks or trade names of their respective companies.

Microwave Journal

CONTENTS

mwjournal.com

Product Feature

Tech Briefs

Departments

Microwave Journal (USPS 396-250) (ISSN 0192-6225) is published monthly by Horizon House Publications Inc., 685 Canton St., Norwood, MA 02062. Periodicals postage paid at Norwood, MA 02062 and additional mailing offices.

POSTMASTER: Send address corrections to Microwave Journal, PO Box 1028, Lowell, MA 01853 or e-mail mwj@e-circ.net.com. Subscription information: (978) 671-0446. This journal is issued without charge upon written request to qualified persons working in the RF & microwave industry. Other subscriptions are: domestic, $120.00 per year, two-year subscriptions, $185.00; foreign, $200.00 per year, two-year subscriptions, $370.00; back issues (if available) and single copies, $10.00 domestic and $20.00 foreign. Claims for missing issues must be filed within 90 days of date of issue for complimentary replacement.

STAFF

Publisher: Carl Sheffres
Associate Publisher: Michael Hallman
Editor: Patrick Hindle
Technical Editor: Gary Lerude
Managing Editor: Jennifer DiMarco
Associate Technical Editor: Cliff Drubin
Copy Editor: Ashleigh West
Multimedia Staff Editor: Barbara Walsh
Contributing Editor: Janine Love
Electronic Marketing Manager: Chris Stanfa
Digital Content Specialists: Lauren Tully, Jaclyn Seigal
Audience Development Manager: Carol Spach
Traffic Manager: Edward Kiessling
Director of Production & Distribution: Robert Bass
Art Director: Janice Levenson
Graphic Designer: Ann Pierce

EUROPE

Office Manager: Nina Plesu

CORPORATE STAFF

CEO: William M. Bazzy
President: Ivar Bazzy
Vice President: Jared Bazzy

EXECUTIVE EDITORIAL OFFICE
685 Canton Street, Norwood, MA 02062
Tel: (781) 769-9750
FAX: (781) 769-5037
e-mail: mwj@mwjournal.com

EUROPEAN EDITORIAL OFFICE
16 Sussex Street, London SW1V 4RW, England
Tel: Editorial: +44 207 596 8730 Sales: +44 207 596 8740
FAX: +44 207 596 8749

SUBSCRIPTION SERVICES
Send subscription inquiries and address changes to:
Tel: (978) 671-0446
e-mail: mwj@e-circ.net

BPA WORLDWIDE

www.mwjournal.com

Printed in the USA

Microwave Journal Online

Visit us @ mwjournal.com

E LEARNING CENTER

Access webinars on-demand from the archived webinars and events page at www.mwjournal.com/events

Executive Interviews

Karim Hamed, general manager of **Analog Devices**' microwave communications segment, discusses how ADI is supporting the communications market from "bits to antenna," including nascent mmWave and phased array opportunities.

Jonathan Rowntree, senior VP & GM, Advanced Connectivity Solutions at **Rogers Corporation**, discusses the challenges facing high frequency PCB designers and market demands for laminates to meet the demanding thermal and electrical requirements for 5G, satellite and automotive radar applications.

WHITE PAPERS

KEYSIGHT TECHNOLOGIES — Tips for Better Signal Generator Measurements

NATIONAL INSTRUMENTS / AWR — A Designer's Primer on Internet of Things (IoT)

ROHDE & SCHWARZ — 5G

RF MW Frontends

Check out MWJ's podcasts on iTunes and Google Play

https://podcasts.microwavejournal.com/

Join Us Online

Follow us
@Pathindle
@MWJGary
@MWJEditor

Join us at the RF and Microwave Community

Become a fan at facebook.com/microwavejournal

Catch *Frequency Matters*, the industry update from *Microwave Journal*,
microwavejournal.com/FrequencyMatters

COM

Blue Chip Performers

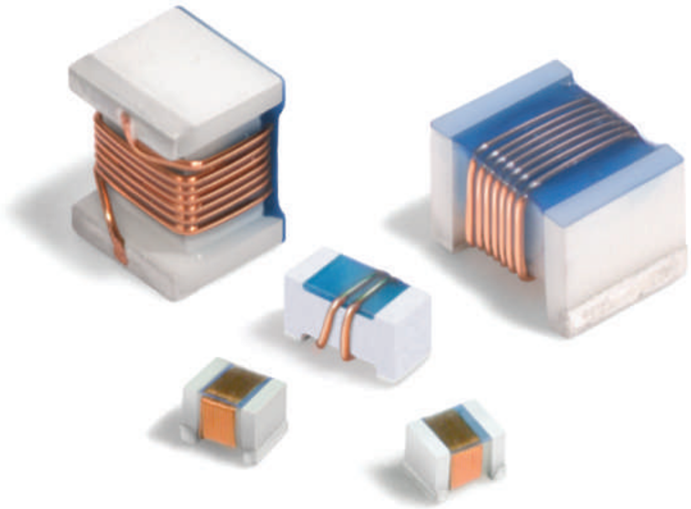

Exceptionally high Q, low DCR and a wide range of inductance values make our wirewound chip inductors a sure bet!

Engineers love our high-performance, low-cost, wirewound ceramic chip inductors; considered by most to be the best performing wirewounds available.

For example, our 0201HL Series is offered in seven inductance values ranging from 22 to 51 nH – the highest currently offered in an 0201 (0603) package – making them fully optimized for impedance matching in 700 MHz band LTE and 5G applications.

Our 0402DC and 0805HP Series provide the industry's highest Q factors in their respective sizes for super low loss in high frequency circuits. Select values from 2.6 to 820 nH, including 0.1 nH increments from 2.8 to 10 nH in the 0402DC Series.

Find out why our customers are so bullish on our wirewound ceramic chip inductors. Order your free samples today at **www.coilcraft.com.**

Coilcraft®

coilcraftdirect.com
No min order. Next day delivery.

WWW.COILCRAFT.COM

See us at EuMW

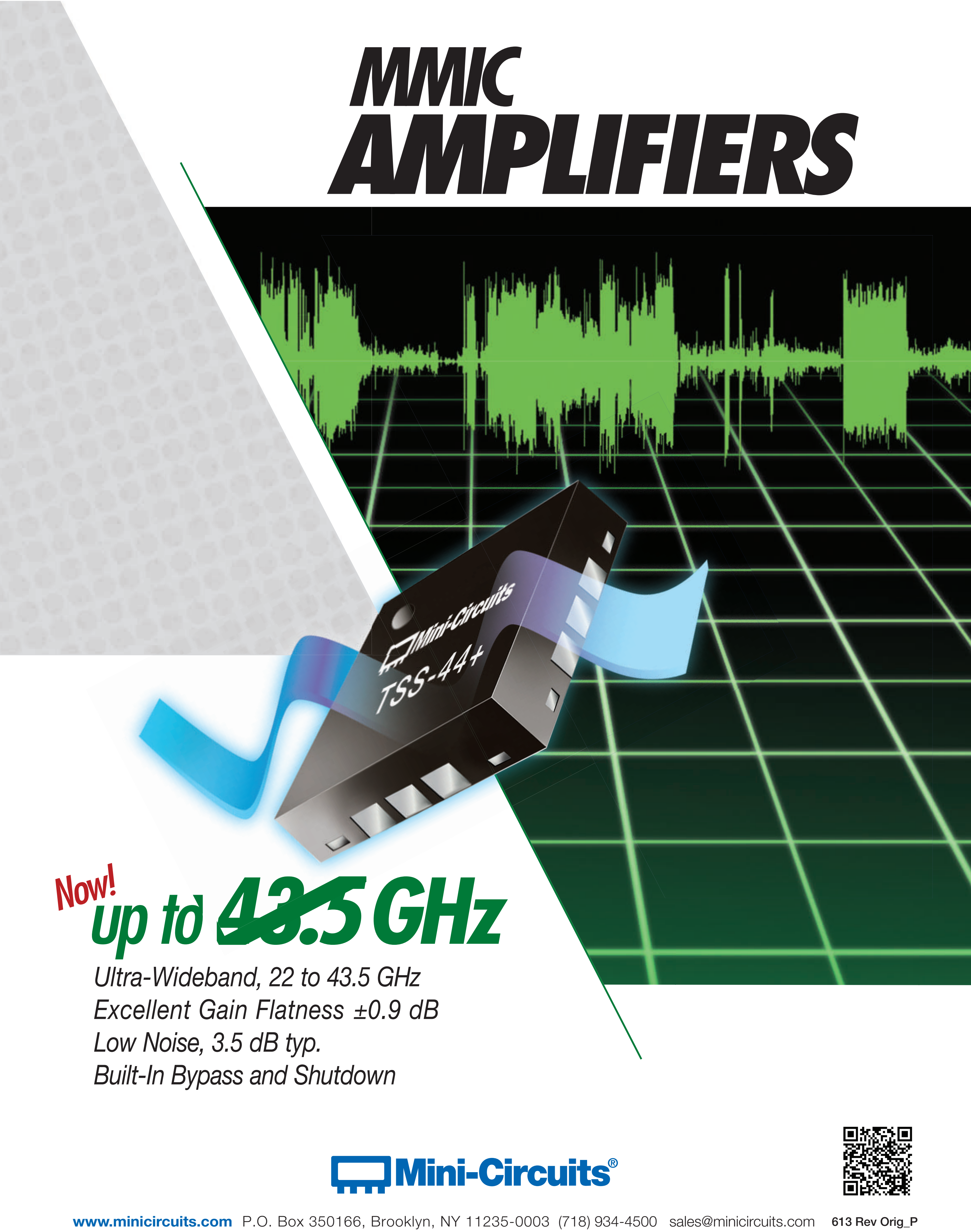
MMIC
AMPLIFIERS
Mini-Circuits
TSS-44+
Now!
up to 43.5 GHz
Ultra-Wideband, 22 to 43.5 GHz
Excellent Gain Flatness ±0.9 dB
Low Noise, 3.5 dB typ.
Built-In Bypass and Shutdown
Mini-Circuits®
www.minicircuits.com P.O. Box 350166, Brooklyn, NY 11235-0003 (718) 934-4500 sales@minicircuits.com
613 Rev Orig_P

DECEMBER MARK YOUR CALENDAR

4

Call for Papers Deadline

IMS

The IEEE MTT-S 2020 International Microwave Symposium (IMS2020) will be held June 21-26, 2020 in Los Angeles, Calif. IMS2020 is the centerpiece of Microwave Week 2020 comprising the RFIC Symposium and the ARFTG Conference. Microwave Week, with more than 9,000 participants and 600 industrial exhibits of state-of-the-art microwave products, is the world's largest gathering of RF and microwave professionals. Authors are invited to submit technical papers describing original work microwave, mmWave and THz theory and techniques.

https://ims-ieee.org/authors-organizers

7-11

IEDM 65th International Electron Devices Meeting

Washington, DC

IEEE International Electron Devices Meeting (IEDM) is a preeminent forum for reporting technological breakthroughs in the areas of semiconductor and electronic device technology, design, manufacturing, physics and modeling. IEDM is the flagship conference for nanometer-scale CMOS transistor technology, advanced memory, displays, sensors, MEMS devices, novel quantum and nano-scale devices and phenomenology, optoelectronics, devices for power and energy harvesting, high speed devices, as well as process technology and device modeling and simulation.

https://ieee-iedm.org

10-13

2019 Asia-Pacific Microwave Conference APMC 2019 10 - 13 DECEMBER 2019 SINGAPORE Microwaves bridging Smart Cities

Singapore

The 2019 Asia-Pacific Microwave Conference (APMC) will be held in Singapore, December 10-13, 2019. APMC will offer a rich scientific program of the highest quality with invited speakers from all over the world and provide a broad forum of exchange for both academia and industry alike. The conference will cover the entire scope of microwave and mmWave engineering, including RF/microwave/THz, antennas and propagation and EMC/EMI.

https://apmc2019.miceapps.com/client/sites/view/SP8f993

13-15

IMaRC

Mumbai, India

The IEEE MTT-S, with technical co-sponsorship from IEEE Bombay Section and IIT Bombay, announces the 7th IEEE MTT-S International Microwave and RF Conference (IMaRC) in Mumbai, India. This conference is held annually in India and provides a forum for the international community of microwave engineers to meet and present their latest technical achievements in the field of microwave and RF components, circuits, systems and modelling techniques.

https://imarc-ieee.org/

FOR DETAILS, VISIT MWJOURNAL.COM/EVENTS

Coming Events

CALL FOR PAPERS

IEEE IMS2020
December 4

EDI CON China 2020
January 6, 2020

IEEE EMC+SIPI 2020
January 13, 2020

IEEE IMBioC 2020
January 31, 2020

WAMICON 2020
February 7, 2020

EuMC 2020
February 7, 2020

95th ARFTG Microwave Measurement Symposium
February 14, 2020

IEEE AUTOTESTCON 2020
February 15, 2020

ITC 2020
March 13, 2020

APMC 2020
May 15, 2020

mwjournal.com

NOVEMBER

Space Tech Expo Europe 2019
November 19–21 • Bremen, Germany
www.spacetechexpo.eu/

IEEE WiE Forum USA East 2019
November 21–23 • Arlington, Va.
https://attend.ieee.org/wie-forum-usa-east-2019/

DECEMBER

65th Annual IEEE International Electron Devices Meeting (IEDM)
December 7–11 • San Francisco, Calif.
https://ieee-iedm.org/

Asia Pacific Microwave Conference 2019
December 10–13 • Singapore
https://apmc2019.miceapps.com/client/sites/view/SP8f993

IEEE IMaRC 2019
December 13–15 • Mumbai, India
https://imarc-ieee.org/

JANUARY

CES 2020
January 7–10, 2020 • Las Vegas, Nev.
www.ces.tech/

94th ARFTG Microwave Measurement Symposium
January 26–29, 2020 • San Antonio, Texas
www.arftg.org

Radio and Wireless Week 2020
January 26–29, 2020 • San Antonio, Texas
https://radiowirelessweek.org/

DesignCon 2020
January 28–30, 2020 • Santa Clara, Calif.
www.designcon.com

FEBRUARY

MWC Barcelona 2020
February 24–27, 2020 • Barcelona, Spain
www.mwcbarcelona.com/

MARCH

SATELLITE 2020
March 10–12, 2020 • Washington, D.C.
https://2019.satshow.com/

GOMACTech 2020
March 17–18, 2020 • San Diego, Calif.
www.gomactech.net/2020/index.html

EMV 2020
March 17–19, 2020 • Cologne, Germany
https://emv.mesago.com/events/en.html

Microwave & RF 2020
March 18–19, 2020 • Paris, France
www.microwave-rf.com

APRIL

Expo Electronica 2020
April 14–16, 2020 • Moscow, Russia
www.expoelectronica.ru/en-GB

WAMICON 2020
April 15–17, 2020 • Clearwater Beach, Fla.
www.wamicon.org/

MAY

CS Mantech 2020
May 11–14, 2020 • Tucson, Ariz.
http://csmantech.org/

EDI CON China 2020
May 12–13, 2020 • Beijing, China
www.ediconchina.com

Space Tech Expo USA 2020
May 18–20, 2020 • Long Beach, Calif.
www.spacetechexpo.com/


ANALOG.COM/ADEF

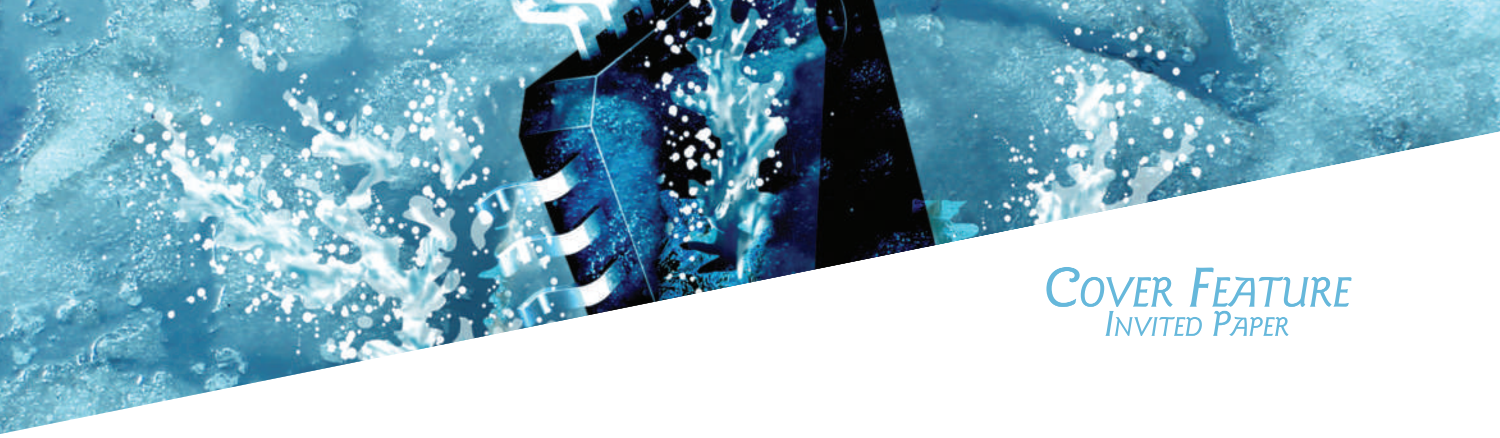

COVER FEATURE
INVITED PAPER

New Thermal Interface for High-Power Density GaN Devices in Space

Jordan Mizerak
JETCOOL Technologies Inc., Littleton, Mass.

The onset of GaN as a semiconductor material is enabling the next generation of electronic devices. Because GaN is a wideband gap (WBG) semiconductor material, it can sustain higher breakdown electric fields and electron drift velocities than conventional semiconductors such as Si and GaAs.[1] GaN also exhibits enhanced thermal characteristics, sustaining higher temperatures and more effectively conducting heat. Because of these desirable material properties, GaN devices can operate at higher frequencies and higher powers in smaller package sizes, an enabling development in the field of high-power semiconductors.

SOLID-STATE POWER AMPLIFIERS

GaN has great promise to revolutionize solid-state power amplifiers (SSPA) for space applications. GaN is a particularly good fit in space applications due to its small size, light weight and radiation tolerance from enhanced atomic bond strength. In traditional satellite architectures, amplifying a signal for transmission has typically been achieved either by using travelling wave tube (TWT) amplifiers, which are relatively large in size and weight, or lower power GaAs SSPAs, which require numerous units and additional signal combining hardware. With costs still near $10,000 per pound to get into low Earth orbit (LEO),[2] the ability to shrink from ~150 in^3 TWT amplifiers to operationally equivalent ~0.05 in^3 GaN high-power amplifiers (HPA) will result in significant cost reductions as well as payload capability enhancements.

The byproduct, however, of shrinking the power amplifier to a package smaller than a penny is the increased power density. In SSPAs, device temperatures spike to very high local values at the microscopic gate fingers as power density increases, making the removal of heat a far more difficult task. Moreover, with an Arrhenius relationship between device mean time to failure (MTTF) and operating temperature, small changes in the device temperature can result in orders of magnitude differences in lifetime.[3] It is therefore critical in high value, low-maintenance space payloads to have a reliable and effective cooling technique compatible with the shrinking package sizes and increasing power densities of GaN HPAs.

With current power densities of HPAs on space payloads eclipsing 50 W/cm^2, traditional heat spreading cooling methods are reaching their limits. Moreover, with the enhanced material properties of GaN devices, power densities over 1500 W/cm^2 are imminent in space payloads which is almost two orders of magnitude higher than those supported using standard thermal architectures. Therefore, a fundamentally different approach to thermal management is needed to fully capture the exceptional capabilities of GaN semiconductor devices while maintaining temperatures compatible with long-term, reliable operation on space platforms.

FUNDAMENTAL HEAT TRANSFER CONSIDERATIONS

Radiation heat transfer, assuming a perfect view factor to the surrounding cold sky, is governed by the Stefan-Boltzmann Law:

$$\dot{q}_{rad} = \epsilon\,\sigma\left(T_H^{\,4} - T_C^{\,4}\right)$$

where $\dot{q}_{rad}$ is the radiative cooling flux (W/cm^2) from a surface of emissivity ϵ with temperature T_H (K), radiating to surrounding cold sky temperature T_C (K) often taken to be around 3 K. The Stefan-Boltzmann constant, σ, is a physical constant of proportionality denoting the total radiative transfer of a black body over all wavelengths, which takes the value

$$\sigma = 5.67\times10^{-12}\,\frac{W}{cm^2K^4}$$

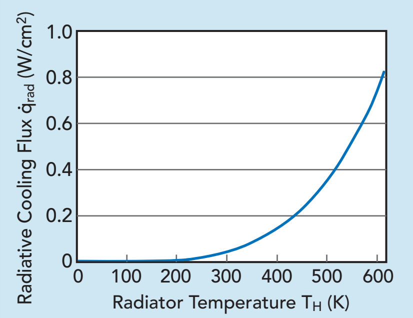

▲ Fig. 1 **Radiative cooling flux as a function of surface temperature, applying best case scenario of a 3 K cold sky with perfect emissivity and view factor.**

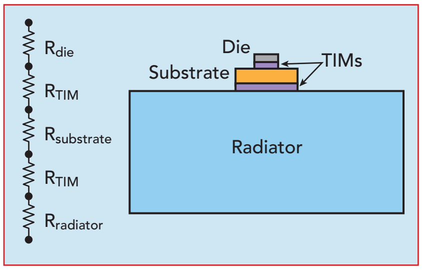

▲ Fig. 2 **Schematic of conductive heat spreading thermal stackup. The heat generated in the die passes through multiple layers of interface materials and heat spreaders before reaching the radiator (not to scale).**

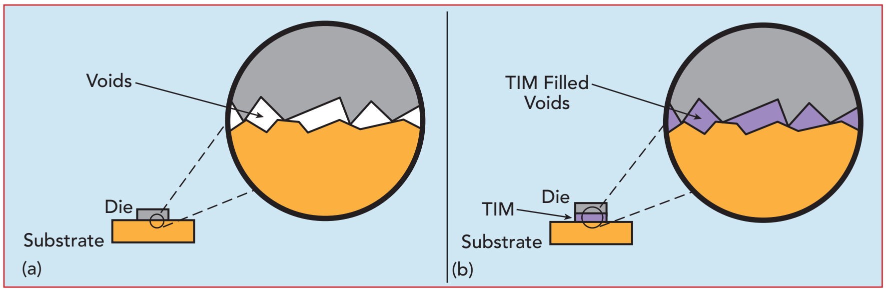

▲ Fig. 3 **Illustration of microscale roughness of adjoining surfaces, resulting in voids causing poor heat transmission between surfaces (a). TIMs are applied to fill in the gaps with a conductive intermediate layer, improving the thermal contact (b).**

Unlike conduction and convection, which are linear with temperature difference, radiation has a quartic dependence on absolute temperature. Because the Stefan-Boltzmann constant is small, radiation is negligible at temperatures typically seen on Earth. In space, however, radiation becomes the only viable option as an ultimate heat sink. Therefore, the hot radiator surface temperature T_H becomes the major determining factor in heat transfer capability per unit area in space, due to the quartic dependence in an otherwise low temperature, cold sky. Taking best case conditions at perfect emissivity $\epsilon = 1$ and cold sky temperature $T_C = 3$ K, the radiative cooling flux $\dot{q}_{rad}$ can be plotted against hot surface temperature T_H.

Most GaN devices have recommended maximum operating temperatures of about 250°C (523 K). As seen in ***Figure 1***, even at power densities of current devices, ~50 W/cm^2, the power density of GaN SSPAs is far higher than the heat transfer capability of radiative techniques. This makes the required radiator area for a given SSPA much larger than the device footprint area, and often heat management tradeoffs such as low duty cycle operation, onboard thermal storage and other indirect thermal pathways must be employed to keep the equilibrium temperature low.

It is therefore paramount to optimize the heat pathway from where the heat is being generated (microscopic hot spots on the die) to where it is ultimately rejected (the large area surface of the radiator). As power densities increase, temperatures on the die spike to very high local values, requiring high capability thermal management techniques to effectively transfer the heat to the radiator, which may be over a meter away. Minimizing the thermal resistance between the die and the radiator is what facilitates high-power density devices maintaining safe temperatures for high performance and long lifetime.

CONDUCTIVE HEAT SPREADING APPROACH

The standard method of removing heat from PAs on space payloads relies on heat spreading via conduction. The PA die is attached to a heat spreader substrate with a matched coefficient of thermal expansion (CTE) via a thermal interface material (TIM), often a solder. This substrate is then attached to a large radiator via a second TIM, often a filler paste or epoxy. This thermal stackup is shown in ***Figure 2***. As described previously, the radiator's surface area needs to be much larger than that of the die footprint. Therefore, there needs to be a method of connecting the die to the radiator in order to spread the heat out.

The most direct thermal pathway would be to attach the die directly to the radiator. The first issue is that, when attempting to mate surfaces, numerous voids are introduced due to the inherent roughness of each surface at the microscale. These voids cause reduced contact area between the surfaces and result in an insulating layer, thereby inducing a large resistance for heat to flow. To remedy this, thermal interface materials are applied when mating two surfaces. The goal with TIMs is to fill those voids with a thermally conductive material to minimize the resistance for heat to flow from one surface to the next, as shown in ***Figure 3***.

Attaching the die to the radiator via a TIM would be the next most direct thermal pathway. However, for the radiator to maximize heat rejection to the cold sky, it is ideally made of a high thermal conductivity material (aluminum, copper, etc.) to ensure a high surface temperature over the entirety of its area. Unfortunately, these high thermal conductivity materials often have large values for their CTE, introducing a mismatch with the lower CTE die. This will introduce high stress to the die and/or TIM, especially under conditions of thermal cycling seen from diurnal variations in space.

Therefore, the final solution is to attach the die to a CTE matched substrate via a first TIM, and subsequently, attach the substrate to the radiator via a second TIM. The substrate ideally has the highest thermal conductivity possible while matching the CTE of the die, which is typically a tradeoff as most CTE-matched substrate materials (Molybdenum, Tungsten, etc.) have low thermal conductivities. These substrates are made thicker to sustain stresses induced from the CTE mismatch to the high conductivity radiator, thereby relieving stress on the die while also offering some heat spreading as an intermediate step before the high conductivity radiator. Thermal con-


Has Amplifier Performance or
Delivery Stalled Your Program?

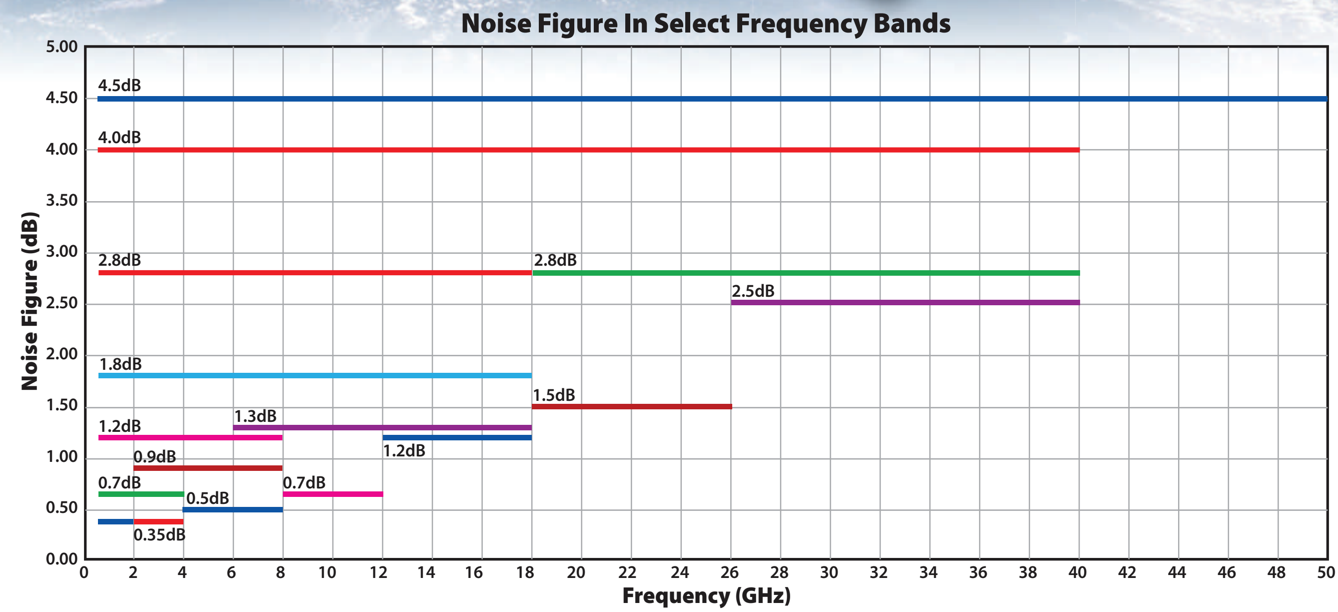
Noise Figure In Select Frequency Bands
Noise Figure (dB)
Frequency (GHz)
5.00
4.50
4.00
3.50
3.00
2.50
2.00
1.50
1.00
0.50
0.00
0
2
4
6
8
10
12
14
16
18
20
22
24
26
28
30
32
34
36
38
40
42
44
46
48
50
4.5dB
4.0dB
2.8dB
2.8dB
2.5dB
1.8dB
1.5dB
1.3dB
1.2dB
1.2dB
0.9dB
0.7dB
0.7dB
0.5dB
0.35dB

TABLE 1

THERMAL CONDUCTIVITY AND COEFFICIENT OF THERMAL EXPANSION (CTE) VALUES OF COMMON MATERIALS.[4]

Table fill colors correspond to typical materials of layers shown in Figure 2

Type	Material	Thermal Conductivity (W/cm-K)	CTE (ppm/K)
Die	GaN	1.7	3.2
Die	SiC	3.9	2.8
Die	Si	1.3	2.6
Substrate	Copper Tungsten 10%/90% (CuW)	2.0	8.0
Substrate	Copper Molybdenum 30%/70% (CuMoCu)	1.9	7.6
Substrate	Cu-CuMo-Cu 1:4:1 (CPC)	2.2	7.1
Radiator	Copper (Cu)	4.0	17
Radiator	Aluminum (Al)	2.4	23

ductivity and CTE values of common materials in the stackup are shown in ***Table 1***.

The drawbacks of this robust solution include three additional thermal resistances: one from the CTE matched substrate and two from the TIMs. The resistance of the substrate is not usually problematic—it is a relatively high thermal conductivity metal material, employed in a manageable thickness. This typically adds a modest thermal resistance and may even help with initial heat spreading from the die. There are also promising new materials such as aluminum diamond and silver diamond which can be used (thermal conductivities up to 5 to 8 W/cm-K and CTE ~7.5 ppm/K) for even further reduction in resistance through the substrate.[4]

The TIMs, however, often become a bottleneck. Even though TIMs allow much improved conduction between surfaces compared to voids, in general, they are not very conductive. Most TIMs operate around 0.05 W/cm-K, which is a significant drop compared to the substrate and radiator materials over 2 W/cm-K. Even with attempts to enhance the conductivity of TIMs by adding complex metal microbeads or other high conductivity nanoparticles, it is rare to see filler based TIMs exceed 0.1 W/cm-K.

The thermal resistance of a TIM per unit area can be quantified based on its thermal conductivity and thickness. Taking a TIM thickness near 0.1 mm and thermal conductivity near 0.1 W/cm-K:

$$\frac{\Delta T_{TIM}}{\dot{q}_{device}} = (RA)_{TIM} = \frac{L_{TIM}}{k_{TIM}} = \frac{0.01\ \text{cm}}{0.1\frac{\text{W}}{\text{cm}-\text{K}}} = 0.1\frac{\text{K}}{\text{W/cm}^2}$$

Therefore, for a 50 W/cm^2 die, there is a ~5 K temperature jump

across each TIM layer (depending on TIM type and level of spreading in the substrate). This results in needing yet a larger radiator, as the rejection temperature of the radiator cannot match the actual device temperature due to the intermediate resistances. At such power levels, a drop on the order of 10 K through the TIMs is salvageable. However, with upcoming power densities near 1500 W/cm^2, a drop > 100 K across each TIM layer will be prohibitive.

In addition to the baseline heat transfer limitations at ideal conditions, there are a number of practical considerations which can make working with TIMs challenging. There are a variety of different types of TIMs applied in various circumstances depending on the application, including solders, low melting point alloys, structured carbons and various fillers (pastes, epoxies, adhesives). A few of the common challenges are listed below, some of which are more relevant to certain TIM types than others:[5]

- The interfacial contact resistance between the TIM and the substrate at the molecular level can add additional resistance beyond conduction through the bulk TIM. For example, carbon nanotube (CNT) TIMs have high thermal conductivity and good mechanical compliance, but often suffer from contact resistances at their interfaces with the adjacent substrates. Conceptually, this is similar to the voids that occur when no TIM is used, but at the molecular level.
- Some TIMs are challenging to integrate into the thermal stackup. Special tools, multi-step application procedures, high temperature/vacuum application conditions and long cure times are examples of things that may be required to achieve the TIM's rated performance.
- Even with perfect application, many TIMs experience outgassing/oxidation, causing dry out and degradation over time. This results in the performance of the electronic device faltering over its lifetime, likely experiencing premature failure. There is preliminary research underway to add nanoscale coatings of higher stability compounds to prevent degradation; this may help mit-

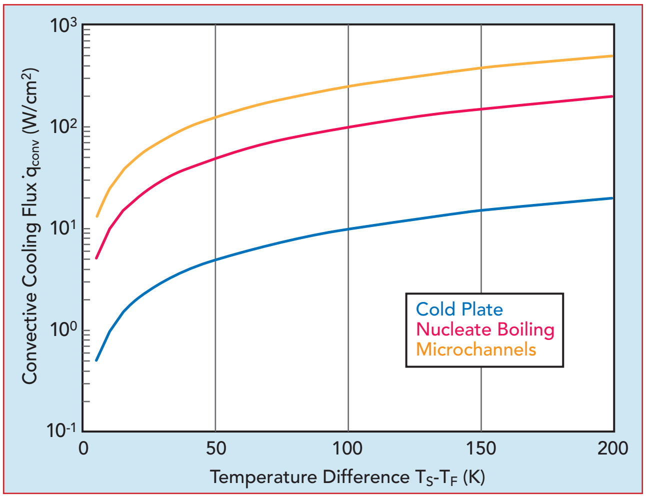

Fig. 4 **Semi-log plot showing achievable convective cooling fluxes from standard liquid convection methods.**

igate the longevity concerns but may result in tradeoffs regarding cost and reduced bulk conductivity.

- Complex verification techniques must often be employed to ensure the TIM was applied properly. Because uniform coverage of the TIM over the entire footprint area with no voids is critical to the TIM's functionality, advanced inspection hardware such as scanning acoustic microscopes are necessary to confirm the quality of each TIM layer in mission critical applications.

Short of TIMs that can match the thermal conductivity of the metals they bind, the conduction approach for heat spreading is starting to fall behind the capability of the devices to which they are being applied. A different technique will be necessary to support devices coming on the near horizon.

DIRECT DIE CONVECTIVE COOLING

In seeking alternatives for conduction-based heat spreading methods, convection-based approaches may be promising candidates due to their high cooling capabilities. In terrestrial systems, a variety of convective approaches are employed, such as air natural convection, forced air convection, forced liquid convection and two-phase convection. Given the long desired operational lifetimes and the lack of a surrounding atmosphere in space, closed loop liquid convection approaches are the most likely candidates. Convective cooling flux $\dot{q}_{conv}$ is prescribed as:

$$\dot{q}_{conv} = h\left(T_S - T_F\right)$$

In this equation, T_S is the temperature of the surface in contact with the coolant, T_F is the fluid coolant temperature, and h is the heat transfer coefficient, which denotes the cooling flux per degree of temperature difference achievable by a given cooling technique (W/cm^2-K). Therefore, the convective cooling flux, $\dot{q}_{conv}$, is linearly proportional to the difference in temperature of the heated surface and the fluid coolant temperature. While in radiative cooling the cold sky is near 3 K, the fluid temperature cannot be taken to be as low in the convective case due to freezing considerations and the inherent thermal resistance of the radiator. ***Figure 4*** displays what cooling fluxes can be achieved for various common liquid cooling techniques over a range of practical surface-fluid temperature differences ($T_S - T_F$).

The plot shows convective cooling fluxes up to 500 W/cm^2 which appears promising for higher power density devices. However, an important distinction must be made as to the applicability of these cooling fluxes. Typical implementations of closed loop liquid cooling are not holistically different from the stack-up shown in Figure 2, for the same reasons of CTE match and high conductivity heat sink requirements. TIMs are still applied between the die and the substrate, and further from the substrate onto a convective cooling module. That is, even if liquid cooling methods can match

the power density of a device, they often cannot be integrated into the system without using thermal interface materials and suffer from the same thermal resistances as shown in ***Figure 5***.

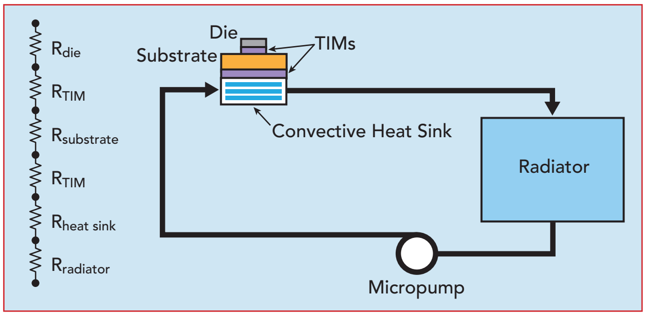

Fig. 5 **Standard convective cooling implementation. The convective heat sink is not integrated at the die level and therefore suffers from the same TIM issues as conductive heat spreading approaches.**

However, new methods of applying convection can change the paradigm of the thermal stackup altogether. A unique, new thermal interface concept is via direct die-attach, where the cooling module is configured such that the fluid impacts the die directly. In this methodology, fluid is brought directly to the die surface, which eliminates the TIMs and heat spreader substrates from the thermal pathway. To perform this task, the convective cooling method has two major requirements:

- It must be integrable with the die such that no intermediate affixing or spreading surfaces are required in its integration or operation.
- In order to cool devices without a heat spreader to expand the area, the convective cooling flux must match or exceed the power density of the device itself.

An emerging method called microconvective cooling by JETCOOL Technologies Inc. appears poised to meet these two requirements for cooling advanced GaN SSPAs in space. Microconvective cooling utilizes high momentum microscale fluid jets that impinge upon the heated die surface, causing strong thermal boundary layer suppression and resulting in high heat transfer capability.

This method has produced heat transfer coefficients over 40 W/cm^2-K, which at a 200 K surface to fluid temperature difference, achieves convective cooling fluxes over 8000 W/cm^2. The direct die-attach methodology with microconvective cooling has been successfully implemented and experimentally demonstrated cooling devices with power densities over 5000 W/cm^2 in radar-based applications.[6] A schematic of the thermal stackup for this new technique is shown in ***Figure 6***. By directly bringing the fluid in contact with a passivated die surface, multiple TIM layers and heat spreaders can be removed from the thermal stackup, greatly reducing thermal resistance to the radiator in high-power density applications.

As an additional benefit, because the fluid is now directly contacting the die, the cooling module does not need to be made of a thermally conductive material. Therefore, the cooling module can be a closely

matched CTE material, removing the tradeoff between thermal conductivity and CTE mismatch. Further, although the die-attach needs to be robust, it no longer needs to be perfect, as was the case in applying thermal interface materials. The thermal performance of the direct die-attach method is unaffected by the quality of the die-attach, meaning the die-attach method can focus on a strong, robust attachment mechanism instead of a high quality workmanship solution requiring high thermal conductivity, minimal thicknesses and complete, void free coverage.

Of course, the ultimate heat sink will still be via radiation to the cold sky, so there needs to be a fluid loop containing a pump and method of exchanging heat from the fluid to the radiator. Because the radiative cooling flux limitations still apply regardless of the thermal interface method, a large area radiator will still be required to reject the heat on the radiator side.

Continually advancing developments in 3D printing can be leveraged to produce optimal radiator designs containing integral cooling channels, allowing seamless integration of fluid cooling loops into the radiator workflow at low size, weight and power (SWaP). As the die level heat rejection has been decoupled from the radiator, this methodology is fully compatible with thermal storage strategies and fits seamlessly with different duty cycles and temperature cycling, with minimal control and input power requirements.

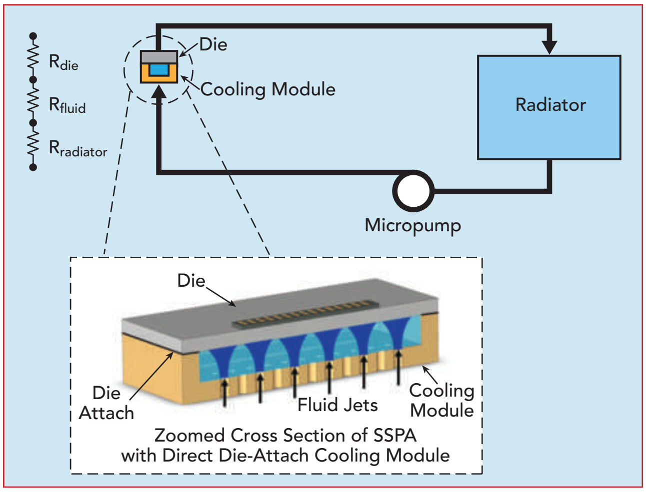

Fig. 6 Direct die-attach cooling methodology, integrated with ultra-high cooling effectiveness microconvective cooling including a zoomed 3D cross section of the die level cooling approach shown at the top.

SUMMARY

With increasing power densities made possible via advanced semiconductor materials, adequate thermal management of devices is becoming increasingly challenging. The traditional method of cooling electronic devices via heat spreading through thermal interface materials and high conductivity heat spreaders is quickly reaching its limits. By employing direct die-attach cooling methodologies with high capability convective techniques, significant reductions in thermal resistance from the die to the radiator can keep devices at safe temperatures. One potential technique involving direct die-attach microconvective cooling via high velocity fluid jets shows promise as an enabling technique to facilitate devices with long lifetimes and low weight, enabling future cost-effective and highly capable space-based missions.■

References

1. J. Y. Tsao et al., "Ultrawide-Bandgap Semiconductors: Research Opportunities and Challenges," *Advanced Electronic Materials*, Vol. 4, No. 1, January 2018, Article No. 1600501.
2. M. LaMarche, "GaN SSPA Technology for Space-Based Applications," *Microwave Journal*, Vol. 62, No. 4, April 2019, pp. 20–28.
3. P. D. T. O'connor, "Arrhenius and Electronics Reliability," *Quality and Reliability Engineering International*, Vol. 5, No. 4, 1989, pp. 255–255.
4. R. S. Pengelly et al., "A Review of GaN on SiC High Electron-Mobility Power Transistors and MMICs," *IEEE Transactions on Microwave Theory and Techniques*, Vol. 60, No. 6, 2012, pp. 1764–1783.
5. K. M. Razeeb et al., "Present and Future Thermal Interface Materials for Electronic Devices," *International Materials Reviews*, Vol. 63, No. 1, 2018, pp. 1–21.
6. S. M. Walsh et al., "Embedded Microjets for Thermal Management of High Power-Density Electronic Devices," *IEEE Transactions on Components, Packaging and Manufacturing Technology*, Vol. 9, No. 2, 2018, pp. 269–278.

LM Skunk Works' Project Riot Demonstrates Multi-Domain Operations

Lockheed Martin (LM) Skunk Works®, the Missile Defense Agency and the U.S. Air Force successfully connected an F-35, U-2 and a multi-domain ground station in a ground-breaking test demonstrating multi-domain operations and the secure distribution of sensitive information across multiple platforms.

During the demonstration, called Project Riot, an F-35 detected a long-range missile launch with its on-board sensors and shared the information through the U-2 to the air defense commander on the ground, enabling the commander to quickly make the decision to target the threat. This next-level connectivity reduces the data-to-decision timeline from minutes to seconds, which is critical in fighting today's adversaries and advanced threats.

Project Riot
(Source: Lockheed Martin)

In partnership with the Air Force Life Cycle Management Center at Hanscom Air Force Base in Massachusetts, and the Missile Defense Agency, Skunk Works' Project Riot builds on a series of open systems architecture demonstrations proving how incremental increases in capability can be rapidly fielded to enable a connected network across air, ground, sea, space and cyber domains.

"This demonstration continues our commitment to provide complete battlespace awareness and seamless interoperability to enable multi-domain operations," said John Clark, vice president of ISR & UAS at Lockheed Martin Skunk Works. "With its long-range standoff sensors, on-board processing and ability to operate in and around contested environments, the U-2 continues to play a critical role in demonstrating new capabilities today, while transforming operations for tomorrow's battlespace."

Leveraging common industry standards to drive down cost and shorten schedules, the team achieved four mission critical data points in less than four months:

- Demonstrated the ability to leverage F-35 sensor data for missile defense.
- Leveraged the modernized U-2's extensive payload capacity, modular design and open architecture to provide beyond line of sight communications between the F-35 and a multi-domain ground station.
- Established two new data paths to securely transmit 5th generation sensor data at multiple levels of security to the warfighter, enabling a multi-domain network of legacy and 5th generation systems.
- Disseminated 5th generation data using the Air Force's Universal Command and Control Interface and Open Mission Systems standards for faster capability deployment and seamless connection between systems.

"The F-35, with its advanced sensors and connectivity, is able to gather and seamlessly share critical information enabling the joint force to be safer and more effective," said Greg Ulmer, Lockheed Martin vice president and general manager for the F-35 program. "No other fighter jet in the world has this capability—and this test was a critical step on the path to unlocking its full potential for multi-domain operations."

This demonstration builds on successful flight tests completed since 2013 that establish the foundation for a distributed, systems-of-systems architecture in the not-too-distant future.

MBDA Working on New SPEAR-EW Electronic Warfare Weapon

The compact size of the SPEAR family allows four weapons to be carried internally in each of the two internal weapons bays of the F-35, or three per station on the Eurofighter Typhoon. MBDA has been awarded a contract to demonstrate SPEAR-EW, a new electronic warfare (EW) version of the SPEAR weapon system family on order for the Royal Air Force (RAF).

SPEAR-EW is being developed by MBDA in partnership with Leonardo to complete a wide range of suppression of enemy air defense (SEAD) missions, under a Technical Demonstration Program (TDP) contract awarded by Defence Equipment & Support (DE&S). SPEAR-EW will integrate a cutting-edge miniaturized EW payload from Leonardo, which will act as a stand-in jammer to greatly increase the survivability of RAF aircraft and suppress enemy air defenses, acting as a significant force multiplier.

Defense Minister Anne-Marie Trevelyan said: "These state-of-the-art electronic jammers will confuse our adversaries and keep our pilots safer than ever in the air. Paired with the devastating power of precision Brimstone and Meteor missiles, our world-class F-35 and Typhoon jets will continue to rule the skies in the years to come."

Mike Mew, MBDA UK director of sales and business development, said: "SPEAR-EW is a revolutionary new capability that, alongside the existing SPEAR3 weapon, marks a fundamental change in the ability of friendly air forces to conduct their missions despite the presence of enemy air defenses. Our vision for SPEAR is to create a swarm of networked weapons able to saturate and neutralize the most sophisticated air defenses.

For More Information Visit mwjournal.com for more defense news.

SPEAR-EW (Source: MBDA)

"Adding SPEAR-EW to the family alongside our existing SPEAR strike missile demonstrates the principle of introducing complementary variants to the SPEAR family that will add significant capability and force multiplication without the need to repeat platform integration. We have an exciting roadmap of variants, spirals and technology insertions in the pipeline to further enhance the family as we move forward."

The core of SPEAR-EW's payload is Leonardo's advanced, miniaturized digital RF memory (DRFM) technology, which offers an advanced and future-proof electronic jamming and deception capability. It will complement the SPEAR network enabled miniature cruise missile, which is designed to precisely engage long range, mobile, fleeting and relocatable targets in all weather, day or night, in the presence of countermeasures, obscurants and camouflage, while ensuring a safe stand-off range between the aircraft and enemy air defenses.

Powered by a turbojet engine the SPEAR missile offers over double the range, and a far more flexible operating envelope, when compared to a conventional glide weapon. SPEAR-EW utilizes this long endurance through its capacity to be launched at enhanced stand-off ranges and loiter while carrying out its jamming mission.

The compact size of the SPEAR family allows four weapons to be carried internally in each of the two internal weapon bays of the F-35, or three per station on the Eurofighter Typhoon. SPEAR-EW will keep the same form and fit as the baseline SPEAR to enable a single integration pathway and launcher solution. The SPEAR family complements MBDA's wider portfolio of strike weapons, filling the gap between the large and very-long range Storm Shadow deep strike missile and the highly accurate Brimstone close-air-support missile.

The SPEAR weapons system recently completed a set of ground trials and fit-checks of a loaded three-pack SPEAR launcher onto a Eurofighter Typhoon fighter aircraft. The work was undertaken by a joint engineering team from MBDA, BAE Systems and the Ministry of Defence's DE&S, and took place at BAE Systems' flight test site in Warton, Lancashire.

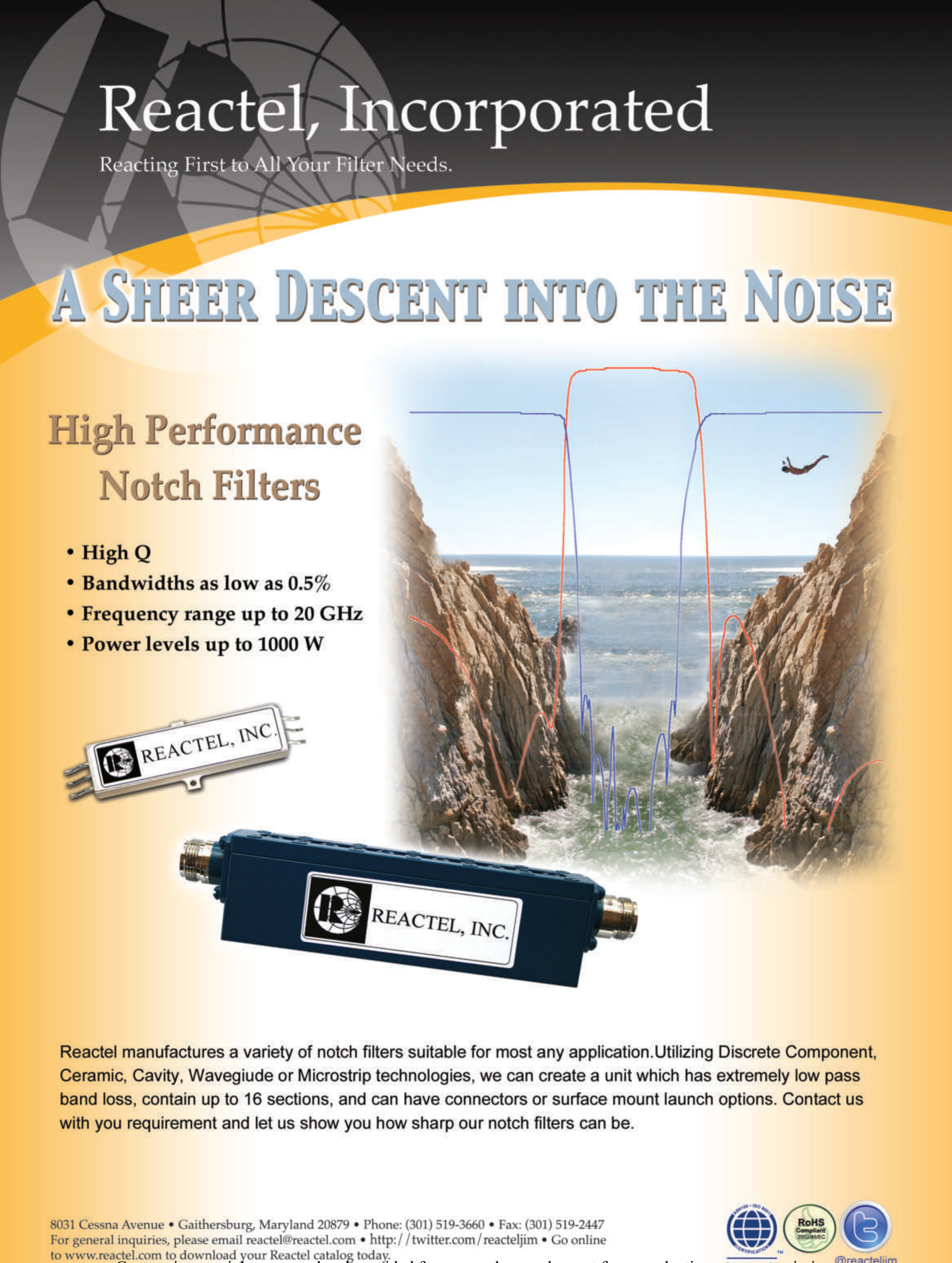
Reactel, Incorporated
Reacting First to All Your Filter Needs.
A Sheer Descent into the Noise
High Performance
Notch Filters
• High Q
• Bandwidths as low as 0.5%
• Frequency range up to 20 GHz
• Power levels up to 1000 W
REACTEL, INC.
REACTEL, INC.
Reactel manufactures a variety of notch filters suitable for most any application.Utilizing Discrete Component, Ceramic, Cavity, Wavegiude or Microstrip technologies, we can create a unit which has extremely low pass band loss, contain up to 16 sections, and can have connectors or surface mount launch options. Contact us with you requirement and let us show you how sharp our notch filters can be.
8031 Cessna Avenue • Gaithersburg, Maryland 20879 • Phone: (301) 519-3660 • Fax: (301) 519-2447
For general inquiries, please email reactel@reactel.com • http://twitter.com/reacteljim • Go online
to www.reactel.com to download your Reactel catalog today.
RoHS
Compliant
@reacteljim


MMIC
SPLITTER/COMBINERS
up to 43.5 GHz
EP2W1+
0.5 to 9.5 GHz
EP2C+
1.8 to 12.5 GHz
EP2K1+
2 to 26.5 GHz
EP2KA+
10 to 43.5 GHz
THE WIDEST SURFACE MOUNT
BANDWIDTHS IN THE INDUSTRY!
▶ Power handling up to 2.5W
▶ Insertion loss, 1.1 dB typ.
▶ Isolation, 20 dB
Mini-Circuits®
www.minicircuits.com (718) 934-4500 sales@minicircuits.com
596_Rev A_P

Pulsed RF Power Semiconductor Device Markets Will Exceed $300M by 2024

While their association with consumer spending fuels the volatility of many global electronics markets, pulsed RF power device markets are supported by quite different priorities. Pulsed RF power transmitters generate tremendous amounts of power in small bursts that are useful for radar, airborne collision avoidance systems and military IFF equipment.

"Ampleon, NXP and Wolfspeed are among the RF power semiconductor manufacturers on a quest to find markets unrelated to the mobile wireless infrastructure," says Lance Wilson, research director, ABI Research. "Device prices in wireless infrastructure are flattening out and more profitable areas are being searched for."

The airborne transportation safety market and military market are both experiencing solid growth in pulsed RF power device shipments. The avionics transponder and air navigation market segments are also seeing growth, which is further lifted by the overall worldwide air traffic control upgrade. Intrinsically less "optional" than many consumer markets, these segments are therefore less sensitive to economic upheavals than consumer-driven markets, although they are not totally immune to the macro economy.

There are several vendors who are already focused to varying extents on the pulsed high-power marketplace, including Integra Technologies, Microsemi, Qorvo and again Wolfspeed, and several semiconductor manufacturers are attempting to enter this market space. Pulsed RF power device markets are becoming very competitive technologically: GaN devices are vying for market share along with the more established Si and GaAs-based technologies. Many companies are rushing into these markets and all vendors are developing GaN products of some form. Qorvo, Sumitomo Electric Device Innovations and Wolfspeed are already producing GaN devices in volume. ABI Research speculates that there may not be the market size to support them all.

Future of 5G Lies in Enterprise, Not Consumer Market

In its new whitepaper, "The Five Myths of 5G," ABI Research finds that use cases across different vertical markets, such as industrial automation, cloud gaming, private LTE and smart transport systems, will become pervasive, and will unlock new opportunities for mobile service providers (MSP) along the way.

However, this bright and lucrative future may be hampered by 5G's past. That is because early 5G implementations were designed to fit the needs of the consumer market first. "The intent was to allow MSPs and their technology suppliers to harvest the low-hanging revenues of the consumer space before gradually extending the network's capabilities to meet the needs of the enterprise," explains Stuart Carlaw, CRO, ABI Research. Unfortunately, this process has proven a lot more costly and time consuming than initially thought. In fact, ABI Research estimates that if MSPs rely solely on consumers to justify their investments in 5G rollouts, it could take up to 15 years to realize any ROI.

MSPs have every hope that 5G will help them reduce the cost per gigabyte of bandwidth and improve ARPU compared to existing access technologies. But, 5G is expected to be much more expensive compared to its predecessors. This is due to the network densification it requires and the addition of a great number of new functions, both at the core and the access sides of the network. As a result, the implementation and democratization of 5G will come at very high costs, notably operational expenditures, which are already increasing at a very alarming pace.

Industrial telcos could potentially become the new cash cow for securing 5G ROI. Indeed, 5G is positioned to be a major component of enterprise digital transformation and a reliable wireless communication platform that could create trillions in economic value across many enterprise verticals. However, as things stand now, implementations for enterprise applications are far from optimized. As a result, MSPs have been unable to accelerate the enterprise digital transformation and unlock new business opportunities in this environment. "Network architecture flexibility, interoperability with legacy operation processes, cost effectiveness, network determinism, security and reliability will be equally important for the enterprise as providing bigger pipes—a value proposition that has long resonated well within the consumer market but is unlikely to attract industrial verticals," Carlaw points out.

The idea of building a 5G network capable of accommodating the needs of multiple markets and industries is a big fantasy of MSPs. "The reality is that the implementation approaches that have been designed for the consumer market will not adequately serve enterprise verticals. The "build it and they will come" approach is simply unrealistic and is one of the myths holding back the 5G market," concludes Carlaw.

Future of AI in Industrial Manufacturing

Artificial intelligence (AI) has been touted as a powerful technology that will revolutionize the industrial manufacturing space. The sentiment has its validity, but the reality is extremely complex. AI in industrial manufacturing is a collection of various use cases at different phases of manufacturing, such as genera-

For More Information Visit mwjournal.com for more commercial market news.

tive design in product development, production forecasting in inventory management and machine vision, defect inspection, production optimization and predictive maintenance in the production phase.

"Since manufacturers are not comfortable having their data transferred to a public cloud, nearly all industrial AI training and inference workloads happen at the edge, namely on device, gateways and on-premise servers," says Lian Jye Su, principal analyst, ABI Research. To facilitate this, AI chipset manufacturers and server vendors have designed AI-enabled servers specifically for industrial manufacturing, and more and more industrial infrastructure is equipped with AI software or dedicated AI chipsets to perform AI inference.

Despite this, the implementation of AI has not been as seamless as was expected. Among the use cases, predictive maintenance and equipment monitoring are the most commercially implemented so far, due to the maturity of associated AI models. The total installed base for these two use cases alone is expected to reach 9.8 million and 6.7 million, respectively, by 2024. It is important to note that many AI-enabled industrial devices support multiple use cases on the same device due to advancements in AI chipsets. Key startups such as Uptake, SparkCognition, FogHorn and Falkonry are introducing cloud- and edge-based solutions that monitor the overall performance of industrial manufacturing assets and process flows.

Another use case currently gaining momentum is defect inspection, with the total installed base expected to grow from 300,000 in 2019 to over 3.7 million by 2024. This is extremely popular in electronic and semiconductor manufacturing, where major manufacturers have been partnering with AI chipset vendors and software providers to develop AI-based machine vision to perform surface, leak and component-level defect detection, microparticle detection, geometric measurement and classification. Conventional machine vision technology remains popular in the manufacturing factory, due to its proven repeatability, reliability and stability; however, the emergence of deep learning technologies opens up expanded capabilities and flexibility. These algorithms can pick up unexpected product abnormalities or defects, go beyond existing issues and uncover valuable new insights for manufacturers.

At the moment, manufacturers are facing enormous competition in building and training in-house data science teams for AI implementation. Most AI talent prefers to work with webscale giants or AI startups, making talent acquisition a challenging task for industrial manufacturers. "As such, they are left with one viable option, which consists of partnering with other players in the AI ecosystem. The diversity in AI use cases necessitates the creation of partnerships," Su concludes.

Around the **Circuit**

Barbara Walsh, Multimedia Staff Editor

MERGERS & ACQUISITIONS

Qorvo announced that it has acquired **Cavendish Kinetics Inc.**, a provider of high-performance RF MEMS technology for antenna tuning applications. The Cavendish Kinetics team will continue to advance RF MEMS technology for applications across Qorvo's product lines and transition the technology into high-volume manufacturing for mobile devices and other markets. Qorvo has been a lead strategic investor in San Jose-based Cavendish Kinetics since 2015.

dB Control has acquired 100 percent of the stock of **TTT-Cubed Inc.** The acquisition of TTT will add high-end frequency locked oscillators, integrated digital control units, RF sources, detectors and controllers to dB Control's existing line of high-power TWT amplifiers (TWTA), microwave power modules (MPM) and high-voltage power supplies (HVPS) for defense and aerospace applications. Specific financial terms and details of the all-cash transaction were not disclosed. TTT will operate as part of dB Control and will relocate to its facility in Fremont, Calif. dB Control is part of HEICO's Electronic Technologies Group. Most of TTT's team will remain with the business post-closing.

TPC Wire & Cable Corp., a portfolio company of Audax Private Equity, announced that it has completed the acquisition of **Cicoil LLC**. Based in Valencia, Calif., Cicoil's technology is widely used in mission critical applications within industries such as mil-aero, semiconductor and medical. This acquisition allows TPC to expand its market reach and strengthen its portfolio of specialized wire and cable solutions to sophisticated, high cost-of-failure environments.

Avnet has signed an agreement to acquire **Witekio**, formerly known as Adeneo Embedded. Witekio is a privately held company with expertise in software and embedded systems that helps developers overcome the technical challenges and complexity of developing IoT solutions. This announcement furthers Avnet's end-to-end IoT strategy by adding more capabilities and expertise in embedded software, edge computing and security, specifically from hardware to the cloud. This acquisition also underscores Avnet's commitment to helping companies reduce the time, cost and complexities of successfully bringing IoT products to market.

SAGE Millimeter will become **Eravant** in March 2020, a change that renews the company's commitment to the RF engineer. The new brand emphasizes building customer relationships on top of a long legacy of mmWave expertise. Read more about the upcoming transformation at www.sagemillimeter.com.

COLLABORATIONS

Keysight Technologies Inc. announced an extended collaboration with **Qualcomm Technologies Inc.**, a wholly owned subsidiary of Qualcomm Inc., to accelerate commercialization of Dynamic Spectrum Sharing (DSS) technology, which will enable mobile operators to quickly and cost-effectively roll out 5G new radio (NR) services. The collaboration utilizes Keysight's 5G network emulation solutions to accelerate the development of Qualcomm® Snapdragon™ 5G Modem-RF System to support DSS, an emerging technology that is part of the 3GPP Release 15. By 2020, mobile operators are expected to start implementing DSS on existing 4G LTE base stations, speeding nationwide deployments of 5G services.

Modelithics Inc. has expanded its partnership with **Mini-Circuits** to develop high-accuracy simulation models for Mini-Circuits' packaged reflectionless filters, power splitter/combiners and LTCC transformers. The substrate-selectable models for the filters are measured/modeled to 40 GHz with the splitters and transformers measured/modeled to 30 GHz. Ten new reflectionless filter models, six power splitter/combiner models and four LTCC transformer models are currently available for free individual download for Keysight Technologies' ADS from the Mini-Circuits MVP page on the Modelithics website. These models will also be available in the Modelithics COMPLETE Library and the Modelithics mmWave & 5G Library in future library releases.

Aptiv and **Hyundai Motor Group** have announced that they are forming an autonomous driving joint venture, which will advance the design, development and commercialization of SAE Level 4 and 5 autonomous technologies. The joint venture will start testing fully driverless systems next year, with a plan to have a production-ready autonomous driving platform available for robotaxi providers, fleet operators and automotive manufacturers in 2022. As part of the agreement, Aptiv and Hyundai Motor Group will each have a 50 percent ownership stake in the joint venture, which is valued at $4 billion.

Mobile operators, enterprises, cities and other key IoT market players gain access to a wealth of new IoT use cases by combining two unlicensed connectivity technologies, as illustrated in a new white paper released by the **Wireless Broadband Alliance (WBA)** and the **LoRa Alliance®**. Developed with input from mobile carriers, telecom equipment manufacturers and advocates of both connectivity technologies, "Wi-Fi & LoRaWAN Deployment Synergies: Expanding Addressable Use Cases For The Internet of Things" illustrates new business opportunities that are created when Wi-Fi networks that are traditionally built to support critical IoT are merged with LoRaWAN networks that are traditionally built to support low data rate massive IoT applications.

For More Information For up-to-date news briefs, visit mwjournal.com

L to K Band Ultra-Wideband

Voltage Controlled Oscillators

Model Number	Frequency	Phase Noise @ 10 kHz offset	Phase Noise @ 100 kHz offset	Tuning Voltage	Output Power
	(GHz)	(dBc/Hz)	(dBc/Hz)	(V)	(dBm)
DCO100200-5	1 - 2	-95	-117	0 - 24	+1
DCYS100200-12	1 - 2	-105	-125	0 - 28	+4
DCO200400-5	2 - 4	-90	-110	0 - 18	-2
DCYS200400P-5	2 - 4	-93	-115	0 - 18	0
DCO300600-5	3 - 6	-75	-104	0 - 16	-3
DCYS300600P-5	3 - 6	-78	-109	0 - 16	+2
DCO400800-5	4 - 8	-75	-98	0 - 15	-4
DCO5001000-5	5 - 10	-80	-106	0 - 18	-2
DCYS6001200-5	6 -12	-70	-94	0 - 15	> +10
DCYS8001600-5	8 - 16	-68	-93	0 - 15	> +10
DCYS10002000-5	10 - 20	-65	-91	0 - 18	> +10

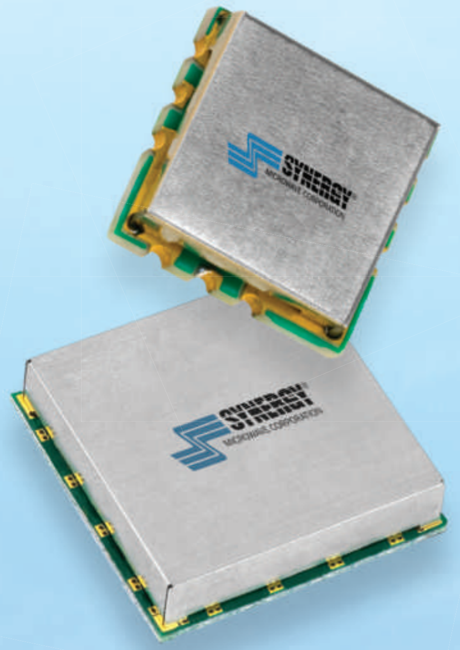

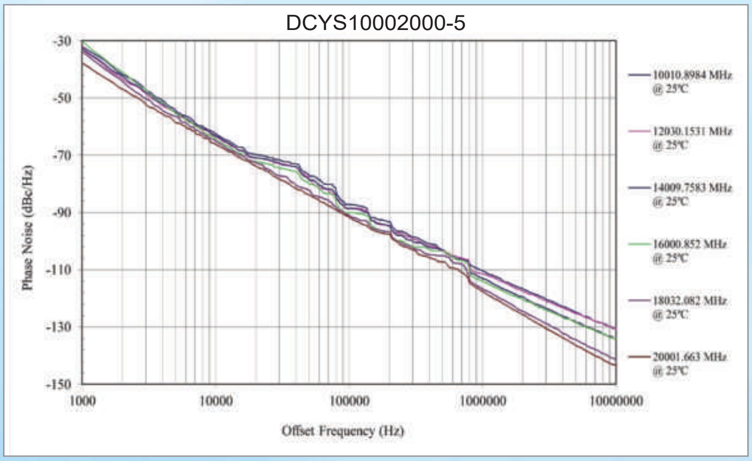

Features:

> Superior Phase Noise

> High Output Power

> Small Size Surface Mount Package

> Vcc: 5 volts

> Future models up to 30 GHz

Talk To Us About Your Custom Requirements.

SYNERGY®
MICROWAVE CORPORATION

Phone: (973) 881-8800 | Fax: (973) 881-8361
E-mail: sales@synergymwave.com | Web: www.synergymwave.com
Mail: 201 McLean Boulevard, Paterson, NJ 07504

Around the **Circuit**

Leonardo announced that they have been selected by the **U.K.'s Royal Air Force (RAF)** to support the next stage of their research and development program. The study will explore the current threat posed by hostile drones and how this is likely to evolve in future, as well as evaluating a range of technologies that could form a future RAF counter-drone capability. The program is expected to last three years and will commence in early 2020. The threat of rogue drones has been well-publicized in recent months, with small, affordable aircraft widely-available on the open market.

Trimble and **Qualcomm Technologies** have announced plans to work together to produce precise-positioning solutions for automotive applications. Trimble will work with Qualcomm Technologies to integrate its RTX technology with Qualcomm Snapdragon Automotive 4G and 5G platforms to deliver a highly accurate positioning solution essential for maintaining absolute in-lane positioning. This new solution will accelerate the adoption of road-level navigation and emergency services applications, as well as satisfy requirements for developing advanced driver-assistance systems (ADAS) and autonomous driving solutions. Qualcomm Technologies' Snapdragon 4G and 5G Automotive platforms feature integrated multi-frequency and multi-constellation high-precision GNSS technology.

Diamond Microwave Limited (DML) has announced a licensing deal with **Diamond Microwave Devices Ltd. (DMD)**. The deal allows DML to continue growing the commercial base for DMD's compact high-power microwave amplifiers, and to take DMD's proprietary technology into new markets. DML's commercial partnership with DMD will focus on the exploitation of the DMD amplifier technology in the global marketplace for high-power microwave systems. DML is a new U.K. company specializing in compact GaN-based high-power amplifiers, designed for application in demanding areas such as radar, communications and EW.

ACHIEVEMENTS

Rohde & Schwarz has carried out 5G NR protocol conformance testing with the new R&S CMX500 radio communication tester. Global Certification Forum GCF has accepted these 41 test cases, defined by 3GPP, in different FR1 and LTE band combinations. By adding the R&S CMX500 to their existing LTE test setups, accredited test houses, cell phone and chipset manufacturers get a smooth upgrade path from LTE to 5G NR testing. The 5G NR protocol conformance tests were presented at GCF's Conformance Agreement Group (CAG) meeting 59. These tests are vital for next-generation mobile communication technology.

WIN Semiconductors has celebrated its 20th foundation day. Since the start of production from its first factory in Taoyuan, Taiwan, WIN has grown faster than the compound semiconductor market and now operates three highly automated wafer fabs, employing nearly 3,000 people. The company has achieved sustained business growth through continuous investment in leading-edge III-V technologies, timely expansion of production capacity and flexible efficient manufacturing. These core competencies provide a competitive advantage for WIN's customers across a broad set of applications and end markets. Key to WIN's 20-year record of success is a portfolio of III-V technologies supporting diverse functions from RF and mmWave frequencies through light-wave applications.

Since its launch in 2017, **GlobalFoundries**' 45RFSOI platform has generated more than $1 billion in design win revenue from more than 20 clients for 5G/mmWave mobile and wireless infrastructure applications. GlobalFoundries (GF) announced this milestone at its annual Global Technology Conference (GTC). GF has a long history of high frequency RF wafer and module test development and implementation. GF's engagement model offers clients comprehensive package design, thermal and electrical modeling services in partnership with leading outsourced assembly and test companies. For example, GF's turnkey testing and packaging services can perform accurate phase measurements between antenna ports for phased array multi-RF channel designs of more than 64 antenna elements.

BAE Systems has completed the first phase of a program to transfer short-gate GaN MMIC technology developed by the U.S. Air Force to its Advanced Microwave Products (AMP) center in Nashua, N.H.; the effort now moves to the second phase. At the end of phase 2, this process will be available to designers through an open foundry service, making the technology available for government programs. The short-gate GaN process provides high efficiency and broad bandwidth that can be integrated into next-generation radar, EW and communications systems.

MCV Technologies Inc. DBA MCV Microwave announced that their Delaware facility, MCV Microwave East has passed the rigorous standards for quality management systems to earn certification to ISO standard 9001:2015 for the design and manufacture of advanced dielectric resonators, RF microwave filters, antennas, connectors and cable assemblies. MCV Microwave was also successfully audited and certified to the AS9100 Rev D standard. This certification is necessary for all aerospace industry suppliers to meet the International Aerospace Quality Group (IAQG) quality initiatives.

CONTRACTS

Raytheon will upgrade the Ballistic Missile Early Warning System (BMEWS) and Precision Acquisition Vehicle Entry Phased Array Warning System (PAVE PAWS) radars with solid-state T/R modules, receiving an **Air Force** contract worth $495 million, if fully exercised. Raytheon will produce 148 qualification units during the first phase of the program, followed by production of some 40,000 T/R modules for all five radar sites, including spares, out of band replacements at the Fylingdales Royal Air Force Station and sensitivity improvement units.

Around the **Circuit**

Lockheed Martin has been awarded a $281 million contract by the **U.S. Army** to develop the Sentinel A4 radar system. Sentinel A4 is a high performance modification of the Sentinel A3 (AN/MPQ-64A3) air and missile defense radar that will provide updates to improve the existing Sentinel capability against cruise missiles, UASs, rotary-wing and fixed-wing threats. The new Sentinel A4 radar will provide improved surveillance, detection and classification capabilities against current and emerging aerial threats in order to protect Army maneuver formations and high-value static assets like command and control nodes, tactical assembly areas and geopolitical centers.

CACI International Inc. announced that it has been awarded a five-year task order, with a ceiling value of nearly $70 million, to assist the **U.S. Navy** in assessing its weapons and integrated combat systems. Under this task order, CACI will provide engineering and information technology expertise, including combat systems acquisition readiness and performance assessment support, to the Naval Surface Warfare Center (NSWC) Corona Division. Awarded under the SeaPort-e contract vehicle, the task order represents continuing work for CACI. In the past year, as part of the Navy's "Clear Decks Initiative," CACI experts at the warfare center have made critical safety improvements to protect personnel during weapons testing.

Minneapolis-based **Humanetics Corp.** has entered into a $6 million cooperative research agreement with the **U.S. DoD**, under the Joint Warfighter Medical Research Program. The agreement funds advanced development of BIO 301, a unique orally administered medical countermeasure to protect warfighters from lethal radiation exposure. BIO 301 is being developed as a prophylactic medical countermeasure that can be taken by warfighters prior to potential exposure to lethal radiation. Currently, no drugs are approved by FDA for this use. The drug may also benefit first responders who must be prepared to address domestic events related to nuclear accidents or terrorism.

Comtech Telecommunications has received a contract valued at more than $1.8 million for Ku- and Ka-Band high-power traveling wave tube amplifiers (TWTA) for a trailer-based SATCOM ground system. Comtech Telecommunications received the contract through its subsidiary, **Comtech Xicom Technology**, a part of Comtech's Commercial Solutions segment. The order was received during the fourth quarter of fiscal 2019 and the amplifiers are expected to ship during the 2020 fiscal year. Comtech Xicom Technology has been providing long-term support for important military communications missions with its rugged and high performance TWTAs.

ZAF Energy Systems Inc. announced that it has been awarded a $1.4 million contract for a nickel-zinc (NiZn) battery system to support the **U.S. Air Force** Intercon-

tinental Ballistic Missile (ICBM) Ground Facility. ZAF's NiZn batteries are helping to meet customer demands for powerful, cost-effective and environmentally-friendly battery solutions and are uniquely positioned to respond quickly to power outages. The project, which will run for 24 months, is expected to result in a prototype stationary energy storage system capable of powering the silo's systems in the event of a power outage, and until standby generators can be started.

PEOPLE

▲ *Dr. William Conley*

Mercury Systems Inc. announced that **William Conley, Ph.D.**, will join the company as senior vice president and CTO, effective immediately. In this role, Conley will direct and accelerate Mercury's technology vision and leadership in innovative technology that provides state-of-the-art solutions to the aerospace and defense industry. Conley brings to Mercury a wealth of experience in research, development, weapon system acquisition, technology road mapping, strategy development & implementation and government. Prior to joining Mercury, he was a member of the Federal Senior Executive Service, serving as the director for EW in the Office of the Secretary of Defense.

▲ *Philip Knights*

RFMW announced that **Philip Knights** has joined their organization as business development manager–RF Power products, reporting directly to Mike Carroll, VP–Global Sales. Knights joins RFMW with more than 35 years' experience in RF design engineering, new business development, sales management and marketing. Knights has a demonstrated history of strong customer relationships, revenue growth and interpersonal skills in complex RF and microwave oriented organizations. Prior to RFMW, Knights served as an RF design engineer in multiple Plessey Semiconductor divisions and Powerwave UK, where he successfully authored and delivered white papers at well attended symposiums.

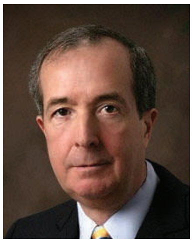

▲ *Thomas Marzetta*

NYU WIRELESS has appointed **Thomas Marzetta**—the originator of antenna technology that is enabling vast improvements in wireless communications—as director of the world-recognized research center at the NYU Tandon School of Engineering. He succeeds another researcher credited with seminal findings that underpin 5G: Theodore (Ted) S. Rappaport, who founded the research center in 2012. Before Rappaport published his 2013 paper, "Millimeter Wave Mobile Communications for 5G Cellular: It Will

Work," few experts acknowledged the possibilities of tapping that underutilized spectrum.

The **SOI Industry Consortium** has announced awards to two luminaries of the semiconductor industry: **Jim Cable**, chairman and CTO of **pSemi**, a Murata Company, and **Herb Huang**, CEO and GM of **Ningbo Semiconductor**. Both received awards for their contributions to the advancement of RF-SOI, a leading technology used extensively in chips for cellular communications. The awards were given during a gala following the SOI Consortium's annual RF-SOI Workshop in Shanghai. The Workshop, which was attended by over 450 industry leaders from China and around the world, is the largest of the SOI Consortium events.

REP APPOINTMENTS

PPM Systems, the U.K.-based division of **Pulse Power and Measurement Ltd. (PPM)**, will now be the seller of RF products from U.S. manufacturer **Corry Micronics**, in the U.K. The new partnership will see the addition of Corry Micronics' RF amplifiers, RF switches, switch matrixes, RF and microwave sub-systems added to PPM's existing portfolio of RF over fibre systems, antennas, software-defined radio (SDR) and more. Corry Micronics has its roots in the U.S. defence and security industries, the same sectors PPM has always been deeply committed to in the U.K. Its components are an ideal complement to PPM's suite of engineering services and products.

PLACES

Cree Inc. announced plans to establish a SiC corridor on the East Coast of the U.S., with the creation of the world's largest SiC fabrication facility. The company will build a brand new, state-of-the-art, automotive-qualified 200 mm power and RF wafer fabrication facility in Marcy, N.Y., complemented by its mega materials factory expansion currently underway at its Durham headquarters. The new fabrication facility, part of a previously announced project to dramatically increase capacity for its Wolfspeed SiC and GaN business, will be a bigger, highly-automated factory with greater output capability.

Altum RF announced the opening of its application support and sales office in Dallas, Texas. The office space is ideally situated in the Telecom Corridor, a technology business center in Richardson, Texas, an inner-suburb of Dallas. Altum RF is an international company, with strategic partnerships and office locations that span the globe.

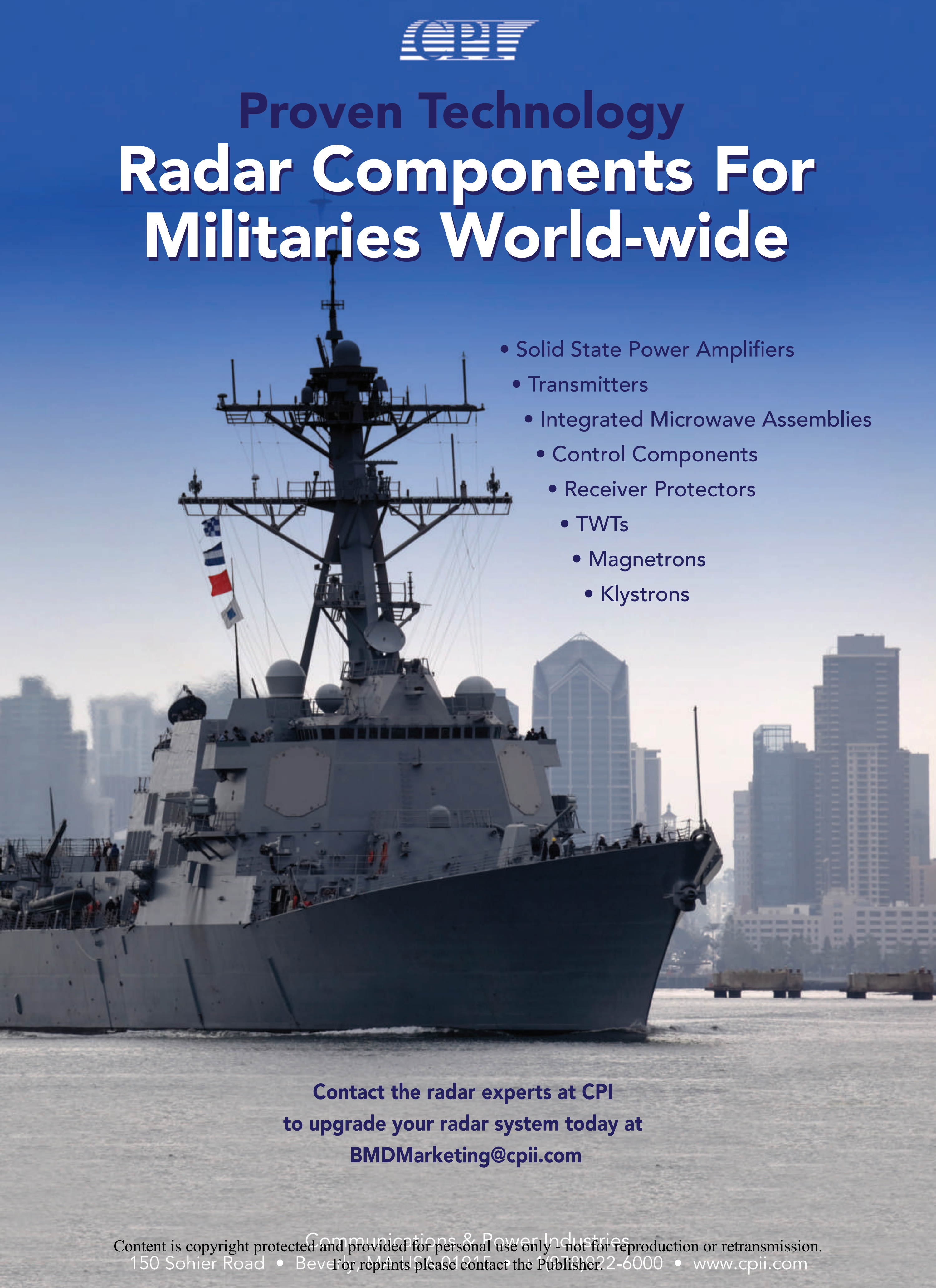
CPI
Proven Technology
Radar Components For Militaries World-wide
• Solid State Power Amplifiers
• Transmitters
• Integrated Microwave Assemblies
• Control Components
• Receiver Protectors
• TWTs
• Magnetrons
• Klystrons
Contact the radar experts at CPI
to upgrade your radar system today at
BMDMarketing@cpii.com
Communications & Power Industries
150 Sohier Road
www.cpii.com

Compact, Low Loss Switched Filter Bank Using MEMS Switches

Ian Burke
Menlo Microsystems Inc., Irvine, Calif.

Purna Subedi
3H Communications Systems Inc., Irvine, Calif.

RF MEMS switches combine extremely low loss and high power-handling in a unique SP4T configuration, which enables the creation of miniaturized and very high performance switched filter banks (SFB).

SFBs are becoming more and more common for both commercial and military applications with the proliferation of communications frequency bands and the deployment of more frequency-agile radios. Traditional SFBs that use semiconductor devices as the switching element to select discrete filters are increasingly preferred over their electromechanical counterparts. In some applications, however, the additional losses associated with semiconductor switches is prohibitive. This is problematic when considering that at least two switches are required, at both the input and output of the filter bank, which can drive losses from switching alone to 3 to 4 dB—or higher depending on the number of filter selections and the frequency range of operation. Such losses can create significant challenges for radio designers, especially in high-power applications where 3 dB corresponds to a significant amount of power dissipation (i.e., heat) that must be managed. Recently, RF MEMS switches have become available that combine extremely low loss and high power-handling capability in a unique SP4T configuration. This enables the creation of miniaturized and high performance SFBs. This article explores the underlying technology, design approach and resulting performance.

THE GROWING NEED

RF filters are some of the most mission critical components in any wireless communications system. Smaller and lighter weight RF filters are desired to meet the demand for smaller and more capable mobile wireless communication devices whether they are used in handheld radios such as cell phones; inside a drone, an airplane, a satellite; or even on mountaintop cell towers.

The degree of rejection needed from a filter is unique to each radio, whether it is to suppress spurs or mitigate interference. This creates the need for custom filters. The significant advantages of SFBs have resulted in their widespread use in diverse applications such as radar, electronic warfare, communications and test and measurement. SFBs combine switches and filters in a single module, where a switch at the input is followed by a filter for each channel and followed by a switch at the output (see ***Figure 1***).

SFBs have significant benefits compared to approaches in which discrete switches and filters are used. The most obvious is less board space and the ease of using a single integrated module. The modules contain all or most of the components required to perform the switching function, including a microcontroller, power management and amplifiers (if required).

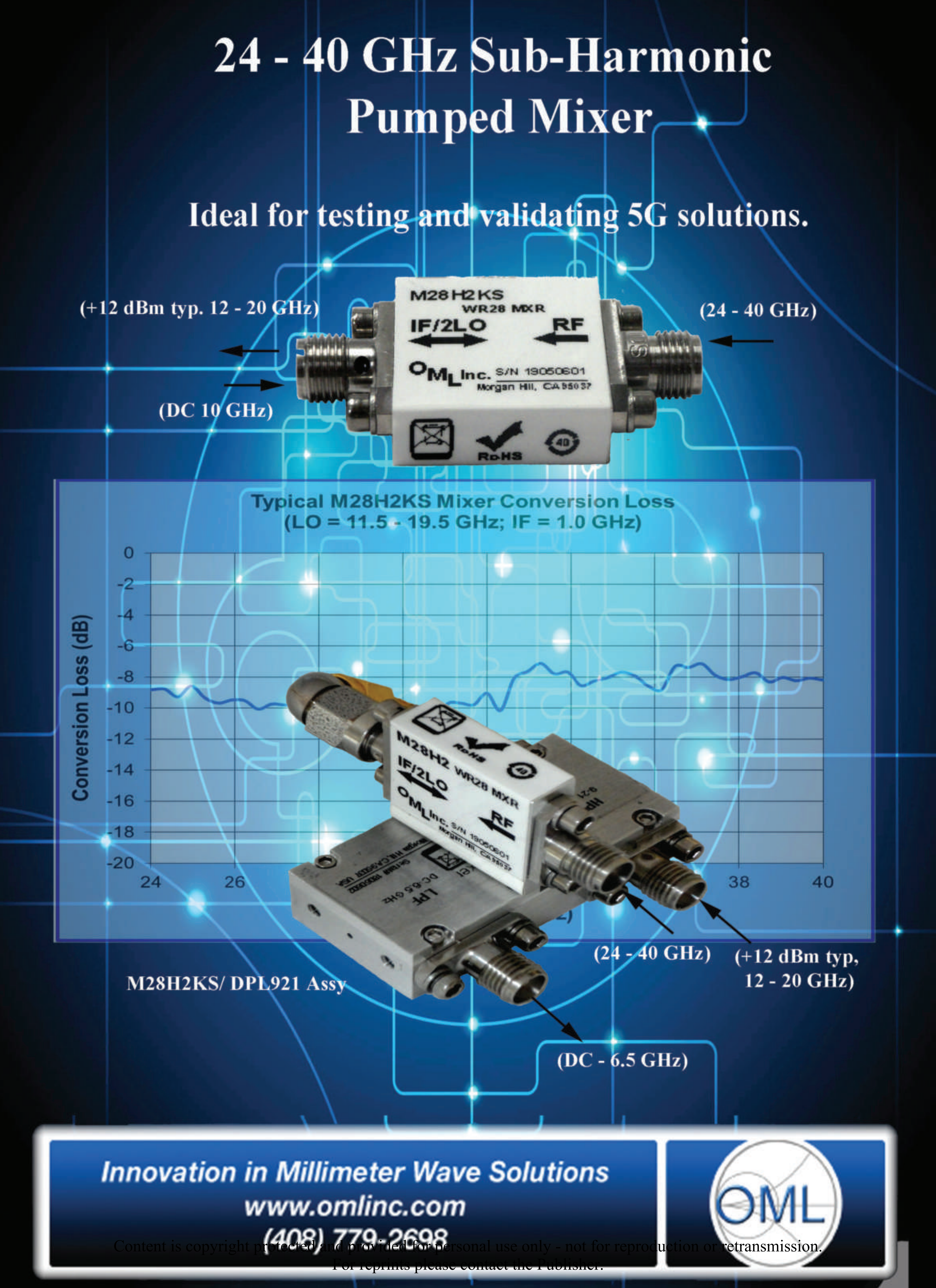
24 - 40 GHz Sub-Harmonic Pumped Mixer
Ideal for testing and validating 5G solutions.
(+12 dBm typ. 12 - 20 GHz)
(DC 10 GHz)
(24 - 40 GHz)
M28H2KS
WR28 MXR
IF/2LO
RF
OML Inc. S/N 19050601
Morgan Hill, CA 95037
RoHS
Typical M28H2KS Mixer Conversion Loss
(LO = 11.5 - 19.5 GHz; IF = 1.0 GHz)
Conversion Loss (dB)
0
-2
-4
-6
-8
-10
-12
-14
-16
-18
-20
24
26
38
40
(24 - 40 GHz)
(+12 dBm typ, 12 - 20 GHz)
M28H2KS/ DPL921 Assy
(DC - 6.5 GHz)
Innovation in Millimeter Wave Solutions
www.omlinc.com
(408) 779-2698
OML

An SFB also eliminates circuit transitions, which enables more precise impedance matching and lower insertion loss. Because the channels are internal to the module, better rejection and isolation are achieved. Any filter topology can be used based on the requirements of the application, including rejection, insertion loss and power handling.

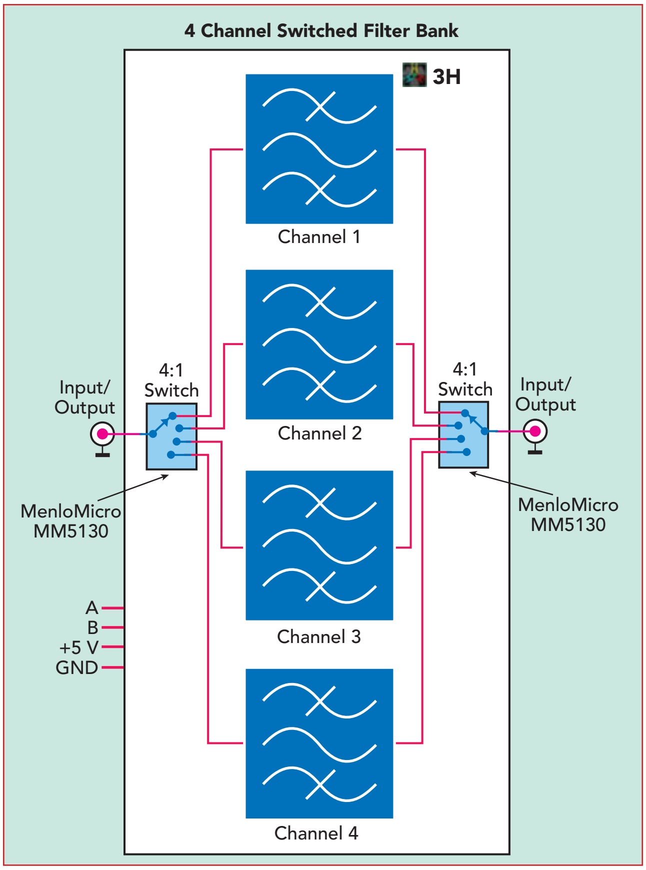

Fig. 1 Block diagram of a 4-channel switched filter bank.

In general, whether in the receive (Rx) or transmit (Tx) path, a key performance metric is insertion loss. To limit out-of-band interference, in receive, the SFB will usually be situated before any low noise amplifier; insertion loss from the SFB will contribute directly to the Rx system noise figure. In transmit, the SFB will be situated between the power amplifier (PA) and antenna to limit spurious and other interference from being radiated. Low insertion loss and high linearity are key to system performance; insertion loss determines radiated power, and linearity determines interference levels and receiver sensitivity. An example of a switched filter bank application is shown in ***Figure 2***.

RF MEMS SFB DESIGN

The four-channel blocking SFB shown in ***Figure 3*** uses two RF MEMS SP4T switches from Menlo Microsystems (MM5130) and four bandpass filters manufactured by 3H Communications Systems. The SFB contains all the components required to provide the drive voltages to turn on the switches, as well as a programmable microcontroller to control switching via either TTL or a PC application using USB control. The SFB measures 2.5 in. × 2.5 in. × 0.81 in. without connectors and weighs 6.5 oz. The specifications for the SFB are shown in ***Table 1***.

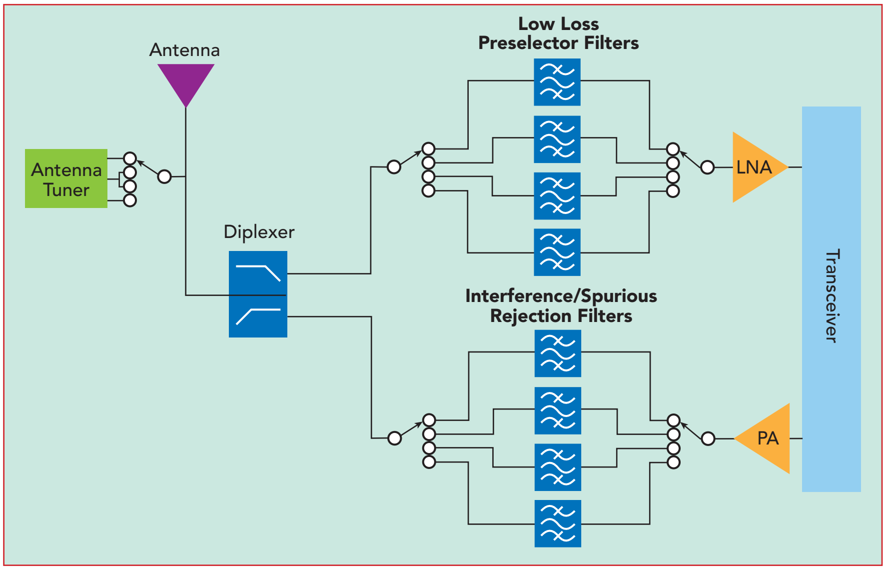

Fig. 2 Switched filter bank use case.

The RF MEMS switches are activated via electrostatic force, requiring a high-voltage source for switching. The gate bias of the switch is set at 0 VDC, which places the metal cantilever beam in a non-deflected (off) state. Thus, the path between RF input and output is isolated with an air gap, similar to a traditional mechanical relay. When the gate is set to its actuation voltage of +88 V, the electrostatic force between the gate and cantilever beam is strong enough to cause it to deflect downward, forming a connection with the contact and closing the switch. This is the deflected (on) state. For the purpose of this design, the +88 V for both SP4T switches is supplied by an Analog Devices LT3482 step-up DC/DC converter that can provide up to 90 VDC output with about 2 mA of current (see ***Figure 4***). Since the switches are electrostatic, requiring only nanoamps of current to operate, an entire switch matrix can be biased with a single boost circuit.

The output current of the LT3482 is converted to a filtered voltage through a fixed load resistor and bypass capacitor that is stable over the temperature range of the SFB. A Microchip HV513 8-channel high-

Fig. 3 Four-channel switched filter bank with four lumped element filters and two SP4T MEMS switches.

ENABLING THE 5G REVOLUTION

Our communication networks are in upheaval as the demand for ever greater data bandwidth has exhausted our current systems. New software defined radio systems leveraging our unique **Antenna Processor Units** promise to drive the next generation of communications.

for further inquiries contact sales@iqanalog.com

FULL SPECTRUM CONVERSION™ ANTENNA PROCESSORS

F1000 APU : F800 APU

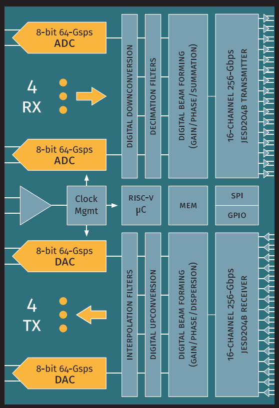

4x4 Transceiver
32-GHz Addressable Bandwidth

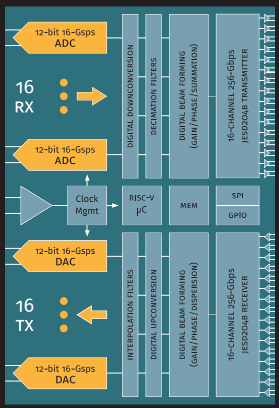

16x16 Transceiver
8-GHz Addressable Bandwidth

TABLE 1

RF MEMS-BASED SFB SPECIFICATIONS

Specification				
Band	1	2	3	4
Frequency Band (MHz)	740 to 1040	1676 to 2274	2970 to 3185	2525 to 2775
Insertion Loss (dB)	<2.7	<3.95	<5.2	<5.2
Rejection, Minimum (dBc)	>60	>60	>60	>60
Return Loss (dB)	>10	>10	>10	>10
Power Handling (W)	25			
Third-Order Intercept (dBm)	>85			
Control	TTL/USB			
Power Supply (VDC)	+5 V/USB			
Switching Time (us)	<10			
Current Consumption (mA)	65			
Size (mm)	63.5 (L) x 63.5 (W) x 12.7 (H)			
Operating Temperature (°C)	–40 to +85			
Vibration (10 to 500 Hz)	10G Mx			
Shock Duration	11 ms			

voltage driver routes the +88 V to each of the switch's four gate control pads. The input to the HV513 is managed by an Atmel ATSSAMD11 microcontroller, which can be controlled via USB or by direct +5 V TTL control. Other interface schemes can easily be implemented.

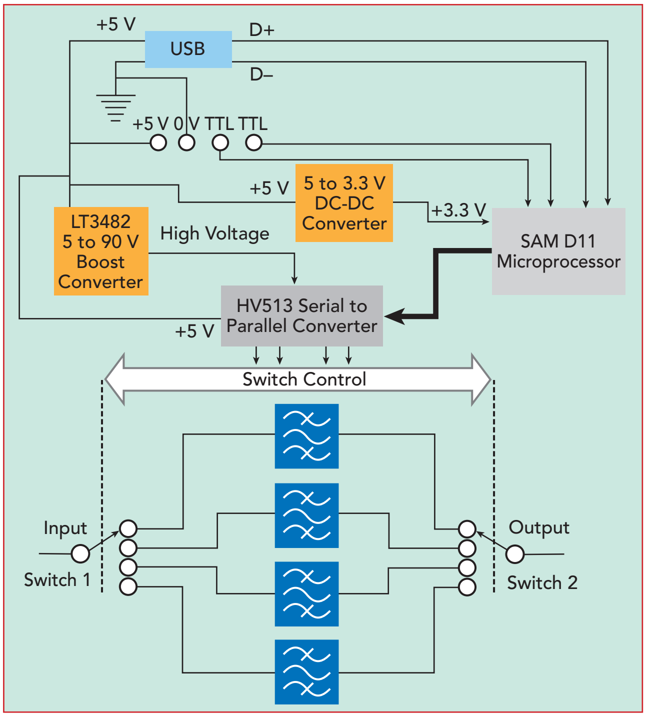

Fig. 4 MEMS SFB control circuit.

Layout

The input SMA connector routes the signal to the center of switch 1 (see ***Figure 5***). As the switch outputs are in the corners of the chip and need to maintain a ground-signal-ground (G-S-G) arrangement for best isolation, a grounded coplanar waveguide (GCPW) interconnection is used. This yields the best isolation while providing an optimum mounting configuration for the switch and bandpass filters. Two rows of vias are used on the ground sides of the GCPW that work to 18 GHz.

To avoid mismatch effects, sharp bends in the GCPW lines are avoided, with swept bends at least 3× the line width. As the board incorporates RF and DC components, the top layer is typically an RF material such as Rogers 4003C, especially for operation at higher frequencies; the other board layers are typically FR-4. In this design, which only operates to 4 GHz, Isola FR408HR is used for both an RF and DC substrate, since it is a more stable and high performance version of FR-4. 6 mil diameter micro-vias are used under the switch to

PERFORMANCE OVER TIME

You can’t trust the performance if you can’t trust the test!

You can’t afford to wonder if your cables are impacting your results. You expect your cables to be reliable. You need your cables to last.

But, with 75% of cables failing during installation or operation, your cable selection needs to be more than an afterthought. Choosing authentic GORE® Microwave/RF Test Assemblies is the only way to be sure your cables will stand up to the rigors of everyday use in demanding applications.

GORE® PHASEFLEX® Microwave/RF Test Assemblies – for proven performance, time and again. Learn what sets GORE® Microwave/RF Test Assemblies apart.

To learn more, visit www.gore.com/test

Together, improving life

GORE

ensure optimum ground and maintain GCPW into the device.

Design Considerations

Depending upon the end application, it is necessary to choose a filter technology and topology to meet the minimum requirements. In this case, the filter vendor uses a proprietary technique where the filter has more zeros than poles, as opposed to traditional filter theory which requires the maximum number of zeros to be one less than the number of poles (i.e., for a n-section filter, the maximum number of zeros would be n-1). This causes the filter skirts of the passband to roll sharply, since many more zeros can be placed. As a consequence, the greater number of transmission zeros enables significantly smaller filters. These small filters used with the miniaturized, high performance RF MEMS switches reduce the size of the SFB significantly. To customize a uniquely different frequency response for each filter band, a lumped element technology with discrete zeros was chosen.

PERFORMANCE

The insertion loss meets the target requirements and is slightly better than simulated (see ***Figure 6***). The RF MEMS switch for this application adds almost negligible

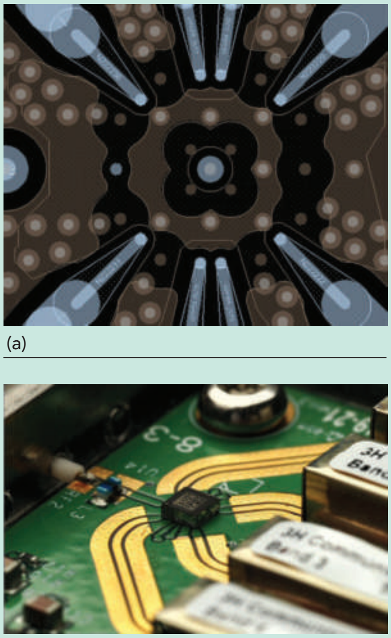

(a)

(b)

Fig. 5 SP4T RF MEMS switch layout (a) and zoom in of trace routing to the SFB (b).

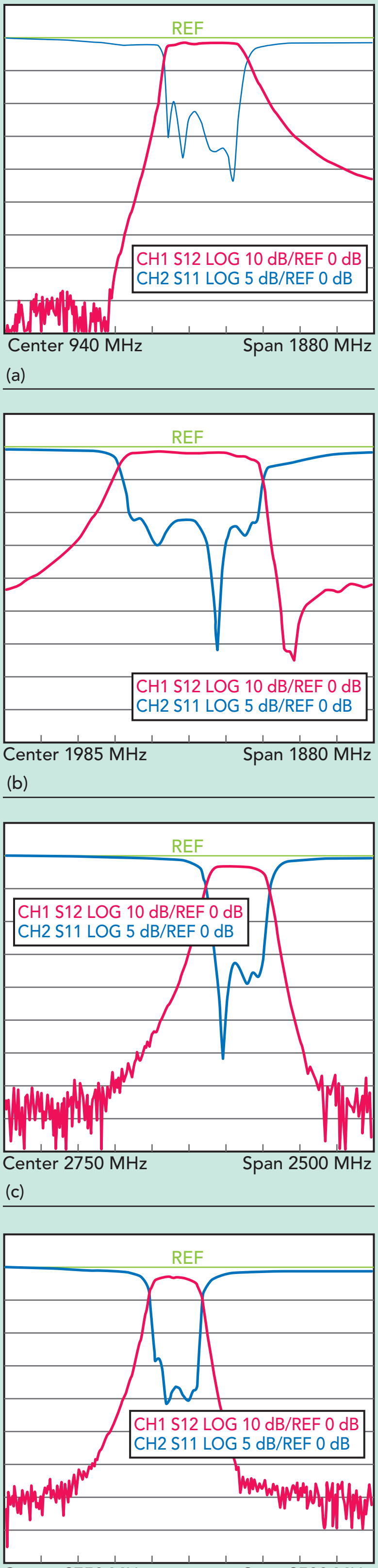

Fig. 6 Insertion loss and return loss for all 4 SFB bands: Band 1 (a), Band 2 (b), Band 3 (c), Band 4 (d).

TABLE 2

HIGH-POWER RF SWITCH PERFORMANCE

Specification	PIN Diode (2 Cascaded)	GaN (2 Cascaded SPDT)	RF MEMS (MM5130)
Input Power, CW (W)	100	20	25
Insertion Loss (dB)	2 x 0.5 = 1.0	2 x 0.7 = 1.4	0.15
Switching Speed	1.5 μs	0.05 μs	10 μs
Settling Time	N/A	0.15 μs	N/A
Return Loss	15	15	20
Isolation (dB)	35	25	30
Switching Cycles	Unlimited	Unlimited	>3 billion
Third-Order Intercept (dBm)	75	60	>85
Switch Dimensions (mm)	4 x 4 x 1.5	4 x 4 x 1.4	2.5 x 2.5 x 0.9

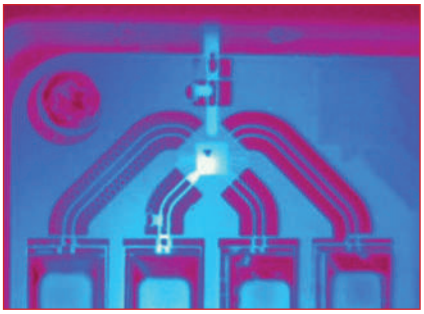

Fig. 7 Thermal profile of RF MEMS SFB under a 25 W CW load.

insertion loss to the overall SFB performance, using a much smaller and less complicated filter design than would normally be possible using solid-state switches.

The RF MEMS switch selected for this design exhibits a low insertion loss of 0.15 dB at 4 GHz and 0.75 dB at 12 GHz, a third-order intercept greater than 85 dBm and the capability to handle 25 W RF input power. Since it is configured as a native SP4T, there is no need to cascade switches, which can increase loss and, for high-power applications, the thermal load.

A comparison of the RF MEMS switch used in this design with traditional solid-state high-power switch technologies is shown in ***Table 2***. It is very challenging to find comparable SP4T monolithic switches that can handle greater than 20 W, so this comparison assumes the use of multiple cascaded SPDT high-power switches on both the input and output of the filters to create 1:4 multiplexing.

The RF MEMS switch used in this design is uniquely manufactured with high temperature electrodeposited metal alloys. This addresses a well-known problem experienced by many previous MEMS switches, where the switch actuator tends to deform over time and high temperature, reducing operating life. In this case, the electroplated metal alloy has a yield strength orders of magnitude greater than gold, which has been commonly used in the past for MEMS switch actuators. The results demonstrated in this SFB design show that these high temperature metal alloys are necessary to provide highly conductive and low loss signal paths and perform at elevated power levels, where some amount of self heating is inevitable. ***Figure 7*** shows a thermal image of the SFB, including the RF MEMS switch. Operating with a 10 W CW input, it exhibits only a 20°C temperature rise above ambient.

The low losses exhibited in this SFB compared to solid-state designs translate to a significantly smaller and lighter weight assembly, since heat sinks or more complicated thermal management can be reduced—even eliminated. As an example, for an SFB on the transmit path, where the radio needs to deliver 25 W to the antenna, a solid-state version would require the PA to generate an extra 2 to 2.5 dB of power into the SFB compared to the RF MEMS version. Not only does this add cost and complexity to the PA, it forces the designer to manage 10 to 14 W of extra heat in the radio.

SUMMARY AND DIRECTION

There are many ways to optimize the design. First, the high-voltage DC control section can be integrated into a single chip with minimal external passive components. There are many variants for high voltage drivers that can scale to 16, 32 or high-

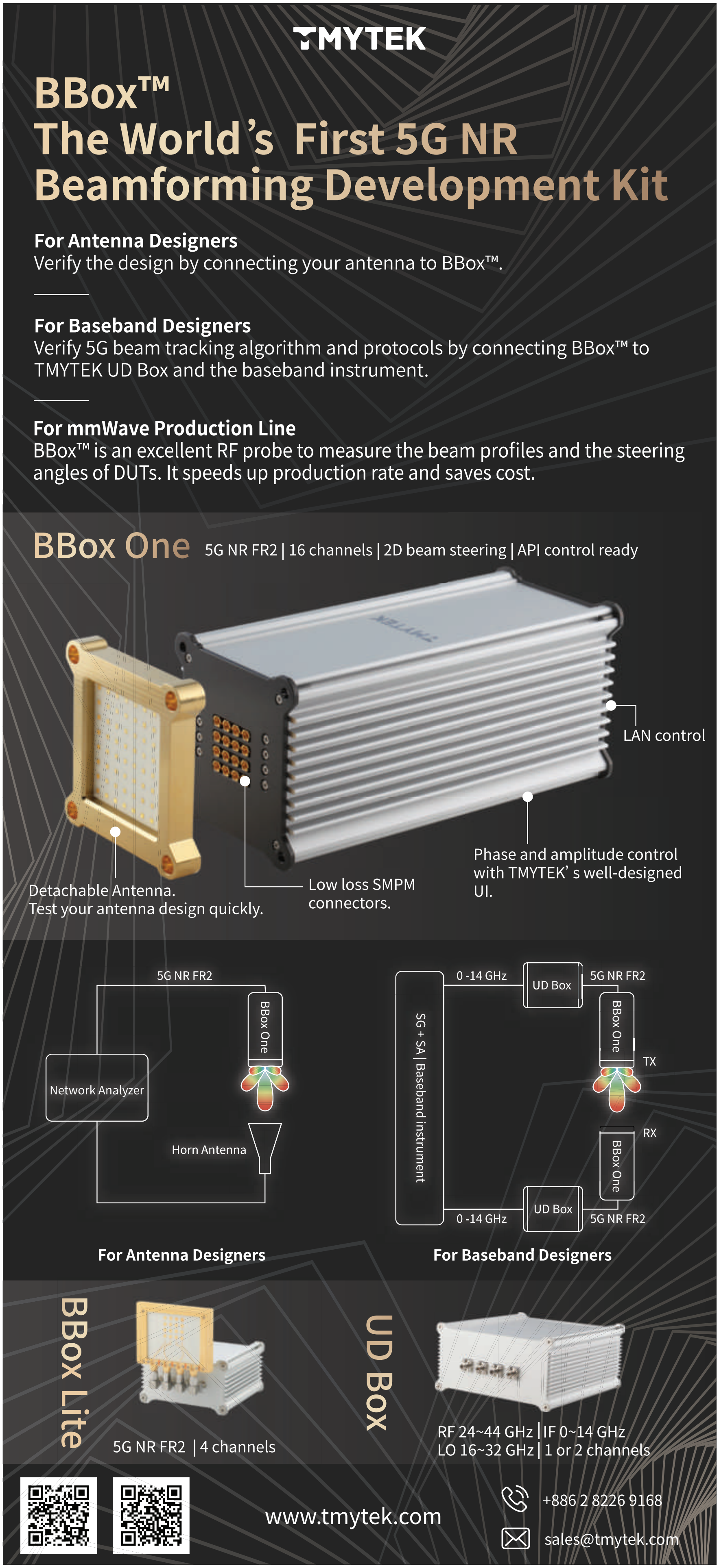

er channels for applications where there are multiple SFBs to control or SFBs with more than four channels.

Additionally, the design can easily be scaled to accommodate a different number of frequency bands (i.e., more channels) and higher frequencies. For example, the SFB in this article can be increased from four to eight channels with center frequencies from DC to 18 GHz with a small penalty in insertion loss and board space. The savings in power dissipation and insertion loss for the overall SFB becomes even greater compared to solid-state when adding more channels.

Finally, there are other ways to take advantage of the extremely low $R_{on}C_{off}$ characteristics of an RF MEMS switch. The on-resistance (R_{on}) of the metal-to-metal contact is very small, typically less than 0.5 Ω, which provides the lowest possible insertion loss. The switch also has very low levels of parasitic capacitance in the off-state (C_{off}), typically less than 15 fF, providing very low signal leakage when open. These unique characteristics provide opportunities where the switch can be used to select different resonators and "actively tune" a resonator to different frequency bands, employing one or multiple switch channels to connect series or shunt elements to the resonator. This type of tunable filter is extremely challenging using solid-state switches, given the non-ideal "on" and "off" characteristics of a transistor. This is especially true for high-voltage and high-power applications that stack transistors, which can significantly degrade the resonator Q-factor. Using RF MEMS for tuning enables further reduction in space over a straight SFB while maintaining very high Q.

Designers have a variety of choices when choosing an SFB. Most of the filter characteristics are determined by the switching element as well as the filter response required by the application. The RF MEMS switch is a new entrant in this market. Owing to its inherently superior electrical characteristics, it provides an appealing alternative for many RF subsystems, especially those where reducing the SWaP are mission critical.■

INVITED PAPER

Removing MMIC Outliers in Production Test Using Real-Time Principal Component Analysis

Grace Remillard**, Charles Trantanella* and Michael Megan*
Custom MMIC, Chelmsford, Mass.*
*University of Massachusetts-Lowell**, Lowell, Mass.*

Many electrical components have wide performance specifications to allow for high yield in production testing. Such an approach, however, comes at a cost. The problem is the outliers, the out-of-family components which pass the electrical specifications but are noticeably different from the rest of the population. These outliers, which represent anywhere from 0 to 4 percent or so of the passing units (depending on the specific definition of an outlier), can often be identified when the data is analyzed in its entirety, post measurement. However, at this point, it may be impossible to separate the outliers from the "pass" population, especially if the units have been placed in storage, such as on tape and reel. Therefore, a preferred approach is to identify and remove outliers in real-time during the production test.

Outlier detection of integrated circuits has been examined in the past as detailed by Stratigopoulos.[1] Here, the author presents a thorough discussion of outlier detection via machine learning, though the specifics of implementing a detection algorithm are not discussed. Others, such as Yilmaz,[2] have used outlier analysis to reduce the defective parts per million and the production test time. Jauhri[3] discussed the identification of outliers at the wafer level and used this information to unearth problems in the manufacturing process. Bossers[4] considered a univariant, real-time approach to detect outliers in production on a rolling basis, but under the assumption the units always followed a normal distribution. Finally, O'Neill[5] considered outlier detection using just one measured parameter, though this technique was intended for post-processing and not real-time.

Table 1 has a summary of this previous work. As shown in the table, the previous work does not adequately address outlier

TABLE 1

PCA ANALYSIS FOR OUTLIER DETECTION IN ICs

Reference	Packaged Circuits	Multivariant	Applied During Measurement	Applied on Production Floor
2	YES	YES	YES	NO
3	NO	YES	YES	Unsure
4	YES	NO	YES	NO
5	YES	YES	NO	NO
This Article	YES	YES	YES	YES

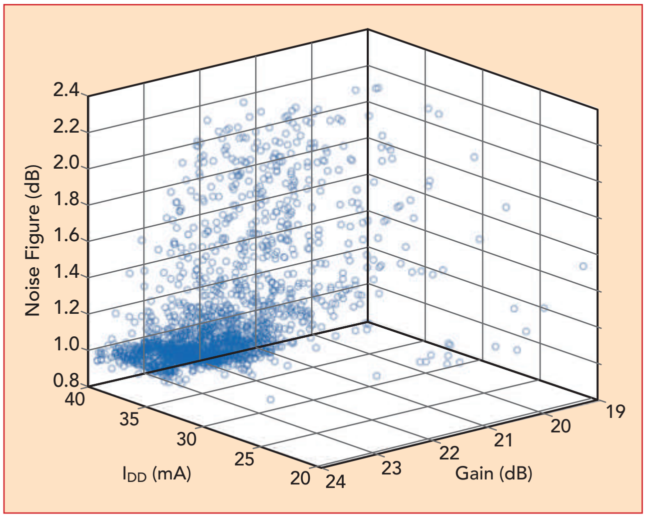

Fig. 1 **Gain vs. noise figure vs. I_{DD} for 2,139 CMD132P3 LNAs.**

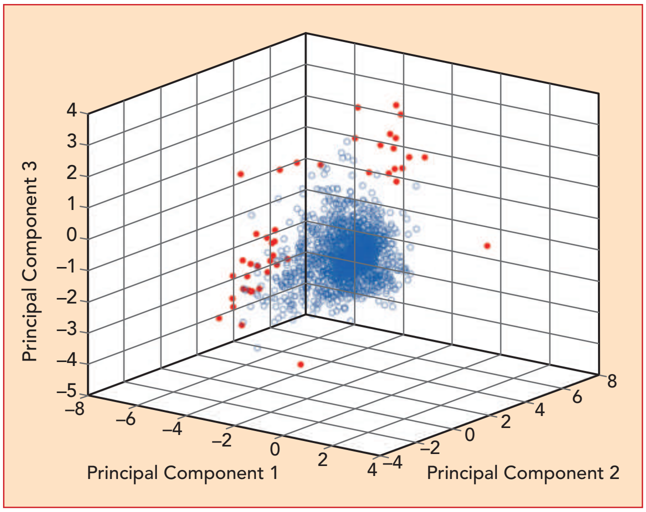

Fig. 2 **T-matrix scores for the LNAs from Fig. 1, showing the outliers in red.**

detection on the production floor. Therefore, this article presents a real-time method for outlier detection using principal component analysis (PCA), beginning by describing the theory behind PCA. Next, we deploy PCA in a post-processing role to examine its ability to detect outliers, then describe a real-time implementation of a PCA algorithm on the production floor, showing the results. Finally, we offer conclusions and plans for future work.

PCA AND OUTLIER DETECTION

PCA is a statistical method used to discover and quantify relationships between variables in a data set.[6-7] Consider a set of measurements, S, organized into an m × n matrix, where each of the m rows represents the measurement of one unit over n parameters.

For example, the CMD132P3, a commercially available low noise amplifier (LNA) from Custom MMIC, has n = 3 measured parameters: gain, noise figure and supply current (IDD). From experience, we know there is some correlation between these parameters: if the gain of the CMD132P3 is low, the noise figure may be higher than average; if the current is high, the gain may be high as well. But this correlation is not easily identified. ***Figure 1*** is a scatter plot of gain versus noise figure versus current for one lot of CMD132P3 LNAs (m = 2189 units). Each circle in the figure represents a unit that passed the electrical specifications. Note the data is not clustered tightly, instead spread over the acceptable range of the three parameters, making it difficult to discern the outliers. With PCA, however, we can quantify the relationship between the measured parameters and more easily discover the outliers.

The first step deploying PCA is to normalize the data in S and generate a new matrix, X. Normalization effectively removes the unit of measure from the data. Without this step, measurements that produce large numbers, such as an IDD of 35 mA, would completely overshadow smaller measured values, such as a noise figure of 1.5 dB, even though

ADVANCED SIMULATION MODELS

Accelerate RF Design Success for Mini-Circuits Components

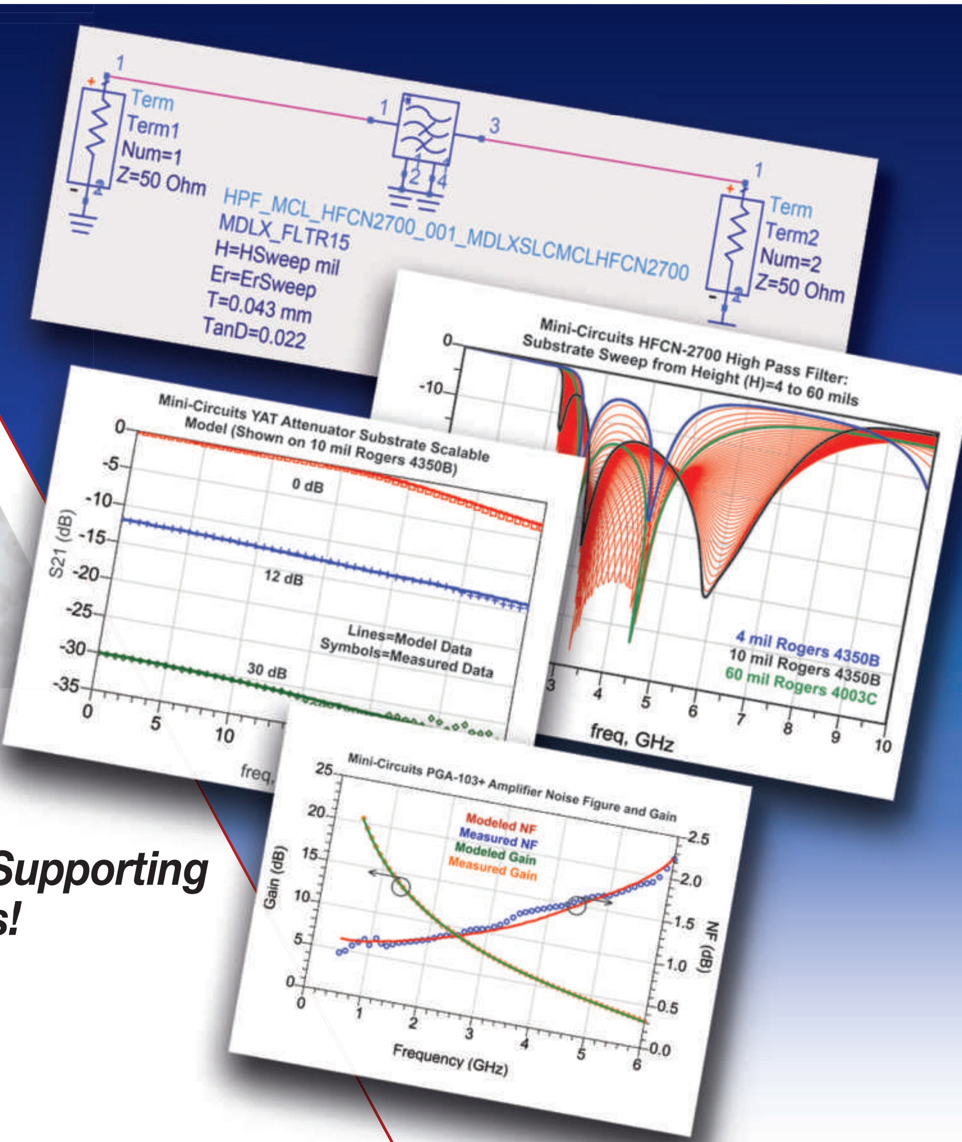

Now Over 50 Models Supporting Over 100 Components!

- *Attenuators*
- *Amplifiers*
- *Filters*
- *Splitters*
- *Transformers*

Download Free Models for PathWave ADS

www.modelithics.com/MVP/Mini-Circuits

Mini-Circuits® Modelithics® World's Best RF & Microwave Simulation Models

www.minicircuits.com P.O. Box 350166, Brooklyn, NY 11235-0003 (718) 934-4500 sales@minicircuits.com 617 RevOrig_P

TABLE 2
VARIABLE DEFINITIONS AND MATRIX SIZE

Variable	Description	Matrix Size
m	Total Number of Units Tested	—
n	Number of Measurements (i.e., Idd, Gain, Noise Figure)	—
S	Complete Set of Measured Data	m x n
S_k	Measured Data Vector for k^{th} Unit (k = 1…m)	1 x n
X	Complete Normalized Set of Measured Data	m x n
X_k	Normalized Data Vector for k^{th} Unit (k = 1…m)	1 x n
X*	Covariance Matrix	n x n
Y	PCA Coefficient Matrix (Ranked Eigenvectors of X*)	n x n
T	PCA Score Matrix	m x n
T_k	PCA Score Vector for k^{th} Unit (k = 1…m)	1 x n

each measurement is equally important. Normalization is accomplished through a straightforward calculation:

$$X_{ij} = \frac{S_{ij} - \overline{S_j}}{\sigma_j} \qquad (1)$$

Here, (i,j) is the row and column identifier of the elements in X and S, $\overline{S_j}$ is the mean of column j, and σ_j is the standard deviation of column j, where j = 1, 2, …, n, and i = 1, 2, …, m. The result of this normalization is each column of X now has zero mean and a standard deviation of 1. Once X has been generated, the covariance matrix, X*, is formed:

$$X^* = \mathrm{Cov}(X) = X^T X \qquad (2)$$

We then find the eigenvalues and eigenvectors of X* and sort the column eigenvectors by the highest to lowest eigenvalue, creating a new matrix, Y. The columns of this sorted matrix, Y, are referred to as the principal component axes. Formally, matrix Y is an orthonormal set of basis functions (i.e., principal components) onto which we can project the normalized measured data. Matrix Y is also called the PCA coefficient matrix. Once we have generated the coefficient matrix, Y, we determine the PCA score matrix, T, for the data set through a simple matrix multiplication:

$$T = XY \qquad (3)$$

Matrix T is an m × n matrix, the same size as the initial data set, S, and each row represents the projection of the normalized measured data onto the n orthogonal principal components. Outliers will generate high scores in their respective row of the matrix T, where normal or typical measurements will generate low scores. We can then set a maximum PCA score to remove the outliers from the population.

Figure 2 plots the elements of T from the CMD132P3 data set used to create Figure 1. The majority of the measured data is clumped around the (0,0,0) coordinate, and a number of outliers (shown in red) can clearly be seen on the fringes of the graph. For this example, the outliers were defined as having a PCA score greater than 7. Analyzing several different LNA data sets using this same approach, in all cases the T-matrix scores identified outliers in a similar manner. For reference, ***Table 2*** provides a summary of the variable definitions and their matrix sizes.

REAL-TIME PCA ALGORITHM

The approach used to generate Figure 2 followed a typical post-processing application of PCA, where the data set was processed as a whole after all measurements were complete. The implementation of PCA in a real-time environment, however, requires a slightly different approach. ***Figure 3*** shows a flowchart of a real-time PCA algorithm.

The first step in the algorithm is to load the PCA coefficient matrix,

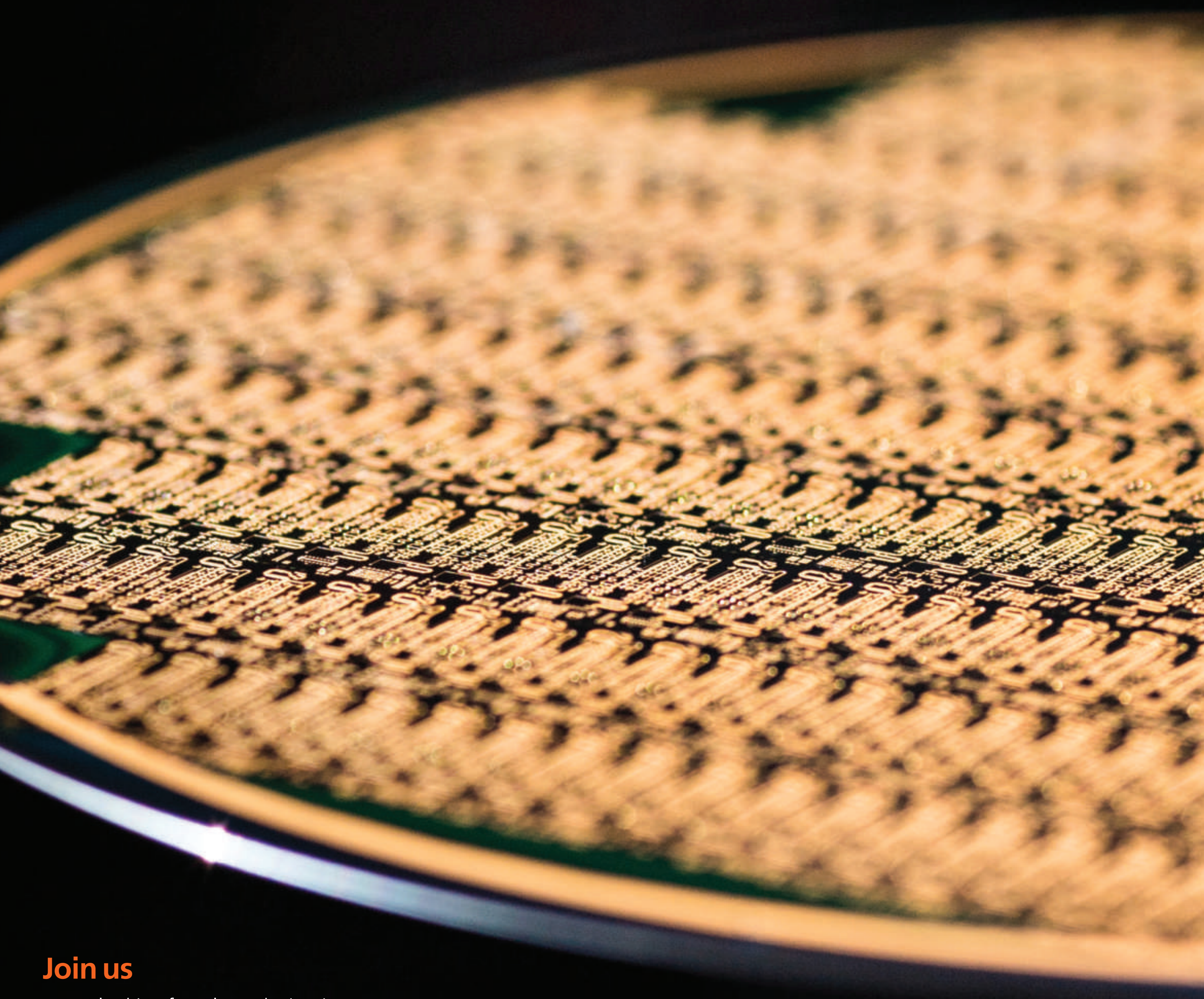

Y, into the automated test equipment. To determine Y, we discounted a real-time method, since the calculations to generate this matrix are computationally expensive and not conducive to a production environment. Instead, we used a series of previous measurements of the same LNA type to determine Y using the method described by Equations 1 through 3. For example, consider the CMD185P3 LNA with n = 3 (IDD, gain and noise figure). ***Figure 4*** shows the absolute value of each element in the Y-matrix as a function of the number of units in the calculation. Note that as the number of units increases, the coefficients begin to converge, especially the larger ones. While convergence is not universal, this result suggests that using a larger set of training data is preferred over a smaller set.

The second step in the algorithm is to run the production test until a fixed number of units pass the electrical specifications. Recall that Equation 1 requires statistics for each of the n parameters to perform the normalization, so an initial set of measurements is needed to generate these statistics. Note that the median instead of the mean is used in the normalization equation, as this approach led to slightly better identification of outliers. The size of the initial window is variable, so

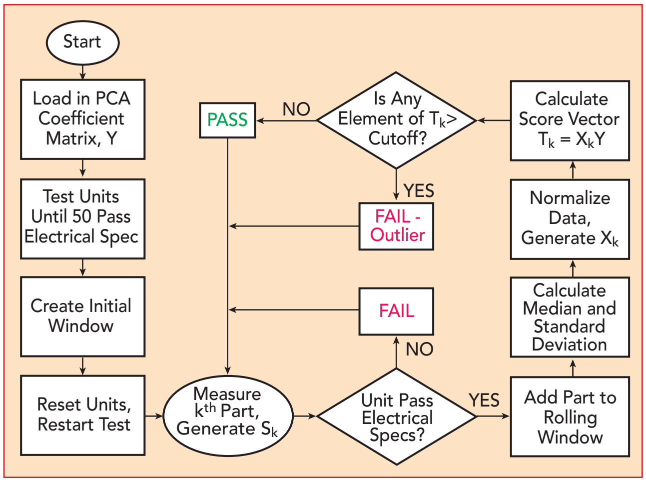

Fig. 3 PCA algorithm for real-time outlier removal at production test.

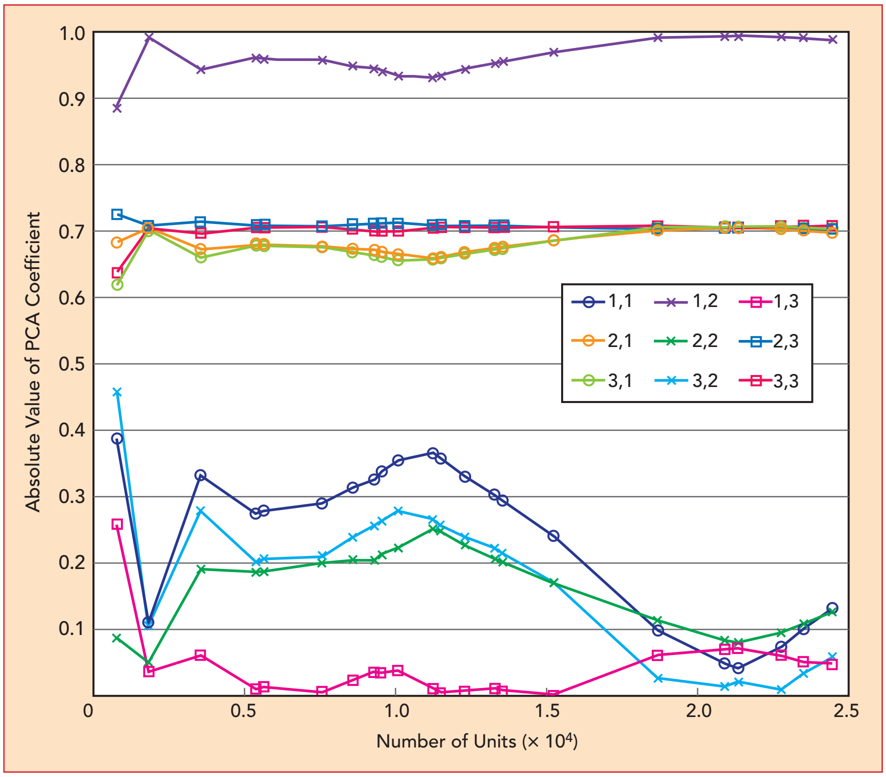

Fig. 4 Absolute value of the PCA coefficients for the CMD185P3 LNA. The legend shows the row, column entry of the Y-matrix.

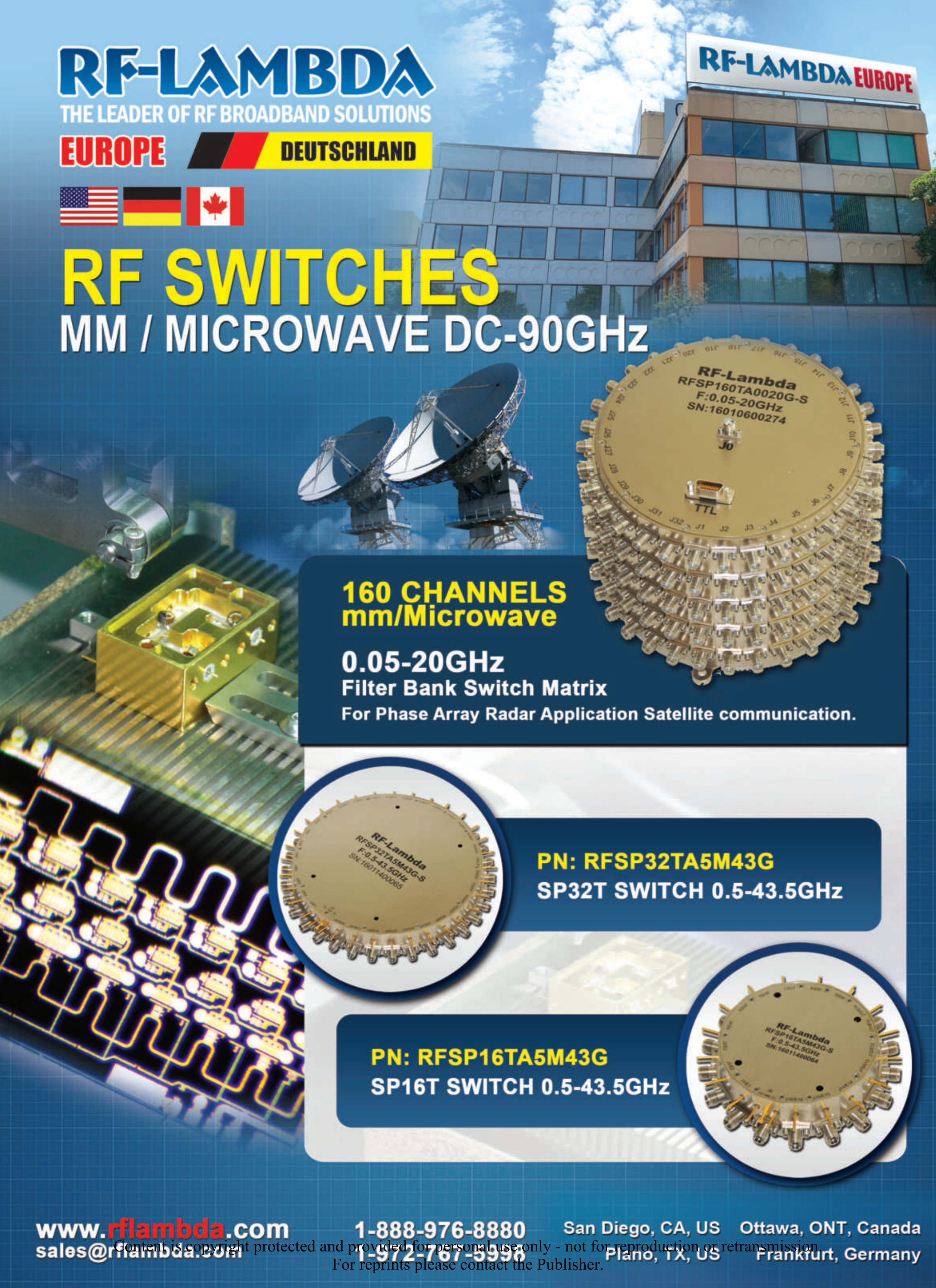
RF-LAMBDA
THE LEADER OF RF BROADBAND SOLUTIONS
EUROPE
DEUTSCHLAND
RF-LAMBDA EUROPE
RF SWITCHES
MM / MICROWAVE DC-90GHz
RF-Lambda
RFSP160TA0020G-S
F:0.05-20GHz
SN:16010600274
J0
TTL
160 CHANNELS
mm/Microwave
0.05-20GHz
Filter Bank Switch Matrix
For Phase Array Radar Application Satellite communication.
PN: RFSP32TA5M43G
SP32T SWITCH 0.5-43.5GHz
PN: RFSP16TA5M43G
SP16T SWITCH 0.5-43.5GHz
www.rflambda.com
sales@rflambda.com
1-888-976-8880
1-972-767-5998
San Diego, CA, US
Plano, TX, US
Ottawa, ONT, Canada
Frankfurt, Germany


SAGE Millimeter, Inc.
SAGE Millimeter will become Eravant in March 2020, a change that renews our commitment to the millimeter-wave industry. Since 2011, we have been delivering quality products and energizing the customer experience to respond to the next generation of RF engineers.
As we continue to grow into an industry leader, we want a new identity that reflects our vision for enabling tomorrow's technology. **Read more about our upcoming transformation at www.sagemillimeter.com.**
TTL IN
SAGE
GND
OUT
+5.0 V
-5.0 V
- 5.0 Vdc
SAGE Millimeter, Inc.
SWD-1040H-15-SB
S/N: 10000-01
D/C: 21/2016
www.sagemillimeter.com
www.sagemillimeter.com 3043 Kashiwa St. Torrance, CA 90505
T: 424-757-0168 F: 424-757-0188 sales@SAGEMillimeter.com

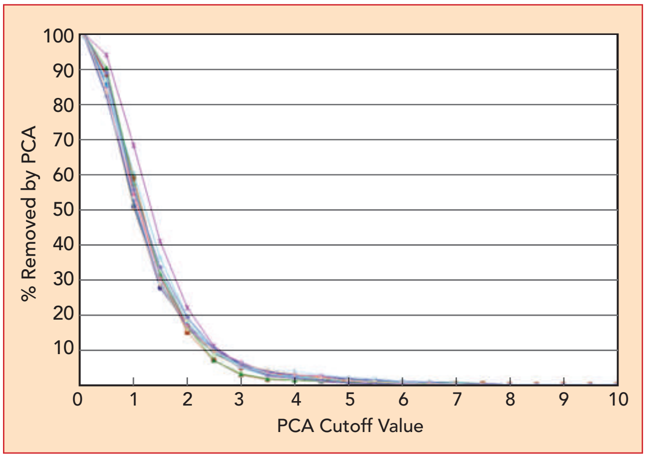

Fig. 5 Simulated percentage of LNAs removed by PCA vs. the cutoff value, using measured data from 16 lots of the CMD132P3 LNA.

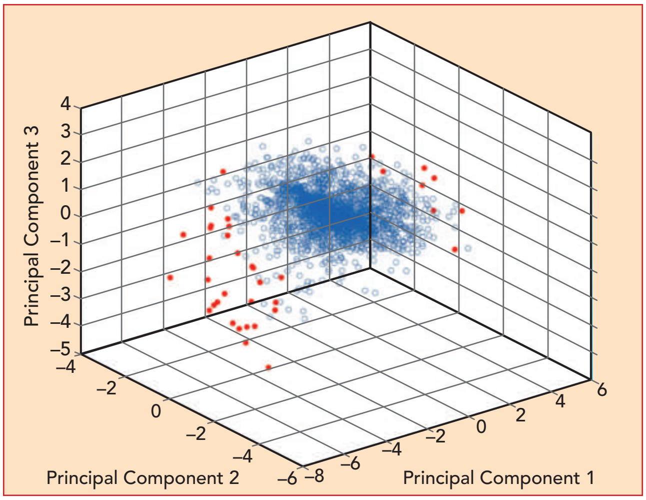

Fig. 6 Real-time Tk vector scores for each CMD185P3 LNA tested in production, with cutoff parameter scores > 4 shown in red.

after some experimentation, we chose 50 units as a compromise between having enough data to generate the statistics and not requiring an excessive amount of test time, since these units are returned to the untested population prior to outlier detection using PCA.

The third step is to restart the production test and apply PCA to each measurement. The k^{th} unit is measured, and if any values in the vector S_k fail their respective electrical specifications, the unit is placed in the "fail" bin without further analysis. If the unit passes electrical specifications, its performance is combined with the previous 49 passing units to determine a new median and standard deviation. By using a rolling window and computing a new median and standard deviation with each unit, the algorithm accounts for a slight drift with time in the measured data. The S_k vector is then normalized to generate X_k, which is multiplied by the Y-matrix to determine the T_k vector score. If any of the values in T_k are outside the PCA cutoff parameter, this unit is considered an outlier and is placed in the fail bin. Otherwise, the unit is placed in the pass bin, and the test moves to the next unit in the

New ATC 560L Ultra-Broadband UBC™ SMT Capacitors

Ultra-Broadband Performance from 16 KHz to 40+ GHz

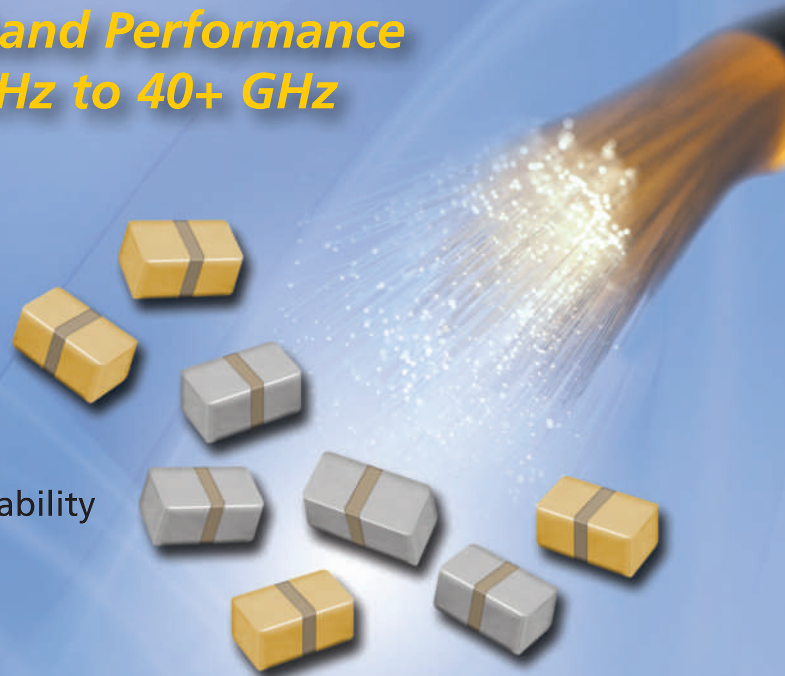

Advantages:

- Ultra-Broadband Performance
- Ultra-Low Insertion Loss
- Flat Frequency Response
- Excellent Return Loss
- Rugged Ceramic Construction
- Unit-to-Unit Performance Repeatability

Features:

- EIA 0402 Case Size
- Capacitance: 100 nF
- Operating Frequency: 16 KHz to 40+ GHz
- Insertion Loss: <0.6 dB typ.
- Orientation Insensitive
- One Piece Construction
- Voltage Rating: 16 WVDC
- Gold Complaint Terminations
- RoHS Compliant

Applications:

- Optoelectronics / High Speed Data
- Transimpedance Amplifiers
- ROSA / TOSA†
- SONET††
- Broadband Test Equipment
- Broadband Microwave Millimeter-wave

† Receive and Transmit Optical Sub-Assembly
†† Synchronous Optical Network

560L Insertion Loss (S21)

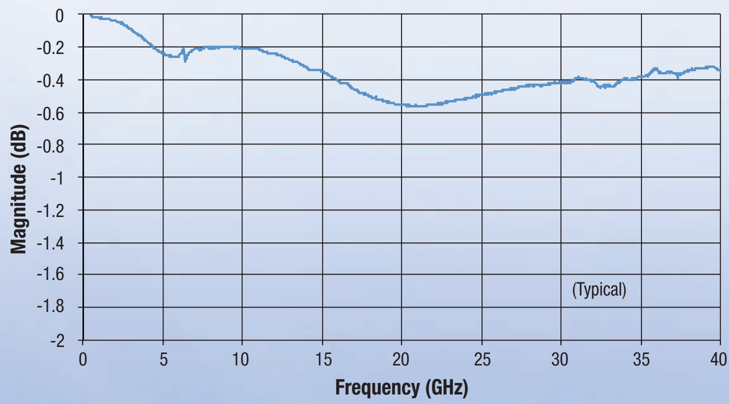

THE ENGINEERS' CHOICE®
ISO 9001 REGISTERED COMPANY

AMERICAN TECHNICAL CERAMICS
AN AVX GROUP COMPANY

RoHS Compliant

sequence. The algorithm is repeated until all units in the lot have been tested.

A major variable is the PCA cutoff parameter. A low cutoff removes too many parts, a high cutoff removes too few. To determine an appropriate value, several simulations were run using the algorithm of Figure 3, where the PCA cutoff parameter was varied to determine the number of outliers removed. ***Figure 5*** shows the results of one set of simulations involving 17 lots of data for the CMD132P3 LNA, where each lot contained 1000 to 5000 units. The plot shows the percentage of units removed as outliers versus the cutoff value, which was varied from 0 to 10.

Although not shown, very similar results were generated from simulations of other LNAs. Based on these simulations, we chose to implement a cutoff score of 4 in the real-time application of the algorithm, which should categorize approximately 1% to 3.5% of the units as outliers and place them in the fail bin.

ALGORITHM ON THE PRODUCTION FLOOR

The algorithm shown in Figure 3 was implemented during a recent production test of a lot of CMD185P3 LNAs containing 2575 units. Again, the measured parameters were gain, noise figure and I_{DD} (n = 3), and

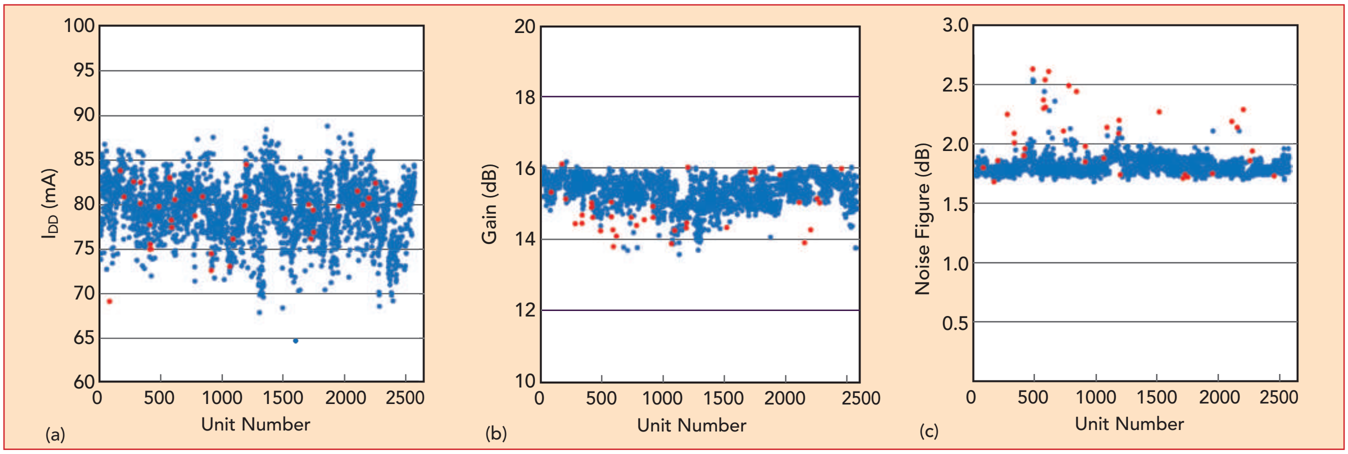

Fig. 7 **Measured I_{DD} (a), gain (b) and noise figure (c) of the CMD185P3 LNA, showing the outliers removed by the algorithm in red.**


CUSTOM DESIGNED
FOR YOUR
APPLICATION
Exceed Microwave's
custom designed WZ-Series
waveguide bandpass filters offer high
frequency selectivity with very low
insertion loss, while handling kWatts of
power for narrowband applications.
EXCEED
MICROWAVE
Phone +1 (424) 558-8341
sales@exceedmicrowave.com
www.exceedmicrowave.com
ITAR
AS 9120 Rev B
CERTIFIED
MADE IN USA
E[redacted]rowave
STAND[redacted]COMPONENTS
• Adapters
• Filters
• Circulators
• Diplexers
• Isolators
IN STOCK AT
HASCO Components
Phone +1 (888) 498-3242
sales@hasco-inc..com
www.hasco-inc.com

the window size was 50 and the PCA cutoff score set at four. ***Figure 6*** is a graph of the T_k vector scores for each unit, where the circles in blue represent a pass, while the red circles represent the units identified as outliers and sent to the fail bin. The algorithm failed 38 outliers and passed 2454 units, an outlier removal rate of 1.5%. An additional 83 units did not pass the electrical specifications and were ignored by the algorithm.

Figure 7 shows this data in a slightly different form: each of the measurements as a function of unit number using the same color scheme, i.e., blue represents a unit that passed and red an outlier that failed. The vast majority of units removed by the algorithm had higher than average noise figure, and many of those correlated with lower gain. The algorithm did not add any time to the production test.

CONCLUSION

We have described a real-time PCA algorithm deployed on the production floor to remove outliers from the testing of the CMD185P3 amplifiers. Of the LNAs meeting the electrical specifications, the algorithm identified 1.5 percent as outliers, which was consistent with the expectation, given the cutoff score of four. We are continuing to deploy this algorithm on the production floor with numerous LNAs as we work to refine the coefficient matrix, Y, and examine the cutoff score to more effectively remove outliers from the passing population. We are also working to deploy the algorithm on other MMICs, such as driver and power amplifiers, distributed amplifiers and switches.■

ACKNOWLEDGMENTS

The authors acknowledge the following for their contributions to this work: Dr. Kavitha Chandra of the University of Massachusetts-Lowell, for her guidance and introduction to PCA. This work would not have been successful without her help. Sarah McKinley and Emma Fournier of Custom MMIC helped run and improve the MATLAB simulations, and Helen Leung of Custom MMIC who deployed the algorithm on the production test equipment.

References

1. H. Stratigopoulos, "Machine Learning Applications in IC Testing," *23rd IEEE European Test Symposium*, 2018.
2. E. Yilmaz, S. Ozev and K. Butler, "Adaptive Multidimensional Outlier Analysis for Analog and Mixed Signal Circuits," *Proceedings of the 2011 IEEE International Test Conference*, 2011.
3. A. Jauhri, B. McDanel and C. Connor, "Outlier Detection for Large Scale Manufacturing Process," *IEEE International Conference on Big Data: Big Data 29*, 2015, pp. 2771–2774.
4. H. C. M. Bossers, J. L. Hurink and G. J. M. Smit, "Online Univariate Outlier Detection in Final Test: A Robust Rolling Horizon Approach," *Proceedings of the 16th IEEE European Test Symposium*, 2011, p. 201.
5. P. O'Neill, "Production Multivariate Outlier Detection Using Principal Components," *Proceedings of IEEE International Test Conference*, 2008.
6. B. Deschamp, "Analysis of Mammalian Cell Culture Data, Ph.D. Dissertation," *University of Massachusetts-Lowell*, 2018.
7. A. Nahar, R. Daasch and S. Subramaniam, "Burn-In Reduction Using Principal Component Analysis," *Proceedings of the IEEE International Conference on Test*, 2005.

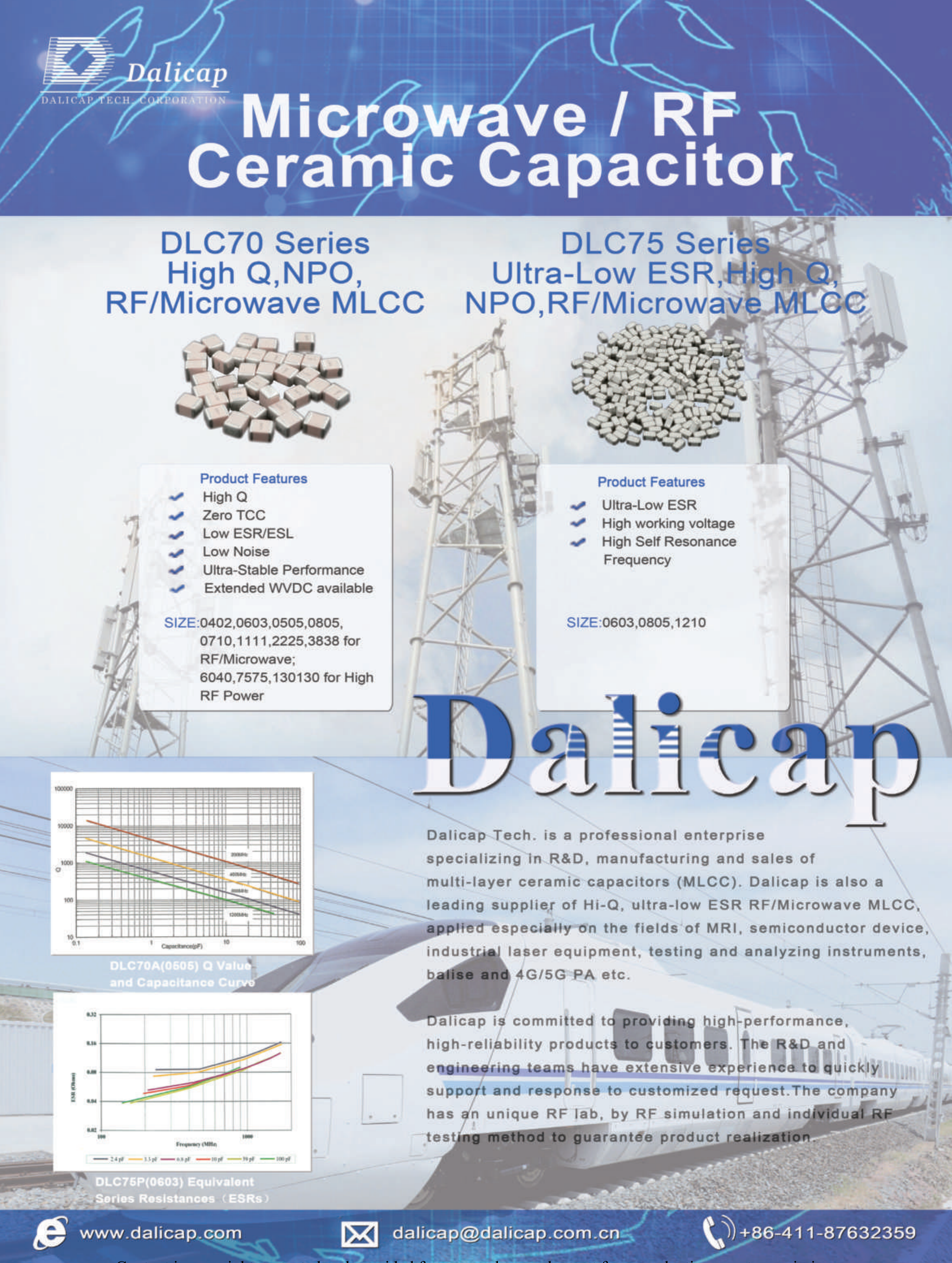
Dalicap
DALICAP TECH. CORPORATION
Microwave / RF
Ceramic Capacitor
DLC70 Series
High Q,NPO,
RF/Microwave MLCC
DLC75 Series
Ultra-Low ESR,High Q,
NPO,RF/Microwave MLCC
Product Features
High Q
Zero TCC
Low ESR/ESL
Low Noise
Ultra-Stable Performance
Extended WVDC available
SIZE:0402,0603,0505,0805,
0710,1111,2225,3838 for
RF/Microwave;
6040,7575,130130 for High
RF Power
Product Features
Ultra-Low ESR
High working voltage
High Self Resonance
Frequency
SIZE:0603,0805,1210
Dalicap
Dalicap Tech. is a professional enterprise specializing in R&D, manufacturing and sales of multi-layer ceramic capacitors (MLCC). Dalicap is also a leading supplier of Hi-Q, ultra-low ESR RF/Microwave MLCC, applied especially on the fields of MRI, semiconductor device, industrial laser equipment, testing and analyzing instruments, balise and 4G/5G PA etc.
Dalicap is committed to providing high-performance, high-reliability products to customers. The R&D and engineering teams have extensive experience to quickly support and response to customized request.The company has an unique RF lab, by RF simulation and individual RF testing method to guarantee product realization.
DLC70A(0505) Q Value
and Capacitance Curve
DLC75P(0603) Equivalent
Series Resistances（ESRs）
www.dalicap.com
dalicap@dalicap.com.cn
+86-411-87632359

INVITED PAPER

The Phase Noise Challenge Pacing the Race to 5G

Bill Linstrom, Ron Parrott and Allen Sweet
VIDA Products, Rohnert Park, Calif.

The wireless communication industry's move toward mmWave frequencies, driven by 5G cellular, is posing a challenge to existing oscillator technologies, particularly phase noise. New techniques and approaches may be required.

5G is pushing the state-of-the-art in virtually every area of cellular radio technology, including higher channel frequencies. To meet the most ambitious 5G goals, including peak data rates of 10 Gbps, cell edge data rates of 100 Mbps and 1 ms end-to-end latency, near-mmWave frequency bands above 20 GHz are needed in the U.S. One of the many challenges posed by near-mmWave frequencies is managing radio link noise and interference. In 1948, Claude Shannon showed that radio system capacity depends not only on the signal strength and bandwidth, but also on the radio link noise level.[1]

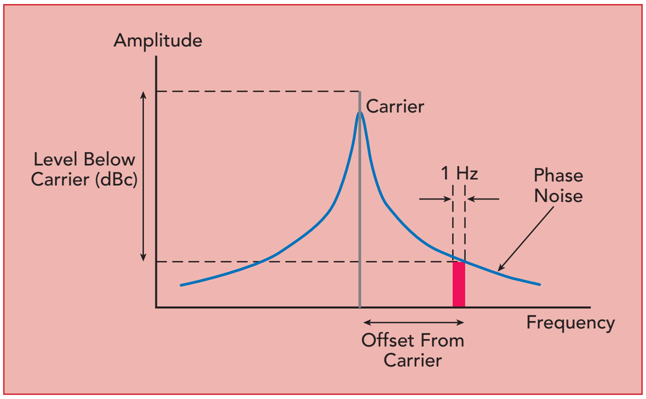

Fig. 1 Oscillator phase noise.

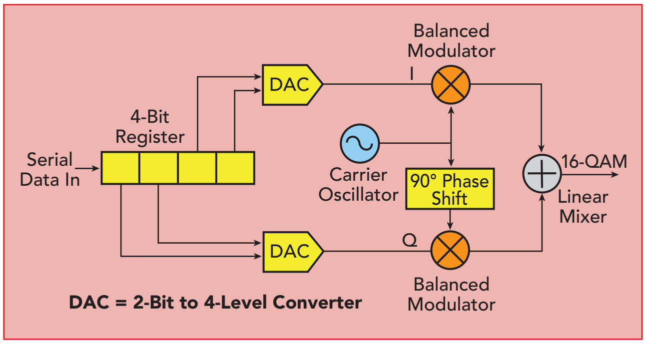

Fig. 2 Typical QAM (I/Q) modulator.

$$\text{Channel Capacity} = \text{Signal Bandwidth} * \log_2 \left(1+\frac{\text{Signal Power}}{\text{Noise Power}}\right) \quad (1)$$

Radio link noise has two broad sources: internal and external. External noise, also termed interference, is related to the environment, while internal noise is related to the radio system's electronic circuitry. The main interest of this article is the internal noise generated in the local oscillator (LO), i.e., the phase noise. From Shannon's Law, it is the key limiter of radio channel capacity. Quoting James Buckwalter, a professor at the University of California Santa Barbara, "Oscillator phase noise is a silent killer in interference limited systems."[2]

Oscillator phase noise is defined as the oscillator's short-term instability resulting in random fluctuation in the frequency or phase of its output (see ***Figure 1***). Phase noise is measured as the power spectral density for each 1 Hz frequency of a single sideband relative to the power spectral density of the oscillator's central frequency, in dBc/Hz. A well-known empirical model for phase noise, the Leeson equation was developed to describe and predict LC tank circuit phase noise performance.[3]

$$L_{(\Delta\omega)} = 10\log\left[\frac{2FkT}{P_{sig}}\cdot\left[1+\left(\frac{\omega_0}{2Q\Delta\omega}\right)^2\right]\cdot\left(1+\frac{\omega_1}{|\Delta\omega|}\right)\right] \quad (2)$$

In Leeson's equation, F is an empirically determined constant for curve fitting, k is Boltzmann's' constant, T is the absolute temperature in Kelvin, P_{sig} is the tank power dissipation, ω_0 is the oscillation frequency, Q is the loaded oscillator quality factor, $\Delta\omega$ is the offset from the oscillation frequency and ω_1 is the corner frequency between the 30 dB/decade and 20 dB/decade slope regions.

EFFECT OF LO PHASE NOISE

LO phase noise performance is critical to modern radio system performance, especially to high data rate orthogonal frequency division multiplexing (OFDM) systems.[4] OFDM is the data modulation technique used by most data transmission systems today, including LTE (4G cellular), Wi-Fi, cable and DSL networks. OFDM enables transmission systems to operate close to the Shannon theoretical capacity, overcoming frequency specific interference but susceptible to oscillator phase noise.

In an ideal OFDM modulator, the data stream is mixed with the ideal oscillator frequency (labeled carrier oscillator in ***Figure 2***) to produce ideal modulated symbols (see ***Figure 3a***). In real life, however, the LO generates the carrier frequency and additional close-in frequencies called additive phase noise. These frequencies, i.e., the carrier plus the additive phase noise, are mixed with the data to produce the modulated signal. The addition of the phase noise around the central carrier frequency

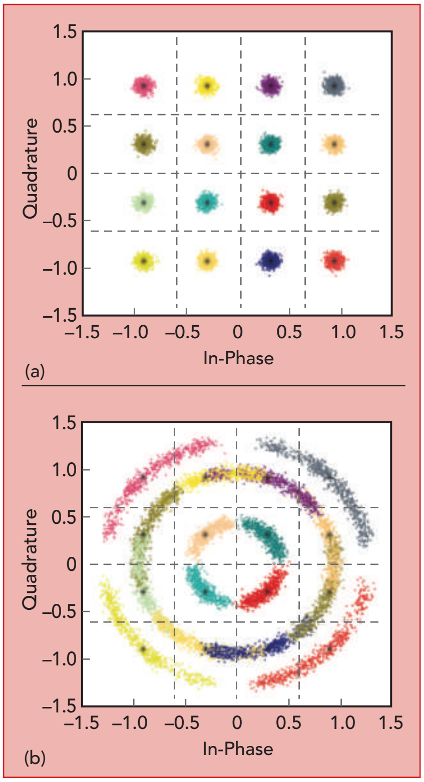

Fig. 3 I/Q constellation (a). If the inter-symbol interference is too high, accurate demodulation is impossible (b).

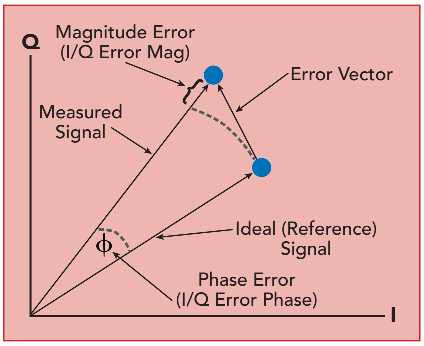

Fig. 4 Error vector magnitude.

Planar Monolithics Industries, Inc.

Integrated RF/Microwave Assemblies & Modules

PMI offers the highest quality multi-function modules and integrated microwave assemblies for industrial and military applications in frequency ranges up to 50 GHz. Built to your specifications with functions that include amplification, attenuation, filtering, switching, phase shifting, power detection, modulation, coupling, limiting and digital/analog control. PMI offers many other standard models with various options that are available at:
https://www.pmi-rf.com/categories/integrated-mic-mmic-assemblies

- Amplifiers
- Attenuators
- Bi-Phase Modulators
- Couplers
- Detectors - RF / Microwave
- DLVAs, ERDLVAs & SDLVAs
- Filters & Switched Filter Banks
- Form, Fit, Functional Products & Services
- Frequency Converters
- Frequency Sources
- Frequency Discriminators & IFM
- Frequency Synthesizers
- Gain & Loss Equalizers
- Integrated MIC/MMIC Assemblies
- IQ Vector Modulators
- Limiters - RF / Microwave
- Miscellaneous Products
- Monopulse Comparators
- Multifunction Integrated Assemblies
- Phase Shifters
- Power Dividers
- Rack & Chassis Mount Products
- Receiver Front Ends & Transceivers
- Single Side Band Modulators
- SMT & QFN Products
- Switch Matrices
- Switch Filter Banks
- Switches - Solid-State
- Systems - Radar Sense & Avoid
- Systems - Fly Eye Radar
- USB Style Product

3U Open VPX Transceiver

PTRAN-100M18G-S[redacted]
http://www.pmi-rf.com/mod[redacted]ah

- 100 MHz to 18.0 GHz [redacted]
- Integrated Up and Down Converters
- IF up to 4 GHz
- Time Gated SDLVA for Pulse Blanking
- -80 to -10 dBm Input D[redacted]
- Customizable Switched [redacted]
- 0 to +10 dBm Transmit Power
- 100 ns Switching Speed
- Fits into a 3U open VPX form factor utilizing the high speed VITA 67 RF connector.
- CW Immunity

Amplified RF Downconverter Modules

LCM-7R7G8R2G-CD-1 & LCM-16G100MBW-CD-1
https://www.pmi-rf.com/model-no-lcm-7r7g8r2g-cd-1
https://www.pmi-rf.com/model-no-lcm-16g100mbw-cd-1

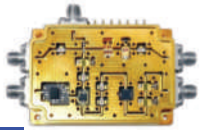

- Customized Frequency Ran[redacted]
  LCM-7R7G8R2G-CD-1: 7.7 to 8.2 GHz
  LCM-16G100MBW-CD-1: 16.0 GHz ± 50 MHz
- IF range of DC to 10 KHz
- Features a 20 dB voltage programmable attenuator and a 360° phase shifter.
- Designed for low spectral noise and high reverse isolation
- Slim line housing measuring only 2.5" x 1.75" x 0.4"

Phase and Amplitude Matched Integrated Modules in sets of four

PCAM-05G18G-INT-S5F
https://www.pmi-rf.com/product-details/pcam-05g18g-int-s5f

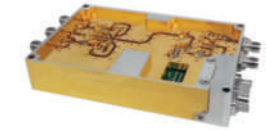

- Operating Frequency Range of 0.5 to 18.0 GHz.
- Built in sets of four, phase and amplitude matched to industry leading levels of ±10º and ±1.5 dB over the frequency range.
- Incorporates limiters, LNAs, switches, and variable digital attenuators.
- These units allow for high and low gain paths, a calibration input, and an auxiliary channel.
- A low noise figure and high output P1dB of +15 dBm are achieved by utilizing system analysis software and in-house hybrid/MIC processes.
- SMA Female connectors and small housing configuration.

Quad Phase and Amplitude Matched Diplexer Gain Module

DGM-18G40G-292FF-DS
https://www.pmi-rf.com/model-dgm-18g40g-292ff-ds

- Operating Frequency Range: 18.0 to 40 GHz.
- Switched output and an integrated power divider feeding the four antenna inputs via a 20 dB coupler for ease of system integration.
- Band select function not only switches bands, but allows the amplified bands not in use to be turned off to reduce power consumption.
- Designed to have better than 60 dB harmonic suppression.

CW immune EW Detector Modules

EWDM-2G8G-65-70MV & EWDM-8G18G-65-70MV
https://www.pmi-rf.com/product-details/ewdm-2g8g-65-70mv
https://www.pmi-rf.com/product-details/ewdm-8g18g-65-70mv

- Customized Frequency Ranges:
  EWDM-2G8G-65-70MV: 2.2 to 8.0 GHz
  EWDM-8G18G-65-70MV: 8.0 to 18 GHz
- Internal switch used to switch between the Bit IN and RF IN with input blanking on both ports.
- RF output port is provided with a gain of 33 dB minimum
- Video output is designed to drive a 150 ft. cable with input dynamic range of 65 dB & TSS of -71 dBm

Active, Filtered, Frequency Doubler Modules

PFDM-3R66R65-13-7R5DC-SFF
https://www.pmi-rf.com/active-filtered-frequency-doubler-module-3-6ghz-to-13-3[redacted]

- Frequency Range: Input: 3.6 - 6.65 GHz
  Output: 3.6 - 13.3 GHz
- Dual RF Output - TTL Switchable, Switching Speed: < 20 ns
- RF Output #1 to RF Output #2 Isolation: >35 dB
- Slim line housing measuring only 3.0" x 1.5" x 0.375"
- Other Frequency Ranges and Output Power Levels Available.

West Coast Operation:
4921 Robert J. Mathews Pkwy, Suite 1
El Dorado Hills, CA 95762 USA
Tel: 916-542-1401, Fax: 916-265-2597

East Coast Operation:
7311-F Grove Road
Frederick, MD 21704 USA
Tel: 301-662-5019, Fax: 301-662-1731

sales@pmi-rf.com • www.pmi-rf.com

ISO9001-2015 REGISTERED

TABLE 1
ERROR VECTOR MAGNITUDE REQUIREMENTS

Modulation	Max EVM (%)
QPSK	18.5
16-QAM	13.5
64-QAM	9.0
256-QAM	4.5

produces an error in the phase angle of the resulting symbol, called its error vector magnitude (EVM)[5], leading to a shift in the placement of the symbol in the constellation (see ***Figure 4***). Too great an error obscures the symbol, making demodulation questionable or impossible, as shown in Figure 3b.

The EVM, an expression of the symbol position in the decoded constellation relative to ideal, is an important specification that cellular system equipment must meet to qualify for commercial use[6] (see ***Table 1***). Symbol position errors, measured as EVM, have multiple causes. The most important source of vector error for high data rate OFDM radio communications is LO phase noise.[7] Symbol vector errors lead to inter-symbol interference, which is measured as symbol error rate. Symbol errors, which corrupt the data stream, slow the data rate by forcing some data to be resent, degrading link performance. In this way, LO phase noise degrades radio link performance.

Phase Noise Power

Total phase noise power is key to understanding the impact of oscillator phase noise on radio link performance. Shannon's Law says with the noise power equal to the signal power, the channel capacity is equal to the bandwidth of the broadcast signal, e.g., 1 Mbps for a 1 MHz broadcast bandwidth. It also says that with every reduction of noise power by a factor of 10 relative to the signal power, the channel capacity goes up by a factor of 3.3. If the noise power is 10 percent of the carrier's power, the channel capacity is 3.3× the bandwidth of the broadcast signal, e.g., 3.3 Mbps for a 1 MHz broadcast bandwidth. If the noise power is 1 percent of the carrier's power, the channel capacity is 6.6× the bandwidth and so on.

From Equation 2, the LC tank circuit oscillator phase noise power increases with the square of the frequency. For example, comparing the phase noise of 2 and 20 GHz VCOs (see ***Figure 5***), the total phase noise power for the 2 GHz VCO is −46 dBc, while the total phase noise power for the 20 GHz VCO is −27 dBc, 19 dBc higher. The results in the figure were calculated using a piecewise linear model assuming the phase-locked loop (PLL) is flat at −70 dBc in both cases. Considering only the phase noise power and not other interference sources, the calculated channel capacity of the system with the 2 GHz VCO and a signal bandwidth of 1 MHz is 15.3 Mbps, while the capacity of the system with the 20 GHz VCO and the same signal bandwidth is only

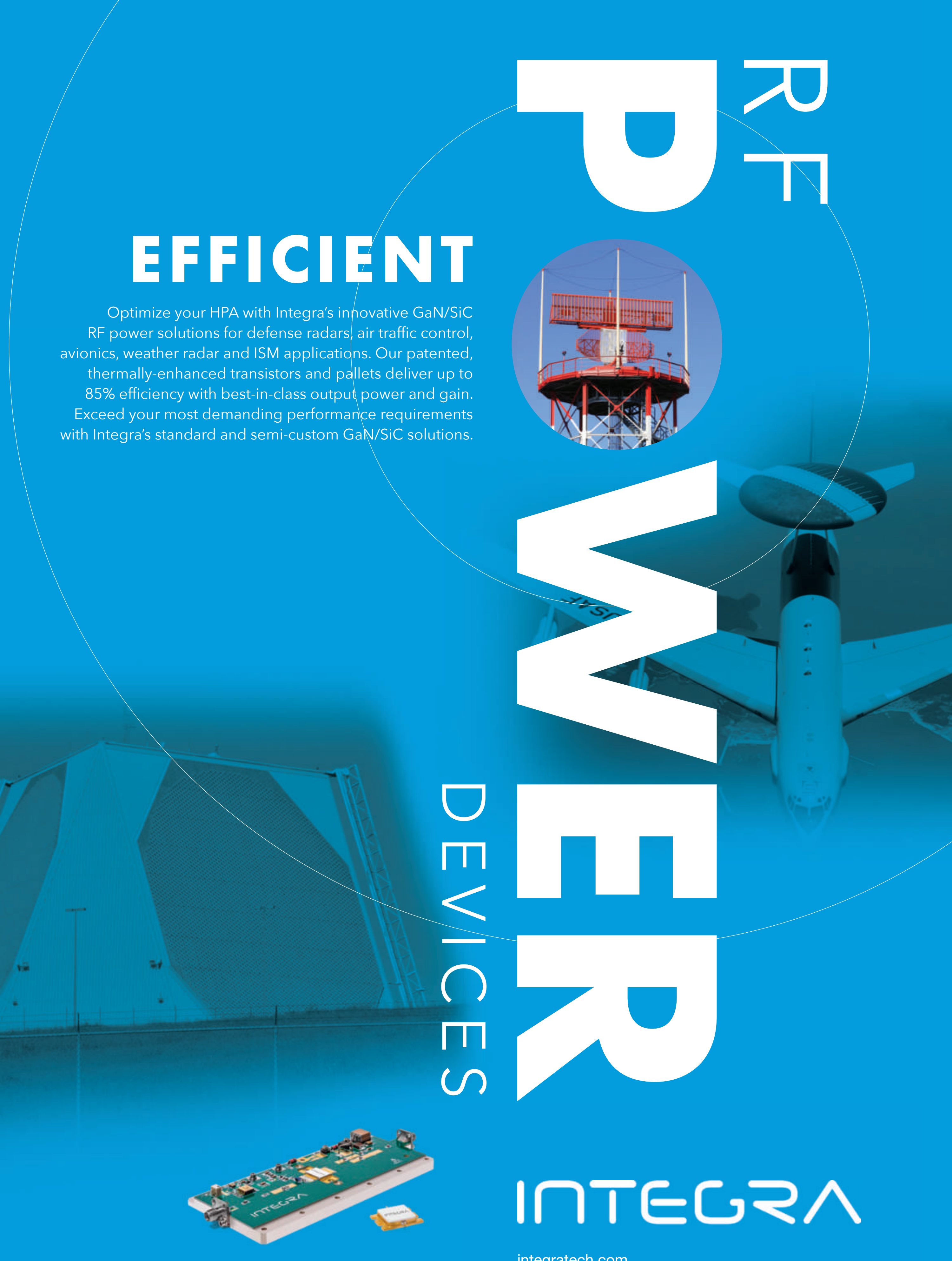
RF
POWER
DEVICES
EFFICIENT
Optimize your HPA with Integra's innovative GaN/SiC RF power solutions for defense radars, air traffic control, avionics, weather radar and ISM applications. Our patented, thermally-enhanced transistors and pallets deliver up to 85% efficiency with best-in-class output power and gain. Exceed your most demanding performance requirements with Integra's standard and semi-custom GaN/SiC solutions.
INTEGRA
integratech.com

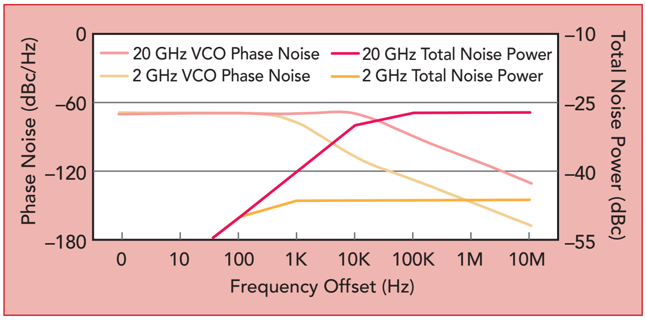

▲ Fig. 5 Phase noise and total noise power of 2 and 20 GHz VCOs.

9 Mbps, a 41 percent reduction in channel capacity (see ***Figure 6***). The reduced capacity is due to the significantly higher phase noise power of the 20 GHz VCO compared to the 2 GHz VCO, i.e., 19 dB or almost 80×.

Challenges at mmWave Frequencies

A fundamental question for 5G and other high modulation density radio systems is what oscillator technology to use. ***Figure 7*** illustrates today's available technologies: SAW, VCO, dielectric resonance oscillator (DRO) and YIG. Tunability is an important feature, as is phase noise. Today's commercially available VCOs, although tunable, suffer increased phase noise between 2 and 3 dBc per GHz, free running, based on publicly available data sheets for commercial VCOs. Phase locking with a PLL will improve noise performance, which is how VCOs are typically used in these applications. SAW oscillators have good phase noise performance, but they are not available above 6 GHz, nor are they tunable. Neither the VCOs nor SAW oscillators appear to be ideal for frequencies above 20 GHz. DROs perform better than VCOs above 20 GHz; however, they also are not tunable. The question of which oscillator technology is best for high bandwidth connections in the near-mmWave spectrum has not been answered. Significant research continues to focus on finding a solution, including exotic VCO/PLL architectures, advanced SAW oscillators, micro/chip-scale atomic clocks

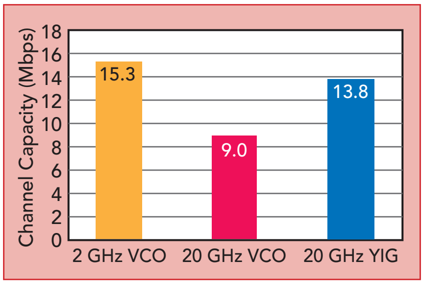

▲ Fig. 6 Oscillator channel capacity comparison at 1 MHz signal bandwidth.

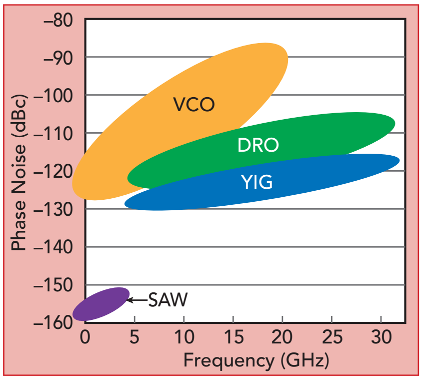

▲ Fig. 7 Oscillator technology phase noise vs. frequency at 100 kHz offset.


XILINX
ZYNQ

and YIG-tuned oscillators. As published in *Microwave Journal*, "The technical approach for supporting mmWave frequencies in handsets is being developed, but the technology is not as mature as for the sub-6 GHz bands."[8]

YIG Oscillators

Of the technological options to provide high quality frequency sources in the near-mmWave and mmWave frequencies, YIG may be a promising option. As background, YIG-tuned oscillators exploit the property that YIG RF permeability is variable, depending on the strength of the encompassing DC-biased magnetic field. The frequency at peak YIG RF permeability tracks the strength of the encompassing magnetic field linearly, at a rate of 2.8 MHz/gauss and is modeled as a parallel resonant inductor and capacitor (i.e., LC tank circuit), with the inductor value varying with the magnetic field strength. The peak YIG RF permeability frequency has very high Q (> 1000), resulting in low phase noise when the YIG is used as an oscillator tank circuit. While an electrically-coupled tank circuit depends on electron movement to realize the resonant frequency, a magnetically-coupled tank circuit depends on an oscillating magnetic field to couple energy in and out of the tank circuit at the resonant frequency of the tank. Instead of direct electron flow of the electrically connected tank, the magnetically connected tank operates as a transformer, inductively conducting energy between two electrically unconnected inductors.

Traditional YIG-tuned oscillators use a "negative resistance" topology to create a high performance oscillator. The negative resistance topology has been proven for decades and is optimized for power, size and performance. However, traditional YIG oscillator designs have not progressed significantly in more than 20 years, since Verticom introduced permanent magnet biasing in 1997.[9] In addition, with microformed wire loops hand-placed and hand-tuned, traditional YIG devices are inherently high cost, with manual assembly and tuning a barrier for high volume applications (see ***Figure 8***). YIG-tuned oscillator design is ripe for innovation.

Next-Generation YIG Oscillators

Next-generation YIG-tuned oscillators use an oscillator design integrated onto a custom MMIC to couple to the YIG resonator. This design approach enables high performance, increased functionality, low power, SMT packaging and low-cost. Although it has been tried repeatedly over the years, the neg-

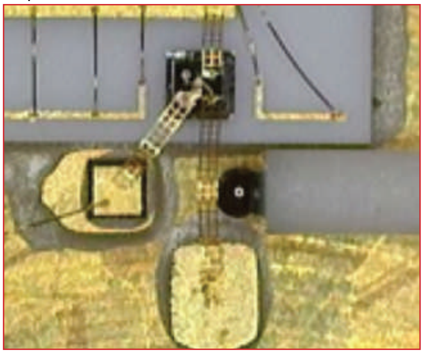

Fig. 8 Traditional YIG assembly.

ative resistance topology used for traditional YIG oscillators has never been successfully integrated onto an IC. This failure is due, in part, to the relatively low RF power in the circuit, requiring a long sense wire to couple the electromagnetic energy back and forth between the YIG and the negative resistance driver circuit. Next-generation YIG-tuned oscillators using a differential resonant ring topology[10,11] overcome the limitations of the negative resistance topology (see ***Figure 9***). By controlling the RF power of the YIG-tuned circuit and controlling parasitic reactances and magnetic interference modes, high performance, low power, small size and low-cost oscillators can be produced.

Critical elements of the design of the MMIC-based YIG oscillator include: assuring a uniform magnetic bias field, efficiently coupling the RF energy into and out of the YIG sphere, achieving 360 degree loop phase shift and managing stray magnetic fields from circuit conductors. The DC magnetic bias field is based on the proven combination of permanent and tunable electromagnets to minimize power and size. RF magnetic coupling is managed within the MMIC, where power levels and impedances are tightly managed with a combination of design elements and active control.

A key difference between the negative resistance and differential resonant ring architectures is the operational mode of the YIG sphere. In the negative resistance circuit, the YIG sphere is modeled as a magnetically-coupled parallel tank circuit. In the differential resonant ring architecture, the YIG sphere is used as a filter element, where only the energy at the tuned frequency is transmitted between the loops in the ring. Naturally, the design of the oscillator must conform to the basic tenants: the loop phase shift must be an integer multiplier of 360 degrees and the loop gain must be greater than 1 at the frequencies of interest.

The differential resonant ring MMIC architecture simplifies the oscillator magnetic design, greatly reducing stray electromagnetic flux. Reducing the stray flux has eliminated the need for the mitigations necessary with traditional YIG oscilla-

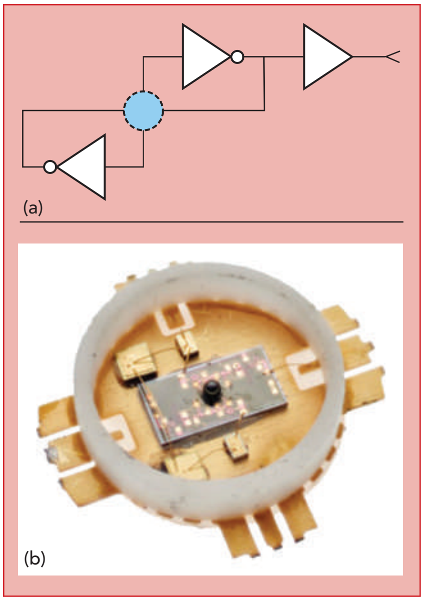

▲ Fig. 9 Differential resonant ring oscillator schematic (a) and early prototype (b).

tors, eliminating any need for hand tuning. A direct consequence of eliminating hand tuning is the ability to use advanced manufacturing assembly processes used for ICs and multi-chip modules. Next-generation YIG oscillators are designed to use this manufacturing flow to keep assembly costs low and yields high.

Beyond the basic improvements achieved with IC integration, next-generation YIG oscillators will offer additional features and functionality, capitalizing on Moore's Law. For example, with the differential resonant ring architecture, doubling the frequency is much simpler compared to traditional single-ended YIG oscillators, as well as dividing the frequency. Combining a new topology with IC manufacturing processes, the next-generation YIG oscillator can evolve into microwave and mmWave synthesizers on a chip.■

References

1. C. Shannon, "A Mathematical Theory of Communication," *The Bell System Technical Journal*, Vol. 27, No. 3 and 4, pp. 379-423, 623-656, July, October, 1948.
2. J. Buckwalter, "Reciprocal Mixing: The Trouble with Oscillators," [Online]. Available: www.ece.ucsb.edu/Faculty/rodwell/Classes/ece218c/notes/Lecture4_ReciprocalMixing.pdf. [Accessed 1 April 2019].
3. D. B. Leeson, A Simple Model of Feedback Oscillator Noise Spectrum, Vol. 54. No. 2, *Proceedings IEEE*, February 1966, pp. 329-330.
4. M. R. Khanzadi, " Phase Noise in Communication Systems Modeling, Compensation, and Performance Analysis," Chalmers University Technology, Göteborg, Sweden, 2015.
5. A. Georgiadis, "Gain, Phase Imbalance, and Phase Noise Effects on Error Vector Magnitude," *IEEE Transactions on Vehicular Technology*, Vol. 53, No. 2, pp. 443-449, March 2004.
6. European Telecommunications Standards Institute (ETSI), "5G," European Telecommunications Standards Institute (ETSI), [Online]. Available: https://www.etsi.org/technologies/5g. [Accessed 3 April 2019].
7. A. G. Armada, "Understanding the Effects of Phase Noise in Orthogonal Frequency Division Mulitplexing (OFDM)," *IEEE Transactions on Broadcasting*, Vol. 47, No. 2, pp. 153-159, 2001.
8. B. Thomas, "5G Brings New RF Challenges for Handsets," *Microwave Journal*, October 9, 2018. [Online]. Available: www.microwavejournal.com/articles/print/31177-g-brings-new-rf-challenges-for-handsets. [Accessed 21 3 2019].
9. Verticom, Inc. (1997). Microwave Ferrite Resonator with Parallel Permanent Magnet Bias. 5,677,652.
10. R. Parrott and A. A. Sweet, "A Wide band, Low Phase Noise Differential YIG Tuned Oscillator," WAMICON, pp. 1-3, June 2014.
11. M. van Delden, N. Pohl, K. Aufinger, C. Vaer and T. Musch, "A Low-Noise Transmission-Type Yttrium Iron Garnet Tuned Oscillator based on a SiGe MMIC and Bond-Coupling Opertating up to 48 GHz," *IEEE Transactions on Microwave Theory and Techniques*, Accepted but not yet published, 2019.

Design of a Broadband Harmonically-Tuned Power Amplifier with Gate-Source Parasitic Compensation

Zhiqun Cheng
Hangzhou Dianzi University, Hangzhou, China, Suzhou Institute of Nano-Tech and Nano-Bionics, Suzhou, China
Lei Xu, Guohua Liu and Han Feng
Hangzhou Dianzi University, Hangzhou, China
Steven Gao
University of Kent, Canterbury, U.K.

A 1.5 to 2.6 GHz broadband power amplifier (PA) based on a GaN HEMT is designed to achieve high-power and efficiency. The transistor's gate-source parasitic effect is reduced with a novel parasitic compensation circuit at the input. To achieve a broadband harmonic match and expand its bandwidth at the fundamental, radial microstrip theory is employed in a harmonic control network. The output power is between 43.4 and 45.6 dBm, and its drain efficiency is 65 to 76.9 percent from 1.5 to 2.6 GHz. Gain is above 10 dB. Second and third harmonic suppression levels are −15.6 to −26.1 and −19.4 to −40.5 dBc, respectively. The measured results are consistent with the simulation.

With the development of wireless communication technology, the need for higher data rates and correspondingly wider bandwidths is growing rapidly. At the RF transceiver, this puts a greater demand on the PA. As it consumes the most prime power, PA efficiency has a large impact on the operating budget of a communications system.

Traditional PAs, i.e., classes A, AB and B, are inefficient. To save energy and increase signal coverage, communication system PAs usually employ high efficiency and high output modes, such as classes D,[1] E,[2] F[3-5] and inverse class F.[6] They also leverage the excellent performance of third-generation semiconductor transistor technology, such as GaN HEMT.[7-8]

CLASS F PA ANALYSIS AND DESIGN

Since the PA operates in a large signal state, harmonics are inevitably generated, reducing output power and efficiency. Class F PAs, however, achieve good performance through harmonic control. The voltage and current waveforms at the transistor drain are shaped with a harmonic control network so the voltage waveform is a square wave, and the current waveform is a half sine wave. The waveforms of the drain voltage and current are expressed as

$$V(\theta) = V_{DD} + V_1 \sin\theta + \sum_{n=3.5.7}^{\infty} V_n \sin\theta \qquad (1)$$

$$I(\theta) = I_{dc} - I_1 \sin\theta - \sum_{n=2.4.6}^{\infty} I_n \cos\theta \qquad (2)$$

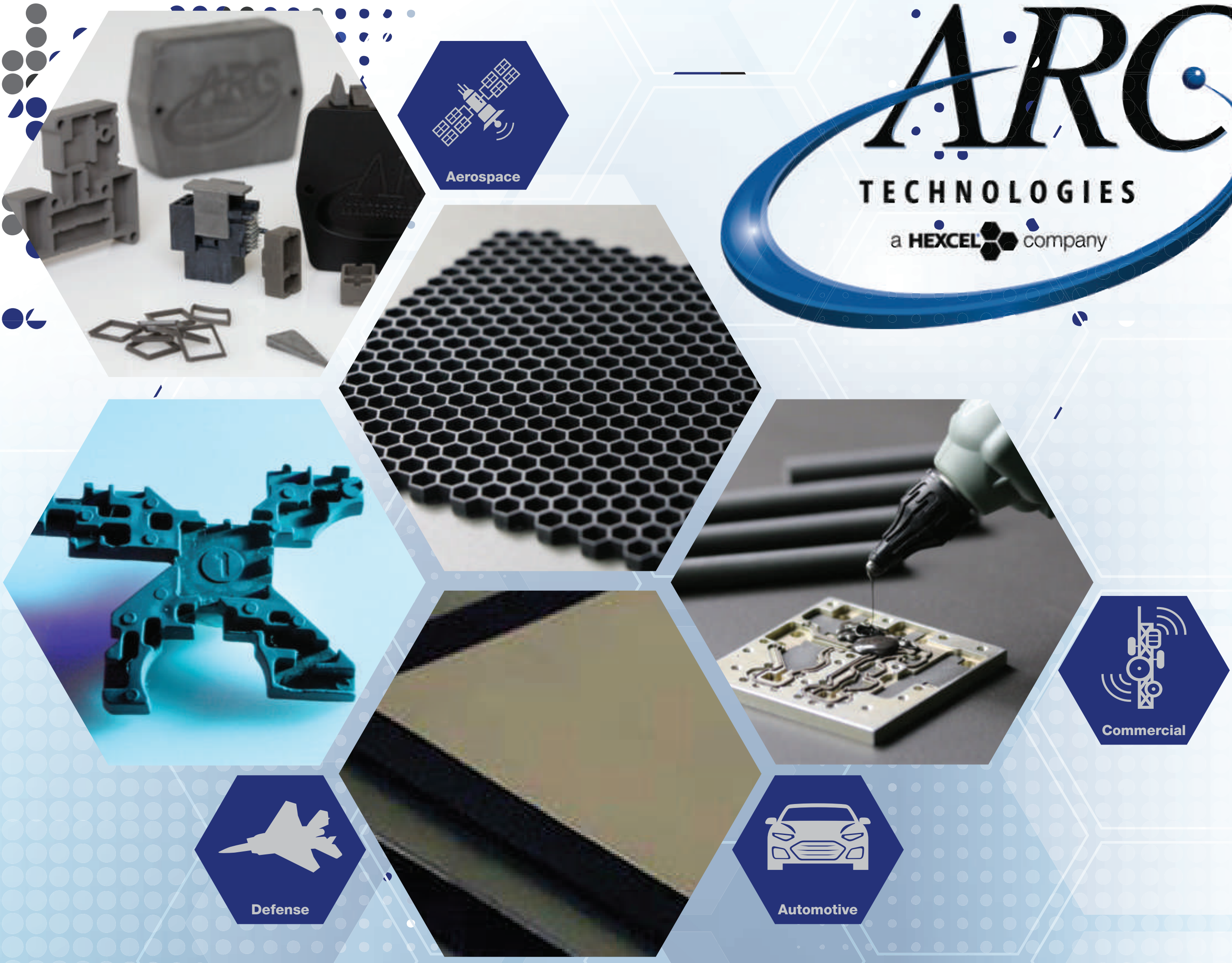
Aerospace
Commercial
Defense
Automotive

According to theory,[5,9] even harmonics are matched to 0 Ω, odd harmonics to infinity and the fundamental to 50 Ω. Due to deficiencies of the class F PA in practical designs, this work describes two improvements: one, because the gate-source parasitics of the GaN HEMT transistor degrade the output power and efficiency of the PA, a gate-source parasitic compensation circuit is employed. And two, because the traditional class F PA uses a high Q output impedance matching transformer, limiting its bandwidth, this work uses low Q radial microstrip lines to control harmonics.

Gate-Source Parasitic Compensation

The GaN HEMT used in this article is an active nonlinear device, with harmonics caused by its parasitics. Gate-to-source parasitics cause the input of the transistor to deviate from a pure sinusoidal wave, reducing PA performance. The transistor model, shown in ***Figure 1***,

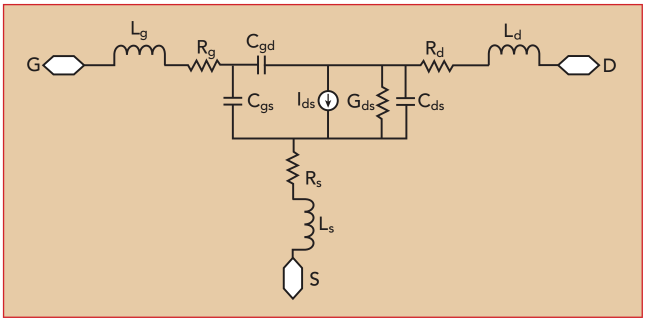

Fig. 1 GaN HEMT model.

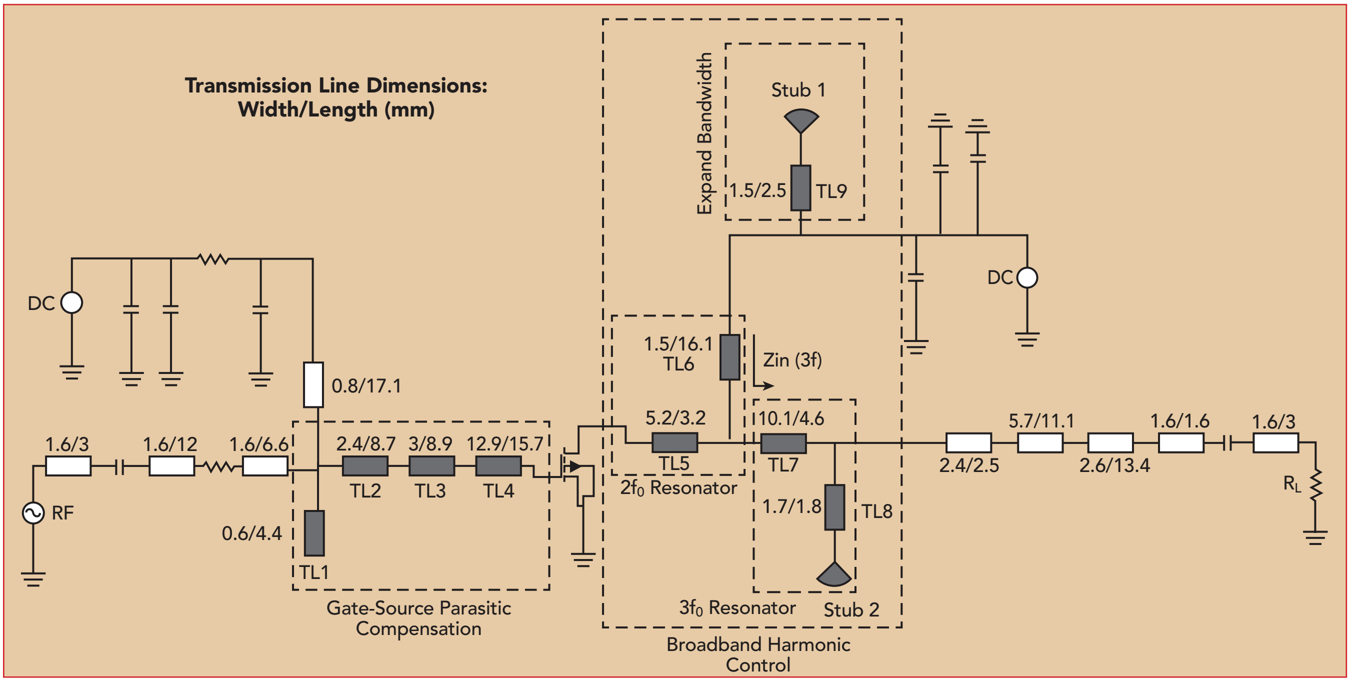

Fig. 2 PA matching circuit design.

includes the parasitic as well as intrinsic elements. Gate-source parasitic parameters include the gate-source capacitance, C_{gs}, gate parasitic inductance, L_g, and parasitic resistance, R_g. C_{gs} is given by the expression

$$C_{gs} = \frac{\varepsilon Z_g}{d} \left[Lg + \frac{\varepsilon\left(V_{bi} + V_{dg}\right)}{q\left(N_{cap}Y_{cap} + NY_A\right) - \sqrt{\left(1.6q\varepsilon N_{cap}\right)} - qn_s} \right] \quad (3)$$

where ε is the dielectric constant of the GaN material, and d is the equivalent depletion depth. The gate parasitic inductance and parasitic resistance are found from

$$L_g = \frac{u_0 d Z_g}{m^2 L_g}$$

$$R_g = \frac{pZ_g}{3m^2 h L_g} \quad (4)$$

where m is the grid index, u_0 is the permeability in a vacuum and ρ is the conductivity of the gate metal.

The gate-source parasitic parameters are calculated from Equations 3 and 4 and are used in the design of the input circuit (see ***Figure 2***). Microstrip lines TL2, TL3 and TL4 compensate for the influence of C_{gs} at the input, where the use of stepped-impedance matching increases the bandwidth. Microstrip line TL1 offsets the effect of parasitic inductance L_g and resistance R_g. The gate-source compensation suppresses the input harmonics, which increases output power and efficiency.

Broadband Harmonic Control

A radial microstrip line, commonly found in mixers and filters, is used in the active bias circuit. The radial microstrip stub input reactance is given by the equations

$$X_{in} = \frac{h}{2\pi r_1} Z_0\left(r_1\right) \frac{360\cos\left(\theta_1 - \varphi_2\right)}{\alpha\sin\left(\varphi_1 - \varphi_2\right)} \quad (5)$$

$$\tan\theta_1 = \frac{N_0\left(kr_1\right)}{J_0\left(kr_1\right)}, \tan\varphi_i = -\frac{J_1\left(kr_1\right)}{N_1\left(kr_1\right)}, i = 1,2 \quad (6)$$

$$Z_0\left(r_1\right) = \frac{120\pi}{\sqrt{\varepsilon_r}}\left[J_0^2\left(kr_1\right) + N_0^2\left(kr_1\right)\right]^{1/2} \cdot \left[J_1^2\left(kr_1\right) + N_1^2\left(kr_1\right)\right]^{-1/2} \quad (7)$$

$$k = 2\pi\sqrt{\varepsilon_{re}} / \lambda_0 \quad (8)$$

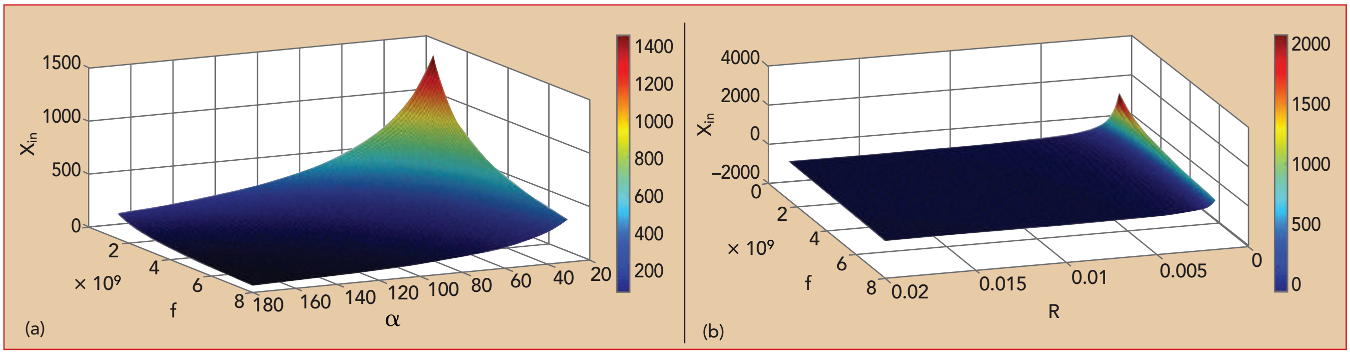

▲ Fig. 3 Radial microstrip stub X_{in} vs. frequency and angle (a) and X_{in} vs. frequency and radius (b).


High Customised Multi-Coax Interconnections for High Speed Digital Testing!
Multi-Cooax Series up to 50GHz
Cables and Adaptors up to 110GHz
Economy type End Launch
Compression Solder-less
Customised Connectors & Adaptors
Multi Coax up to 50GHz
Connectors and Cable Assemblies up to 110GHz
Frontlynk Technologies Inc.
www.frontlynk.com
Tel: +886-6-356-2626 Fax: +886-356-6268
E-mail: info@frontlynk.com

where $J_i(x)$ and $N_i(x)$ are i-order Bessel functions of the first and second classes, α is the angle of the radial microstrip line, ε_{re} is the equivalent dielectric constant and λ_0 is the free space wavelength. r and R are the inner and outer radii of the radial microstrip line, respectively, and h and w are the dielectric substrate thickness and microstrip width, respectively. The relationship between frequency, impedance, radius and angle of the radial microstrip line is shown in ***Figure 3***.[5-8] The open microstrip line is the equivalent of a capacitor.

In the broadband harmonic control network topology shown in Figure 2, the third harmonic impedance can be obtained from

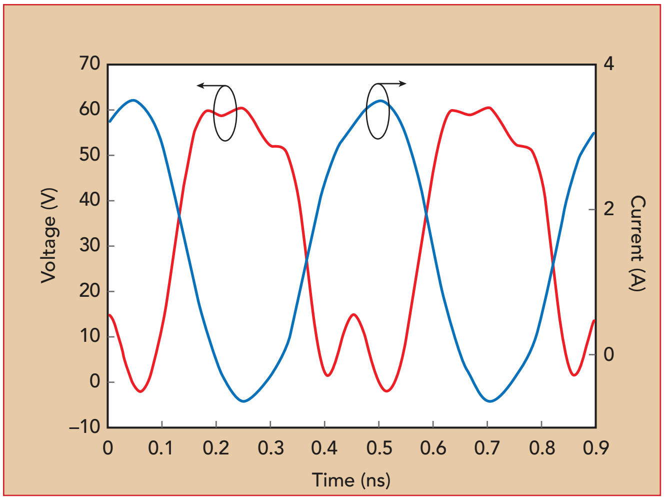

Fig. 4 Drain voltage and current waveforms simulated with ADS.

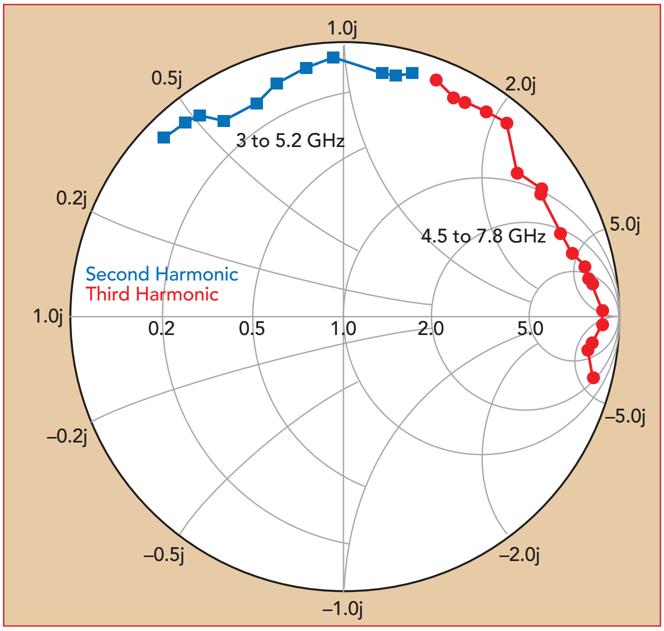

Fig. 5 Simulated second and third harmonic impedances with broadband harmonic matching and gate-source parasitic compensation.

$$Z_{in}+(3f)=jZ_7\frac{X_{in}+Z_8\tan\frac{2\pi}{\lambda}l_8+Z_7\tan\frac{2\pi}{\lambda}l_7\left(1-\frac{X_{in}}{Z_8}\tan\frac{2\pi}{\lambda}l_8\right)}{Z_7\left(1-\frac{X_{in}}{Z_8}\tan\frac{2\pi}{\lambda}l_8\right)-\left(X_{in}+Z_8\tan\frac{2\pi}{\lambda}l_8\right)\tan\frac{2\pi}{\lambda}l_7} \quad (9)$$

$$l_7+l_8+l_{stub2}\approx\lambda/12 \quad (10)$$

where Z_7 and Z_8 are the characteristic impedances of microstrip lines TL7 and TL8. The dimensions l_7 and l_8 are the lengths of the microstrip lines, respectively. The lengths are determined by Equation 10 so the third harmonic is open circuited. At $2f_0$, the microstrip lines TL5 and TL6

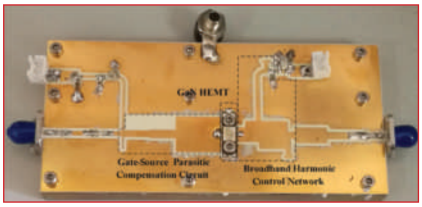

Fig. 6 Fabricated PA.

are stepped to match the second harmonic impedance to 0. Radial stub 1 plays a role expanding the bandwidth.

Simulations of the drain voltage and current waveforms (see ***Figure 4***) show the voltage and current do not overlap in the crests and troughs, which enhances efficiency. By compensating the gate-source parasitic effect and using the broadband harmonic matching circuit, the second and third harmonic impedances of the PA are maintained in the low and high impedance regions, respectively, as shown in ***Figure 5***.

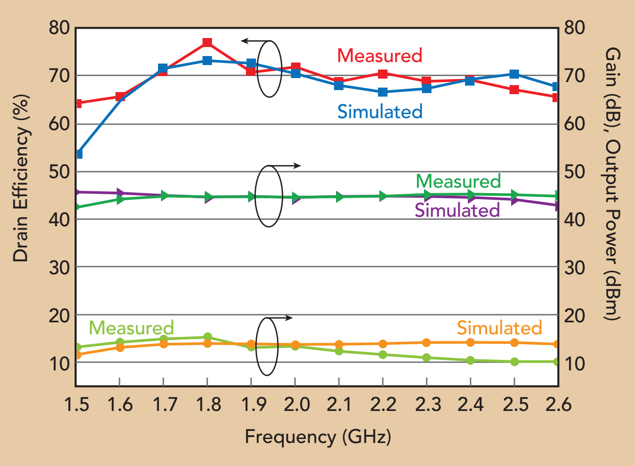

Fig. 7 Measured vs. simulated output power, drain efficiency and gain vs. frequency.

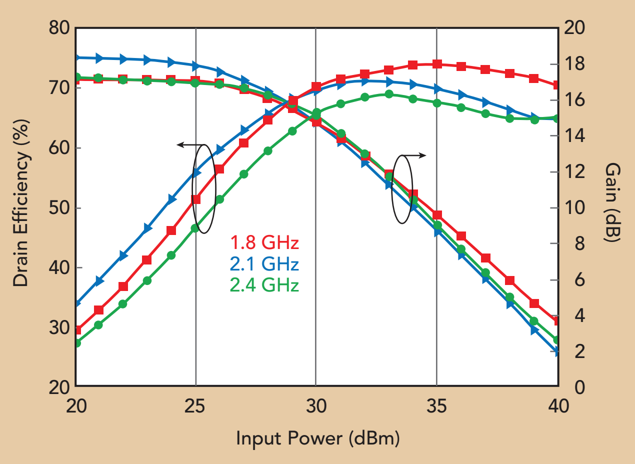

Fig. 8 Measured drain efficiency and gain vs. input power at 1.8, 2.1 and 2.4 GHz.

FABRICATION AND MEASUREMENT

The GaN HEMT used in this design is Wolfspeed's CGH40025F. The broadband PA is fabricated on a Rogers 4350B substrate, which has a dielectric constant of 3.66 and a thickness of 0.762 mm (see ***Figure 6***). The gate bias is −3 V, operating the device class B. To obtain higher power, the drain voltage is set to 32 V instead of the recommended 28 V. The amplifier is operated CW.

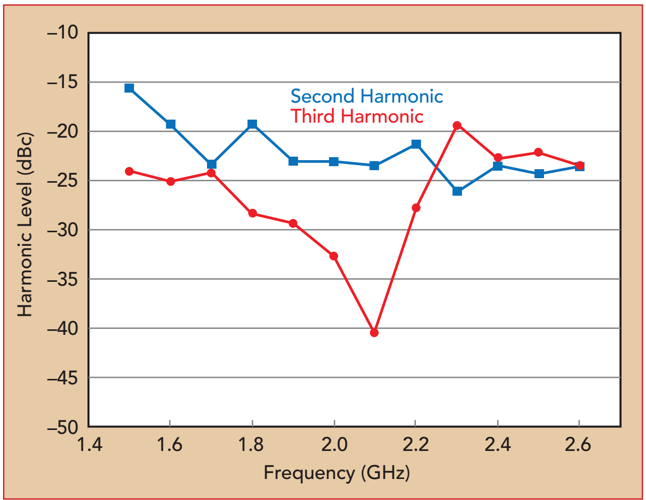

Fig. 9 Second and third harmonic suppression vs. frequency.

The measured output power, drain efficiency and gain are shown in ***Figure 7*** and compared with the simulated performance. The measured output power is between 43.4 and 45.6 dBm between 1.5 and 2.6 GHz, with the drain efficiency between 65 and 76.9 percent. The gain is greater than 10 dB. The maximum measured output power is 45.6 dBm at 1.5 GHz, and the minimum is 43.4 dBm at 2.6 GHz. The

TABLE 1
COMPARISON WITH SIMILAR WORK

Reference	Bandwidth (GHz)	Power (dBm)	Gain (dB)	Drain Efficiency (%)
10	1.6 to 2.2	39	>10	55
11	1.4 to 2.6	39	10	60 to 70
12	1.6 to 2.5	39	>10	55 to 70
4	1.1 to 2.1	40	>10	60 to 73
This Article	1.5 to 2.6	43.4 to 45.6	>10	65 to 77

maximum measured drain efficiency is 76.9 percent at 1.8 GHz.

Measured drain efficiency and gain versus output power at 1.8, 2.1 and 2.4 GHz, respectively, is plotted in ***Figure 8***. These frequencies are chosen to represent the entire frequency range, with 1.8 and 2.4 GHz the lower and higher frequencies, 2.1 GHz the center. As the input power increases, the drain efficiency gradually increases; when the input power reaches a certain level, the gain begins to drop rapidly. The decrease in gain indicates a linear loss and shows that high efficiency and high linearity are difficult to obtain simultaneously. The two parameters must be weighed in the PA design.

Figure 9 shows measured second and third harmonic distortion levels relative to the fundamental. Suppression of the second and third harmonics are 15.6 to 26.1 and 19.4 to 40.5 dBc, respectively.

For comparison, recent broadband PA results are shown in ***Table 1***. The design described here demonstrates greater output power and drain efficiency with equivalent gain over a similar operating band.

CONCLUSION

This article discusses two innovative improvements in wideband PA design: a novel gate-source parasitic compensation circuit reduces the influence of harmonics caused by GaN HEMT gate-source parasitics. At the same time, a broadband harmonic control network increases PA bandwidth. Overall performance results demonstrate an advance in the state of the art.■

ACKNOWLEDGMENT

This work is supported by Key Project of Zhejiang Provincial Natural Science Foundation of China (No. LZ16F010001), Zhejiang Provincial Public Technology Research Project (No. 2016C31070) and National Natural Science Foundation of China (No. 61306100).

References

1. T. Ge and J. S. Chang, "Filterless Class D Amplifiers: Power-Efficiency and Power Dissipation," *IET Circuits, Devices & Systems*, Vol. 4, No. 1, January 2010, pp. 48–56.
2. K. Chen and D. Peroulis, "Design of Highly Efficient Broadband Class-E Power Amplifier Using Synthesized Low-Pass Matching Networks," *IEEE Transactions on Microwave Theory and Techniques*, Vol. 59, No. 12, December 2011, pp. 3162–3173.
3. M. Hayati, A. Sheikhi and A. Grebennikov, "Class-F Power Amplifier with High Power Added Efficiency Using Bowtie-Shaped Harmonic Control Circuit," *IEEE Microwave and Wireless Components Letters*, Vol. 25, No. 2, February 2015, pp. 133–135.
4. M. Iqbal and A. Piacibello, "GaN HEMT Based Class-F Power Amplifier with Broad Bandwidth and High Efficiency," *International Conference on Integrated Circuits and Microsystems*, November 2016, pp. 131–134.
5. E. Cipriani, P. Colantonio, F. Giannini, A. Raffo, V. Vadalà, G. Bosi and G. Vannini, "Extended Operation of Class-F Power Amplifiers Using Input Waveform Engineering," *47th European Microwave Conference*, October 2017, pp. 144–147.
6. S. Goto, T. Kunii, A. Ohta, A. Inoue, Y. Hosokawa, R. Hattori and Y. Mitsui, "Effect of Bias Condition and Input Harmonic Termination on High Efficiency Inverse Class-F Amplifiers," *31st European Microwave Conference*, September 2001.
7. M. Zhang, X. Wang, M. Peng, X. Liu and R. Wang, "Effect of Field Plate Length on DC Characteristics of High Breakdown Voltage GaN HEMTs for Power Switching Application," *10th IEEE International Conference on Solid-State and Integrated Circuit Technology*, November 2010, pp. 1356–1358.
8. P. M. Cabral, J. C. Pedro and N. B. Carvalho, "Nonlinear Device Model of Microwave Power GaN HEMTs for High Power-Amplifier Design," *IEEE Transactions on Microwave Theory and Techniques*, Vol. 52, No. 11, November 2004, pp. 2585–2592.
9. Q. Li, S. He, Z. Dai and W. Shi, "A Method for Designing Generalized Continuous Power Amplifier," *IEEE MTT-S International Microwave Workshop Series on Advanced Materials and Processes for RF and THz Applications*, July 2016.
10. K. Mimis, K. A. Morris, S. Bensmida and J. P. McGeehan, "Multichannel and Wideband Power Amplifier Design Methodology for 4G Communication Systems Based on Hybrid Class-J Operation," *IEEE Transactions on Microwave Theory and Techniques*, Vol. 60, No. 8, August 2012, pp. 2562–2570.
11. P. Wright, J. Lees, J. Benedikt, P. J. Tasker and S. C. Cripps, "A Methodology for Realizing High Efficiency Class-J in a Linear and Broadband PA," *IEEE Transactions on Microwave Theory and Techniques*, Vol. 57, No. 12, December 2009, pp. 3196–3204.
12. L. Ma, F. You and X. Hou, "An Output Match Design Method for High Efficiency and Broadband Class-J PA," *IEEE Topical Conference on Power Amplifiers for Wireless and Radio Applications*, June 2014, pp. 43–45.

INVITED PAPER

DRFM Jammer Test Solutions

Yassen Mikhailov
Rohde & Schwarz, Munich, Germany

This article highlights the test requirements and challenges for digital RF memory (DRFM) jammers, describing the available solutions and pointing out their benefits. The focus is on the three main test areas for DRFMs: system tests, RF/IF stage tests on the module and subsystem and exploration of the digital backend.

DRFM jammers play an essential part in the electronic attack (EA) suite and are instrumental in ensuring mission success and improving platform survivability. DRFMs have been present for quite some time—the earliest reference appears in an article by Sheldon Spector called "A Coherent Microwave Memory Using Digital Storage: The Loopless Memory Loop," published in the January/February 1975 issue of *Electronic Warfare*, a publication of the Association of Old Crows.

During World War II, radar engineers developed the pulse compression technique. Upgrades in radar range resolution came with improvements in signal-to-noise ratio (SNR). This combination, along with phase-coherent klystron-based transmitters, gave radar engineers an advantage that made barrage jamming relatively ineffective, due to the high output requirements for broadband stand-off jammers. In the early development stages, a DRFM jammer was a simple device consisting of a receive path, signal processing with modification and a transmit path. The main objective of the DRFM jammer was to digitally capture and retransmit an altered RF radar return signal with sufficient fidelity to deceive the radar processor.

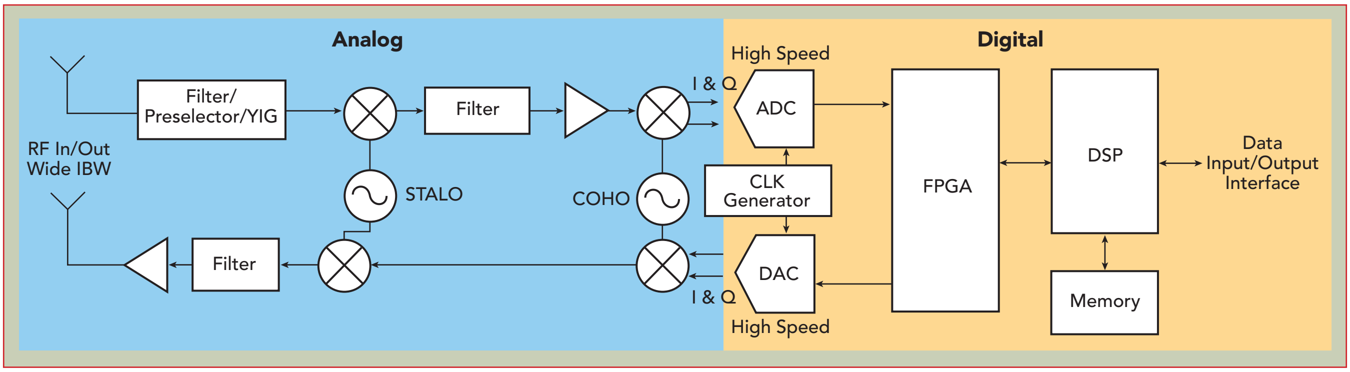

Fig. 1 DRFM block diagram.

Fig. 2 **Test system for DRFM characterization.**

With advancements in semiconductor technology in the 1980s, new signal processing techniques for radar were widely adopted. These techniques, such as moving target and stationary target indication, gave the radar several improvements, one of which was significant signal processing gain. As a result, it became extremely difficult to jam or deceive a radar.

The electronic warfare (EW) community responded by developing complex EW pods and deception techniques to counter radar advancements, giving birth to the modern DRFM jammer. Today, DRFM is an essential part of the EW attack suite. The basic architecture of a DRFM module remains the same: receive, data processing and transmit. A coherent oscillator ensures that both paths have a constant phase difference, the same frequency and the same waveform. Modern DRFMs are characterized by wideband RF front-ends (RFFE) with instantaneous bandwidths exceeding 2 GHz. Wideband analog signals are digitized using high speed analog-to-digital converters (ADC), processed and retransmitted back via high speed digital-to-analog converters (DAC). Access to vast processing power using field-programmable gate arrays (FPGA), digital signal processors (DSP) and flexible, freely configurable deceptive techniques generators make DRFM a formidable asset in the EA arsenal.

A critical requirement of electronic countermeasure (ECM) systems is to provide RF return signals to a radar with sufficient fidelity of the Doppler shift, range and radar cross section to ensure that the radar interprets the return signal as a "real" target. Phase correction is used to correct phase discontinuities resulting from a range update during the coherent processing interval.

For the RFFEs, modern DRFMs employ a range of receiver architectures. One of the highest performance architectures is the channelized receiver, which offers a good compromise between bandwidth, sensitivity and cost. Latency for modern DRFMs is on the order of nanoseconds. A rule of thumb for radar developers is that one microsecond corresponds to roughly 150 m range.

TEST REQUIREMENTS

For this discussion, the device schematic is divided into analog and digital components (see ***Figure 1***). The three main areas of DRFM testing are:

System level or verification and final system test. At this stage, development engineers typically perform an analysis of the deception techniques to ensure proper operation. These tests include direction finding (DF), to ensure the system identifies emitter direction; output stability of the DRFM module (both phase and amplitude); latency; spectral purity; error vector magnitude and global navigation satellite system. Also, electromagnetic compatibility (EMC) measurements are important to ensure the system's EMC compliance.

RF/IF stage or tests focused at the submodule and component levels. Several measurements are performed here, including component and submodule characterization of spurious, dynamic range, compression point, gain and phase response with frequency, noise figure, IP3, receiver sensitivity, quadrature error, local oscillator performance (phase noise, leakage and stability) and antenna radiation.

Fig. 3 **Screen shot of range gate pull-off.**

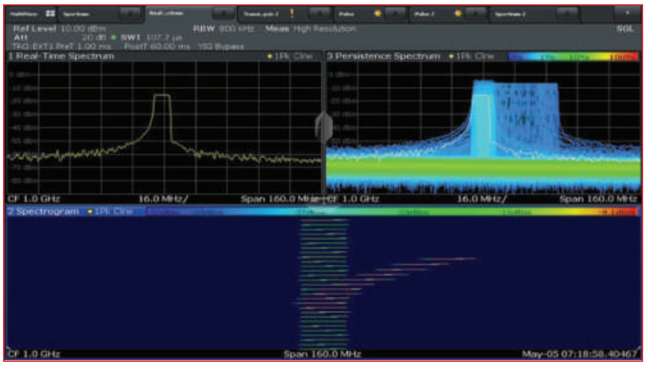

Fig. 4 **Screen shot of velocity gate pull-off.**

Fig. 5 **Spurious measurement.**

DUAL or SINGLE LOOP
SYNTHESIZER & PLO MODULES

Features:

- Proprietary digital Integer and Fractional PLL technology
- Lowest digital noise floor available -237 dBc/Hz figure of merit
- Output frequencies from 100 MHz locked crystal to 30 GHz
- Available with reference clean up dual loop, or single loop for very low noise reference
- Parallel fixed band stepping or SPI interface synthesized up to octave bandwidths
- Reference input range 1 MHz to 1.5 GHz
- Dual RF output or reference sample output available
- +12 dBm standard output power +16 dBm available
- Standard module size 2.25 X 2.25 X 0.5 Inches (LxWxH)
- Standard operating temperature -10 to 60 °C, -40 to +85 °C available

Up to 30 GHz*

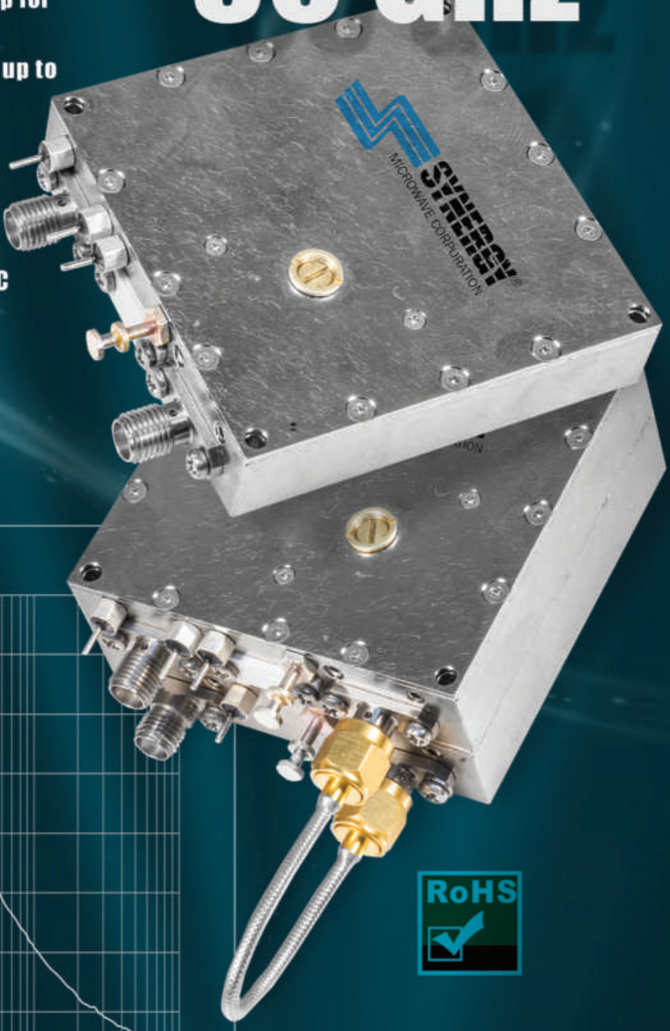

Applications:

- SATCOM, RADAR, MICROWAVE RADIO

* *16 - 30 GHz with added x2 module < 1" in height.*

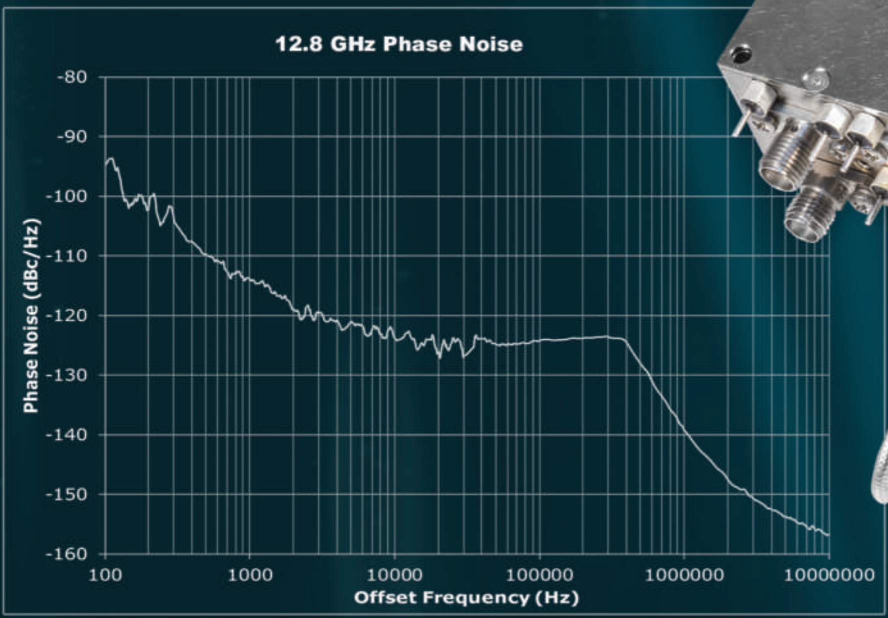

RoHS

Talk To Us About Your Custom Requirements.

SYNERGY®
MICROWAVE CORPORATION

Phone: (973) 881-8800 | Fax: (973) 881-8361
E-mail: sales@synergymwave.com
Web: WWW.SYNERGYMWAVE.COM
Mail: 201 McLean Boulevard, Paterson, NJ 07504

Digital stage testing comprises parameters such as clock jitter, timing and power integrity. A noisy power supply will affect overall performance and can be a beacon for electronic counter-countermeasures (ECCM). Typical measurements include power integrity, clock jitter, latency, timing, equalizer flatness, electromagnetic interference debugging, FPGA, DSP and data converters.

SYSTEM LEVEL TESTS

The spectrum analyzer and signal generator are typical test instruments. In addition, simulating a complex electromagnetic environment is important for stress testing, verification and debugging. To ensure proper emitter location, more advanced DRFM systems perform angle of arrival measurements, which require signals time and phase aligned at a reference plane.

Rohde & Schwarz offers a test system for DRFM testing (see ***Figure 2***), based on the R&S SMW vector signal generator and R&S SGS signal source generator, giving the user the ability to generate up to eight coherent emitters at 20 GHz. Adding the complementary R&S Pulse Sequencer with electromagnetic environment simulation software gives complete control over the system and the ability to generate complex emitter scenarios. The system is calibrated using the R&S NRP-Z81 wideband power sensor to ensure the desired phase at the reference plane. For precise phase accuracy and stability, the multichannel phase-coherent system includes R&S SMW signal generators synchronized via a common local oscillator provided by the R&S SMA100B analog signal generator. The combination of a very low phase noise and high output power makes the R&S SMA100B well suited for this task. A dense emitter environment scenario can be generated using the R&S Pulse Sequencer software. The DF systems are based exclusively on commercial off-the-shelf technology. This provides improved availability, serviceability and the flexible use of test equipment when it is not dedicated to DF tests.

The main purpose of the DRFM system is to deceive the hostile sensor. This task is performed through several deception techniques. Proper design and programming require realistic simulations of the dense emitter environments in which DRFMs operate, with careful analysis of the signals transmitted by the system and comparison with the waveform generated by the hostile emitter. For this, Rohde & Schwarz offers several analysis tools for fast and repeatable results. These tools include a pulse analysis option with automatic pulse capturing and examination, transient signal analysis of signals with time-changing behavior, pulse Doppler waveform streaming to simulate the complex emitter environment and pulse stability analysis to ensure the jammer introduces no unwanted distortion.

Figure 3 shows an example of an EA scenario where the jammer

pulls off the radar range gate. All deception techniques are time-based and require careful synchronization of several parameters. The scenario is created with the pulse sequencer software, transmitted via a function generator, and analyzed with the R&S FSW K6 pulse measurements option. The range gate pull-off or capture and walk technique normally works with velocity gate pull-off (see ***Figure 4***), where the jammer tries to pull off the Doppler gate.

Timing is essential for successful pull-off. If the pulse repetition interval (PRI) or Doppler is pulled off too fast or too far, it might leave the range or velocity gate and alert the radar that it is being jammed. Timing parameters of the PRI or Doppler walk must be carefully considered, so it is important to look at the trend of the selected parameter, which is available in the pulse analysis option. Complex analysis is simplified with a flexible and freely configurable user interface. To speed the measurement, most of the tasks are automated. Nevertheless, one can manually change and configure the setup to fit specific requirements.

Take, for example, the verification of the pulse train transmitted by a jammer in response to a pulse radar with pulse compression used to improve the time-bandwidth product, the range resolution or both. Capturing such a complex signal, modifying some of its parameters and playing it back without disturbing important factors such as phase, compression ratio or sidelobe level is not easy. To ensure that no additional disturbances are introduced by the jammer, one can upgrade the pulse analysis option with the R&S FSW K6S and automatically measure the compression parameters of the modulated pulse transmitted by the system. The main lobe versus sidelobe level and the time difference between them are summarized in a results table. The user can upload reference pulse waveforms in I/Q format and compare phase and frequency within a pulse with the measured values.

RF/IF STAGE TESTING

Spurious emissions ultimately determine jammer effectiveness. Unwanted radiation puts additional strain on the RF systems and acts as a beacon for ECCM. Normally, spurious emissions measurements are tedious, time consuming and expensive. To maximize the analyzer's performance, engineers must manually adjust parameters such as resolution bandwidth and frequency. Using the R&S FSW K50 option, this task is simple: enter a few constraints, such as frequency range and desired spurious level. The instrument then performs the measurements automatically, indicating either a pass or a fail (see ***Figure 5***). The complexity of the task is drastically reduced while the measurement speed is increased by up to 20× compared to the traditional, manual method.

Phase noise measurements are not simple; the more accuracy required, the more complicated the

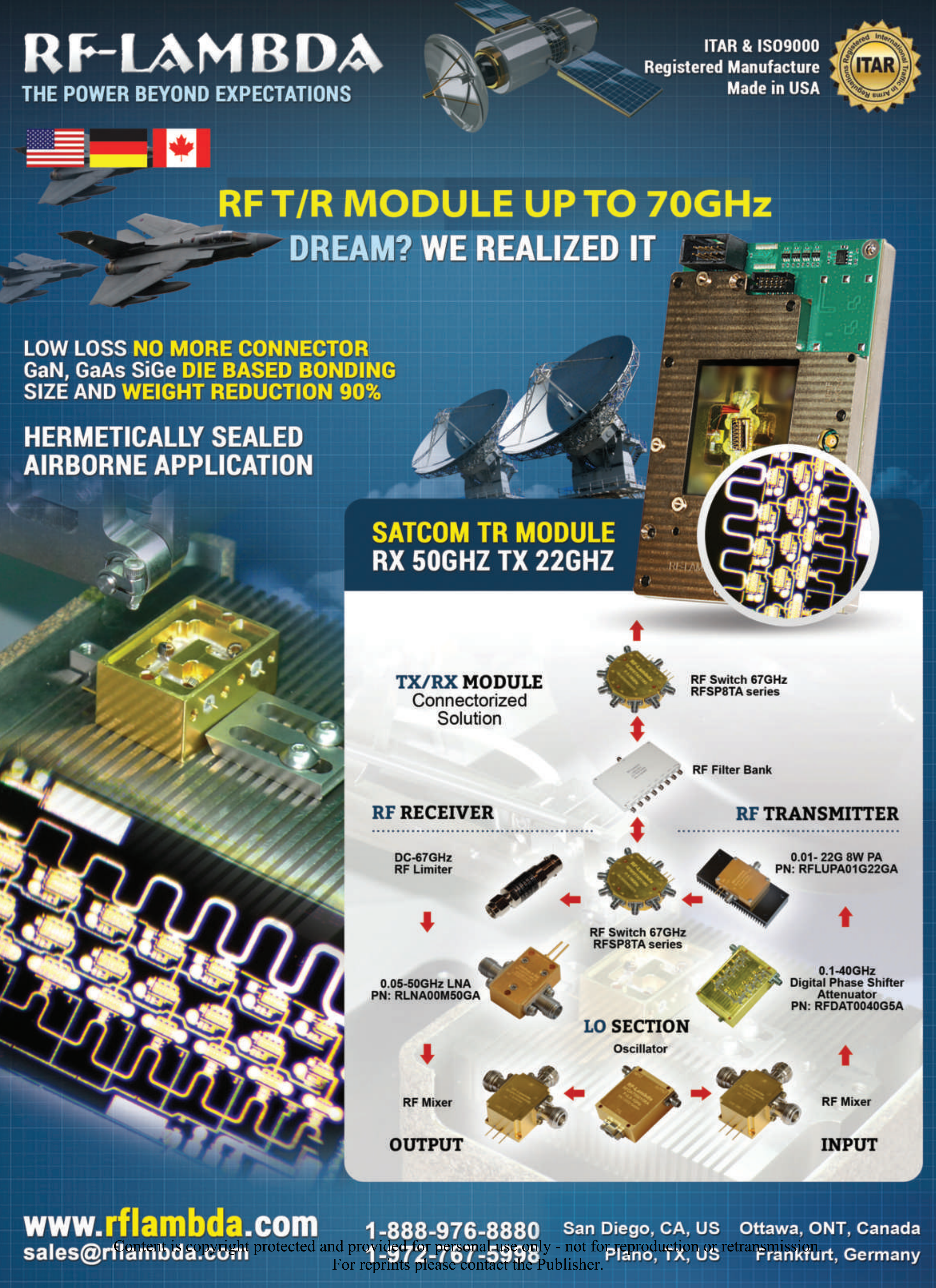
RF-LAMBDA
THE POWER BEYOND EXPECTATIONS
ITAR & ISO9000
Registered Manufacture
Made in USA
ITAR
Registered International Traffic in Arms Regulations
RF T/R MODULE UP TO 70GHz
DREAM? WE REALIZED IT
LOW LOSS NO MORE CONNECTOR
GaN, GaAs SiGe DIE BASED BONDING
SIZE AND WEIGHT REDUCTION 90%
HERMETICALLY SEALED
AIRBORNE APPLICATION
SATCOM TR MODULE
RX 50GHZ TX 22GHZ
TX/RX MODULE
Connectorized
Solution
RF Switch 67GHz
RFSP8TA series
RF Filter Bank
RF RECEIVER
RF TRANSMITTER
DC-67GHz
RF Limiter
0.01- 22G 8W PA
PN: RFLUPA01G22GA
RF Switch 67GHz
RFSP8TA series
0.05-50GHz LNA
PN: RLNA00M50GA
0.1-40GHz
Digital Phase Shifter
Attenuator
PN: RFDAT0040G5A
LO SECTION
Oscillator
RF Mixer
RF Mixer
OUTPUT
INPUT
www.rflambda.com
sales@rflambda.com
1-888-976-8880
1-972-767-5998
San Diego, CA, US
Plano, TX, US
Ottawa, ONT, Canada
Frankfurt, Germany

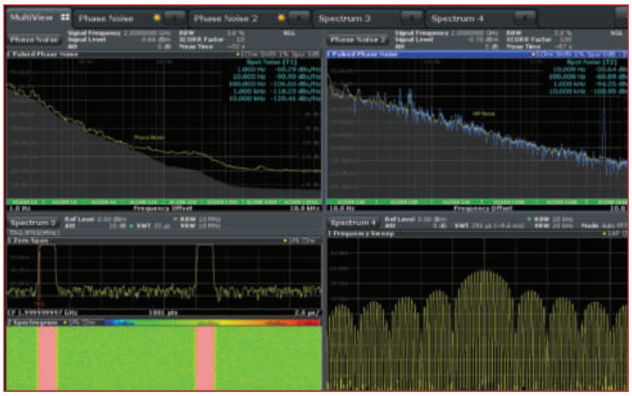

Fig. 6 Phase noise measurement.

measurements become. With the R&S FSWP phase noise analyzer, however, complicated setups, such as pulsed additive phase noise, are accomplished in minutes with high accuracy (see ***Figure 6***). This is also a fully functional spectrum analyzer and voltage-controlled oscillator (VCO) tester. If, for example, the DRFM is acting as a smart (follower) jammer on a hopping signal, then the user must characterize VCO tuning and settling.

Internal DC sources can be used for VCO characterization, providing all VCO parameters at a glance, such as frequency, current, power and sensitivity. Ensuring coherence between transmit and receive paths and the performance of stability measurements are essential parts of the DRFM developer's toolkit. The R&S FSWP phase noise analyzer uses the Allan variance (AVAR) to analyze the time-domain stability of oscillators.

Pulse train stability of the jammer must also be considered. Too much jitter and the return could be filtered by the radar's false alarm rate algorithm—or worse, classified as a jamming signal. Many factors affect pulse stability, for example, memory effects, mismatch between different stages, poor thermal dissipation planning and/or clock/oscillator jitter. The R&S FSWP provides an accurate way to measure phase and amplitude stability, helping optimize jammer design. Typical parameters are difference to average for both amplitude and phase, and 3D visualization makes it easy to spot potential problems.

The free space transducer will always be used, no matter how far digitalization progresses. Even with direct RF-to-digital conversion, an antenna plays the key role in transferring the RF energy to the desired destination. Here, the R&S ZNA vector network analyzer adds fast, non-dedicated receivers for antenna characterization with excellent receiver sensitivity.

DIGITAL STAGE MEASUREMENTS

Testing at the digital stage is as important as performing system level verification or qualifying RF components, sub-modules and

MILITARY AND AEROSPACE INTERCONNECTS AT THE READY

From high-volume production, to low-volume customized products, MilesTek is your source for military, aerospace, communications and industrial interconnect solutions. With quick turnaround and same-day shipping from our stock of more than 10,000 highly reliable products, MilesTek is at the ready to help meet your project deadlines.

The MilesTek Advantage:

- Large In-Stock Inventories
- Same-Day Shipping
- Prototype Development
- CAD Design Capabilities
- Multiple Testing Solutions
- Expert Technical Support
- AS9100 Certified
- SO 9001:2008 Registered

MilesTek
an INFINITE brand

866-524-1553 • MilesTek.com

Available for Same-Day Shipping!

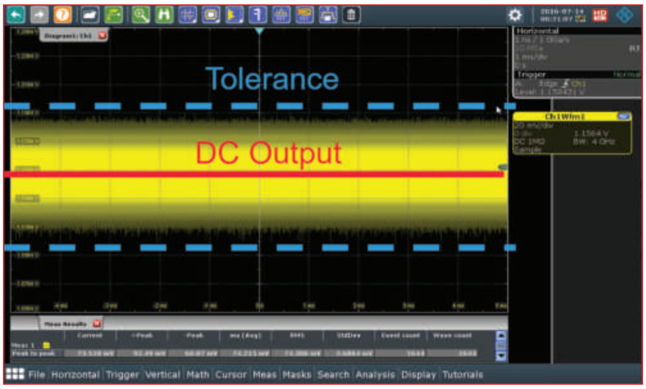

Fig. 7 Power integrity measurement.

modules. Among the key elements are power and signal integrity, clock jitter, latency, timing and qualifying the signal converting components, such as the ADC and DAC. On the digital side, the oscilloscope is the centerpiece of the test kit.

Power integrity tests ensure clean power and no additional coupling of noise or hum on the RF lines. Typical performance parameters are ripple, noise and power distribution network impedance (see ***Figure 7***).

With deeper strides into the digital world, clock synchronization becomes critical. Imagine an active electronically scanned array architecture with thousands of transmit-receive modules, where a significant portion of the calibration time is spent on timing synchronization and clock calibration. Eliminating clock jitter at the design stage simplifies the calibration process in final testing and verification, ensuring a fully functional product.

ADC and DAC measurements are just as important. For the RF side, the R&S FSWP phase noise analyzer or the R&S SMA100B analog signal generator may be used. For the DAC side, testing signal quality, modulation quality and phase noise is common. For the ADC, general testing with CW and real test signals qualify the component for its intended purpose. Wideband tests can be performed with the 2 GHz baseband bandwidth of the R&S SMW vector signal generator. Two RF channels in the same R&S SMW instrument can be stitched together to provide a 4 GHz wide signal with optimal RF performance.

CONCLUSION

The DRFM jammer is an essential and highly complex element of the EA suite. It has evolved from a simple repeater with some fading capabilities to a sophisticated EA asset. Critical test areas involve the operation and timing of deception techniques at the system level, qualifying the individual components, submodules and modules at the RF/IF level and ensuring that clock jitter and power integrity are addressed early in the design stage.■

INVITED PAPER

Reducing EMI/RFI in Microwave Cable Assemblies for A&D Systems

Paul Pino
W. L. Gore & Associates, Newark, Del.

Mitigating electromagnetic interference (EMI) and RF interference (RFI) is a growing concern in aerospace and defense applications. Consumer communications technology is rapidly moving to over-the-air (OTA) transmission, with the need for more information to be communicated over longer distances, driving wider bandwidth, higher frequency and greater transmit power. Defense systems such as electronic warfare (EW) and radar have similar trends toward higher frequency and greater power, placing more stringent demands on the shielding of cable assemblies and electronic components. As the RF environment, which is already filled with noise sources and interference, becomes even more crowded, systems and components resistant to EMI and RFI will play a greater role in system reliability.

Fig. 1 Troubleshooting signal interference problems is challenging, especially in an aircraft.

IMPACT OF EMI/RFI ON CABLE PERFORMANCE

EMI describes noise or interference over a very broad frequency spectrum. For example, the noise source could be a vacuum cleaner motor emitting low frequency interference in the double-digit range. RFI is associated with emissions within the RF spectrum, nominally from 20 kHz to 300 GHz.

For microwave cable assemblies, EMI and RFI are two-way streets. If a cable assembly can produce sizable amounts of interference, it will also be susceptible to receiving the same. The objective of cable shielding is to keep the noise and signals outside of the cable and keep in the signal of interest. When a cable assembly is sensitive to EMI/RFI, the signal of interest—the signal propagating through the cable assembly—can be compromised, even rendered unintelligible by interference.

As frequency increases, between 300 MHz and 300 GHz for microwave applications, shielding a cable assembly becomes more challenging. Higher frequency signals, coupled with increased transmit power, will increase the power radiated through any leakage in the shield. This combination increases the risk of interference with electronic equipment and cable runs adjacent to the radiating component. Troubleshooting a signal interference problem, especially in an aircraft, can be daunting (see ***Figure 1***). Highly effective shielding is critical to system performance.

With cellular communications, 5G OTA testing requires new cell phone designs to

Fig. 2 **RF leakage from a cable assembly can degrade an EW system's capability detecting and countering threats.**

be validated without a cable connection to the device under test (DUT). Instead, all test signals are transmitted OTA in a controlled environment, to approximate real world conditions. In this environment, microwave cable assemblies with poor shielding will be prone to radiating and receiving unwanted signals, which could negatively influence a design validation.

Cable assemblies susceptible to EMI/RFI can have an especially profound effect on airborne EW applications. Modern EW systems gather large amounts of data from the electromagnetic environment surrounding the aircraft, using it to determine threat type, location, proximity and severity. Poorly shielded cable assemblies, or those with compromised shields, can degrade the signals from the system's antennas and the system's ability to identify and determine how to respond to a potential threat—particularly since the design goal for threat detection is to detect a threat with a minimum of 2× the threat's lethal striking distance.

With an EW system, the critical nature of processing time is apparent by considering this scenario (see ***Figure 2***): An aggressor fighter aircraft has just launched a subsonic air-to-air missile against a friendly fighter, as the two rapidly close on one another. At launch, the two aircraft were 4 miles apart, converging at 1200 mph. From the time of launch and at the current closing speed, the friendly aircraft's EW system has less than 12 seconds to identify the threat and determine a course of action, including displaying the threat and its position to the pilot and launching countermeasures. With poorly shielded cable assemblies, the EW system may not extract the threat signal from the cacophony of electromagnetic noise and interference—not unlike trying to pick out a single voice in a stadium full of cheering spectators.

MITIGATING EMI/RFI

With any technical problem, the first step toward resolution is understanding, which comes through testing and characterization. W. L. Gore & Associates performs shielding effectiveness testing of its cable assemblies using the latest mode-stirred chamber technology and incorporates these findings into its cable assembly and connector designs and termination techniques. Shielding effectiveness is not strictly a cable phenomenon; the connector and cable termination are part of the equation (see ***Figure 3***).

For defense aircraft applications, EMI/RFI challenges can be addressed

through the following tactics:
- Use appropriate shielding enclosure designs for the application.
- Where cable installation or aircraft servicing can potentially damage cables, use ruggedized microwave cable assemblies with proven shield designs capable of withstanding installation and servicing.
- Ensure all coaxial connections are clean and tightened to the proper torque.
- In high vibration environments, ensure cables are properly secured using locking connector coupling nuts or coupling nuts drilled for lock wire holes.
- In microwave cable airframe installations, do not stretch a cable that "last little bit" to make a connection; use properly sized P-clamps to secure cables.
- As cable placement is critical, do not position cables close to antennas transmitting high-power.
- In commercial applications, instruct technical personnel on microwave cable assembly care and handling. This is particularly important when using non-ruggedized or general-purpose cable assemblies, as they are considerably more fragile than their ruggedized counterparts.
- Cable shielding problems often result from damage caused by improper handling. Discourage repeatedly bending cables just behind the connector or coiling cables in tight loops for storage, which exposes them to unnecessary wear.
- When bundling cables with plastic zip-ties, use just enough force to contain the bundle; zip-ties can exert damaging crush forces if cinched tightly.
- To maintain performance, proper microwave connector care and maintenance are key to preserving mechanical and electrical integrity.

THE RIGHT CABLE & CONNECTOR

Microwave cable assemblies are often the last component to be designed in a system, often treated as ideal or near-ideal components, assuming not much difference among cables. The common thinking is cables simply link one critical system to another. However, a microwave cable assembly is a critical system itself, capable of causing unintended results that may degrade the per-

Fig. 3 The cable, connector and cable termination determine the shielding effectiveness of an RF cable assembly.

formance of the system. It is rarely considered how poor design or construction can degrade a cable assembly's performance with improper handling, damage inflicted during installation or time.

System designers and program managers should consider the following when selecting microwave cable assemblies for their systems:

- What environmental conditions will the cable assembly be exposed to (i.e., temperature, pressure, humidity)?
- Will the cable assembly be exposed to vibration or excessive flexing, either by hand or mechanized?
- What phase and loss stability over temperature is needed?
- What shielding effectiveness is required and at what frequency?
- What is the expected average power that the connector-cable combination will carry under the prevailing use conditions?
- What is the loss budget for the cable run? What is the VSWR budget?
- Will the cable assembly be subjected to rough handling, either during its service life or installation? If so, consider a ruggedized design.
- Will the cable assembly be housed in the unpressurized portion of an aircraft? If so, consider a sealed assembly to ensure stable phase and loss performance with altitude (i.e., pressure).
- Will the cable assembly be exposed to extreme temperature and moisture? If so, consider a sealed assembly.
- Will the cable assembly be exposed to oil, fuel and chemicals? If so, consider a sealed, ruggedized assembly resistant to chemicals.
- Non-ruggedized or general-purpose cable assemblies will cost less, yet they are vulnerable to damage. Carefully evaluate the risks versus the cost savings when selecting a general-purpose assembly rather than ruggedized.

Consider the connectors selected for the cable assembly, as this drives a myriad of performance aspects inherent to the assembly. As the connector type influences a cable assembly's shielding effectiveness, overall RF performance and mechanical durability, system designers should consider the following when selecting a connector type during the initial design process, then performing thorough testing to ensure the entire interconnect will perform reliably in the intended application.

- Size of the internal components.
- Number of connectors in the entire link.
- Distance between connectors.
- Ease and consistency of termination.
- Noise margin availability.
- Electrical performance of the connector with the selected cable assembly.

Choosing the right microwave cable assembly and connector type that will perform consistently after installation, during use and over time, is well worth the effort and any additional expense, which will pay dividends in system reliability and performance.■

Innovative Waveguide Connector Simplifies mmWave Packages

SAGE Millimeter
Torrance, Calif.

SAGE Millimeter will become Eravant in March 2020.

Microwave and mmWave packaging can turn from mostly routine to highly challenging when waveguide ports are required. Integrated waveguide ports typically require a costly process that is difficult to model and build. An extensive collection of package designs may be needed to accommodate different waveguide bands and numerous port configurations. A common alternative is to employ external coax-to-waveguide transitions. Unfortunately, these can be mechanically cumbersome, and they may have high insertion loss or marginal signal integrity.

The patent pending Uni-Guide™ waveguide connectors from SAGE Millimeter lowers many of these design and manufacturing hurdles. They provide compact, reliable and cost-effective waveguide flanges that are simply added to standard coaxial ports. Easily swapped with coaxial connectors, they

Fig. 1 The Uni-Guide uses the same common RF interface for coaxial connectors, a glass bead hermetically soldered in the housing wall.

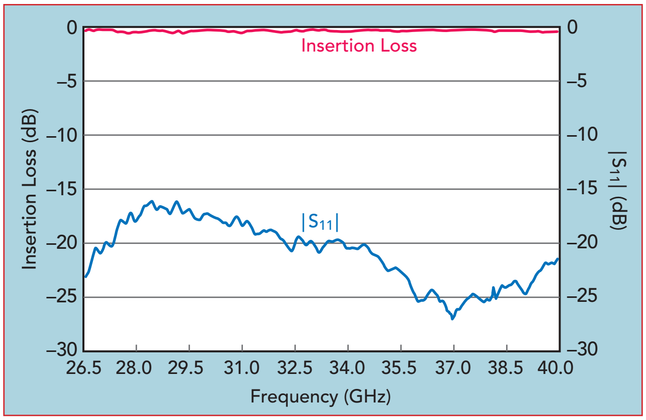

Fig. 2 Typical insertion loss and $|S_{11}|$ of the Ka-Band Uni-Guide connector.

enable greater flexibility for component manufacturers and end-users.

HERMETICAL WAVEGUIDE SOLUTION

A common type of signal port used in hermetic packages uses a glass bead positioned mid-way between a pair of threaded mounting holes (see ***Figure 1***). The threaded holes support a coaxial connector that is easily attached or replaced. This common configuration is used by several connector families, including SMA, 2.92 mm (K), 2.4 mm, 1.85 mm (V), 1.35 mm (E) and 1 mm.

The Uni-Guide waveguide connector joins this group. If the package is designed and manufactured to be hermetically sealed for coaxial connectors, it will retain its hermeticity when using a Uni-Guide waveguide connector. This eliminates the need for an expensive hermetic waveguide process.

A trio of Uni-Guide connectors is available for coaxial ports with a 12 mil center pin and two mounting holes spaced 0.48 in. apart, the same arrangement widely used with the 2.92 mm (K) and 2.4 mm connectors. The model SUF-2812-480-S1 is a WR-28 connector covering 26.5 to 40 GHz with 0.5 dB typical insertion loss. The SUF-2212-480-S1 WR-22 connector covers 33 to 50 GHz and has 0.6 dB insertion loss, and the SUF-2812-480-S1 WR-19 connector, covering 40 to 60 GHz, has 0.7 dB insertion loss. All three have 20 dB typical return loss and handle 100 W RF power. The measured insertion loss and $|S_{11}|$ of the Ka-Band Uni-Guide is shown in ***Figure 2***.

Additional Uni-Guide models designed for glass beads with pin diameters of 9, 15, 20 and 50 mils and various mounting configurations are being developed to cover all standard waveguide bands from 8.2 to 110 GHz.

Fig. 3 Pairs of Uni-Guide connectors can be combined to create band-to-band adapters or 90 degree twists.

PORT TYPE & ORIENTATION CHANGES

While they provide an easy way to implement waveguide ports, Uni-Guide connectors have additional benefits. Rotating them yields a 90 degree change in port orientation to form various integration options, and a polarity inversion is achieved when a connector is rotated 180 degrees. Pairs of Uni-Guide connectors can be cascaded to create common waveguide components, such as band-to-band waveguide adapters or 90 degree twists (see ***Figure 3***). A center pin bridges the signal path between back-to-back connectors, yielding a compact component that rivals the performance of larger and more costly alternatives.

In many situations, Uni-Guide connectors allow component manufacturers to offer various port configurations so that either coaxial or waveguide test equipment can be implemented. This can reduce the number of costly test systems required for a flexible production environment.

TIME AND MONEY

A custom package design requires electromagnetic simulation, mechanical modeling, design, machining and validation, which can easily take 12 to 16 weeks. A second iteration, if required, extends the development time to 20 to 26 weeks. Using the Uni-Guide waveguide connector with a standard coaxial housing can provide any waveguide port needed—instantaneously, without design or prototyping.

To handle a portfolio of waveguide sizes and port interfaces, a manufacturer could have tens to hundreds of package sizes and styles, building costly inventory that becomes large and wasteful. Now, only a few standard housings and Uni-Guide connectors will support many coaxial, waveguide or mixed interface products. The flexibility of the Uni-Guide waveguide connector eliminates many adapters, transitions and waveguide twists.

VENDORVIEW

SAGE Millimeter
Torrance, Calif.
www.sagemillimeter.com

10 MHz to 40 GHz Phase Noise Analyzer

The Holzworth HA7062D Real-Time Phase Noise Analyzer is born from the company's history of industry leading phase noise analyzers with proven accuracy, high-reliability, automation and flexibility. The real-time engine covers the full measurement bandwidth with extremely fast measurement speeds to reduce product development time and optimizes ATE manufacturing throughput.

The HA7062D base model operates from 10 MHz to 26 GHz with a frequency extension available to 40 GHz. The RF input measurement level ranges from –5 to +20 dBm. For phase noise measurements, RF tracking range is typically ±10 ppm, offset frequency ranges from 0.1 Hz to 100 MHz and the phase noise uncertainty is ±4 dB from 1 Hz to 10 Hz, ±3 dB from 10 Hz to 1 kHz and ±2 dB from 1 kHz to 100 MHz.

While many companies provide a measurement confidence factor, which is often misinterpreted as the noise floor of the instrument, Holzworth has architected the instrument's front-end so that the noise floors limits can be measured. The unique architecture of the HA7062D allows for direct access to key internal modules in order to measure the actual noise floor of the analyzer at any given frequency versus minimum frequency offset and number of correlations.

The HA7062D has high-speed digital processors for speed, but the proven accuracy and speed starts with the analog front-end. A key component of the analog front-end is a pair of Holzworth HSX Series RF Synthesizers as the test system's internal LOs. These ultra-low noise RF sources not only complement the dual core FFT engine to provide one of the most advanced phase noise analyzers available, but they are also made available to the user at the front panel's LO Output ports.

The HA7062D has a 1U high, rack mountable chassis form factor. The fully shielded, fan-less chassis eliminates ground loops and troublesome microphonics for uncompromised performance and repeatability. A universal rack mount bracket kit is an available accessory.

VENDORVIEW

Holzworth Instrumentation
Boulder, Colo.
www.holzworth.com
sales@holzworth.com

30 kW Solid-State HPA for P-Band Radar

Daico Industries has developed a solid-state high-power amplifier (HPA) for P-Band radar systems, which is scalable to other bands and applications. The CTX09651 delivers 30 kW peak pulsed power and 40 percent power-added efficiency (typical) from 850 to 942 MHz, transmitting pulse widths to 64 μs up to 5 percent duty cycle. Pulse rise and fall times are less than 800 ns, pulse droop no greater than 0.25 dB and phase variation during a pulse no greater than 6 degrees.

The HPA combines seven, 4.2 kW solid-state HPAs using Daico's patented (m+n)ART™ architecture. With hot swap capability, if the CTX09651's control system detects a failure in one of the seven, it substitutes an eighth HPA to maintain uninterrupted operation. If more than one HPA fails, the multiple amplifier design exhibits graceful degradation. The CTX09651 will not fail with a short or open on the output and, using LDMOS and GaN transistors, achieves 80,000 hours mean time between critical failure.

Spurious signals from the CTX09651 are no greater than –60 dBc from 962 to 1212 MHz, and harmonics are no greater than –30 dBc (second) and –40 dBc (third). The RF input and output connectors are TNC and 7/16 DIN, respectively, with an RS-485 interface for digital control and monitoring. The HPA weighs 175 lb and measures 12.2 in. × 18.4 in. × 12.2 in., achieving a power density of nearly 20 kW/ft^3.

Daico's solid-state designs outperform klystron and other TWT amplifiers, a result of the (m+n)ART design approach, which is flexible, maintainable and scalable for other bands and power levels. Daico's HPAs meet the requirements of mission-critical applications.

Daico Industries Inc.
Carson, Calif.
www.daico.com

High-Power Emitters for Open Air Range Threat Simulation

Open air range testing simulates complex and reactive threats that cannot be simulated with one-dimensional, indoor test amplifiers. To address this, Empower RF Systems has developed its Next Generation family of high performance solid-state amplifiers with embedded high speed computing for precise power control, pulse replication and multi-mode operation. The result is a dynamically configurable transmitting amplifier for generating real-time threat scenarios.

System integrators can take advantage of the hardware and software capability and commonality across the commercial off-the-shelf (COTS) Next Generation product family, with features that simplify system integration and enable faster dynamic threat mode changes. The Next Generation architecture overcomes the historical reliance on single purpose and mission specific amplifiers in system designs. The architecture is a well-conceived combination of hardware engineering—achieving size reductions not seen at these power levels—and a microprocessor/FPGA software architecture, enabling multi-mode, multi-mission support.

A critical requirement in many high-power applications is emitter mobility and reliability. The Next Generation electro-mechanical architecture eliminates virtually all internal connectors, achieving an inherently rugged COTS amplifier with lower losses in the RF chain for improved efficiency and power density.

This Next Generation family offers scalability through an expandable system hardware architecture with electronic phase adjustment: the embedded software adjusts the phase, so any number of like models can be combined in any order without manual phase matching. The scalable architecture makes it straightforward to provide very high power emitters for threat simulation, CW and pulse radars, jamming and broadband communications.

VENDORVIEW

Empower RF Systems Inc.
Inglewood, Calif.
www.empowerrf.com

Customizable 2 kW Broadband Jammer Covers HF to Microwave

Albrecht Telecommunications has developed a digital, broadband jammer for communications jamming and a range of electronic warfare (EW) scenarios. With ultra-fast digital synthesizers, the SAJ-2000MD covers HF to microwave, its output power adjustable to 2 kW. Individual frequencies or frequency bands can be jammed using frequency-agile techniques such as fast frequency hopping and spread spectrum. The customizable jammer can be configured to handle multiple threats, simultaneously transmitting at different frequencies while protecting specific frequencies or bands defined by a blocking list. Frequency lists can be downloaded from a search receiver for spot jamming. Various modulation sources are available so the jammer can be used as a decoy. Spoofing can operate on one or multiple channels simultaneously in near real-time.

The SAJ-2000MD is controlled via computer and a graphical interface, with the synthesizer fully programmable from a PC. For remote control, Albrecht provides wired or an optional wireless control channel, including encrypted VPN. Using encrypted remote control, the jammer can be operated securely in unmanned locations. A comprehensive built-in test system monitors the status of the system, automatically reporting errors with a full description of the issue.

The SAJ-2000MD will operate autonomously as a stand-alone system or can be integrated within a larger EW system. The rack-mounted unit is portable, suitable for the lab or on platforms in the field, including airborne and shipboard. With a modular architecture, the jammer can be customized and upgraded to incorporate changing tactical requirements and new technology.

In addition to communications jamming, the SAJ-2000MD can be used as a programmable transceiver, expanding the applications.

Albrecht Telecommunications GmbH
Hünenberg, Switzerland
www.albrecht-telcom.ch

Software and Mobile Apps

On-Line Filter Synthesis Tool

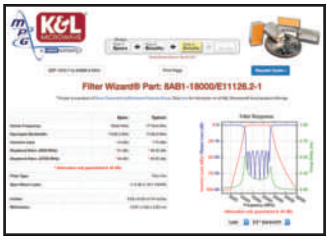

K&L Microwave's Filter Wizard® filter synthesis and selection tool streamlines identification of filter products meeting customer specifications across a large portion of K&L's standard product offerings. Filter Wizard® accelerates user progress from specification to RFQ for RF and microwave filters spanning an ever-increasing range of response types, bandwidths and unloaded Q values. Provide the application with your desired specifications, and the software will return a list of products that match, placing response graphs, outline drawings and downloadable S-parameters at your fingertips. Visit their website to get started today.

K&L Microwave
www.klfilterwizard.com

MCL Microwave Calculator App

VENDORVIEW

The MCL Microwave Calculator, developed by Mini-Circuits, performs 21 calculations commonly needed by RF and microwave system designers in a wide range of applications. Quickly compute the effect of VSWR or return loss on transmitted power; cascaded gain and noise figure for up to five amplifier stages; and power-to-voltage conversion. It is the perfect tool to help you solve problems and save time, whether you are working in the lab or in the field.

Mini-Circuits
www.minicircuits.com/applications/microwave_calculator.html

COMPLETE Library™ v19.5

VENDORVIEW

Modelithics has released Version 19.5 of the COMPLETE Library for use with Keysight Technologies' PathWave Advanced Design System (ADS) software. This update includes 16 new models and compatibility with PathWave ADS 2020. The COMPLETE Library is backward compatible with previous versions of the library as well. This release launches the addition of 16 new models enhancing the library content representing over 700 models for more than 17,000 components. New Microwave Global Models™ for passive components are available for Coilcraft and DLI (Knowles) as well as four new capacitors for Exxelia.

Modelithics Inc.
www.modelithics.com/

sNpViewer to Assist 5G and RF Measurements

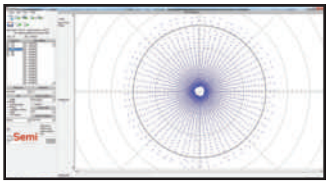

pSemi Corp. (formerly Peregrine Semiconductor), a Murata company, is offering the industry free beta software for viewing S-parameters. The pSemi sNpViewer allows for in-depth S-parameter viewing graphically. This comprehensive viewer includes Smith, polar, magnitude, phase and phase vs. amplitude charting. Time-domain analysis is also available. The pSemi sNpViewer allows you to perform searches through thousands of S-parameter files to determine and record optimal performance. The LUT feature can be especially useful for 5G beamforming or for any other device where a phase and/or amplitude LUT is required.

pSemi Corp.
www.psemi.com/snpviewer

Real-Time Spectrum Analyzer

With the introduction of Signal Hound's SM200B, the company now offers 160 MHz instantaneous bandwidth (IBW) I/Q capture, accessible via an API. The SM200B still has the dynamic range, phase noise, 1 THz/s sweeps and 100 kHz to 20 GHz range that made the SM200A popular, but now features two seconds of segmented I/Q capture memory with triggering options such as frequency mask triggering (FMT) to satisfy the ever-increasing analysis bandwidth demands of the wireless industry. Available now for $12,300.

Signal Hound
https://signalhound.com

VSim 10

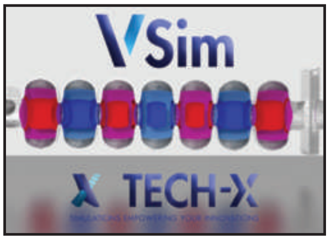

Tech-X Corp. announces the release of VSim 10. Use VSim's radiation generation feature in design and manufacture of high-power (THz) RF devices ranging from spectrometers to oscillators for applications in fields as diverse as biophysics and radio astronomy. VSim for Microwave Devices accurately models particle beams with space charge, simple to complex field absorbers and conformal dielectrics.

Tech-X Corp.
www.txcorp.com

35764

NEW PRODUCTS

FOR MORE NEW PRODUCTS, VISIT WWW.MWJOURNAL.COM/BUYERSGUIDE
FEATURING VENDORVIEW STOREFRONTS

COMPONENTS

Frequency Multipliers

VENDORVIEW

Cernexwave's CFM series active frequency multipliers cover the frequency range of 10 MHz to 500 GHz. They can be designed to multiply an RF signal 2, 3, 4 or as many as 36× with their custom multiplier chain assemblies. These multipliers utilize state-of-the-art MIC and MMIC technologies to provide highly stable, reliable and efficient frequency extenders for system applications.

Cernexwave
www.cernexwave.com

High-Power Coaxial Packaged Limiter

Fairview Microwave Inc. has expanded its line of broadband, high-power coaxial packaged limiters. Typical applications for these RF limiters include military communications, EW, fiber optic communication systems, instrumentation, SATCOM, radar, telecom,

point-to-point wireless and R&D applications. Fairview's line of high-power RF limiters is now made up of 13 unique models that are designed to help protect sensitive components in the receive chain and other microwave circuits in close proximity to high-power signals.

Fairview Microwave Inc.
www.fairviewmicrowave.com

Digital Phase Shifter

Kratos General Microwave manufactures a complete line of broadband fast switching phase shifters. Model 7929 offers a full tuning range of 360° covering a frequency range of 18 to 40 GHz. Excellent phase accuracy and PM/AM performance are achieved by utilizing double balanced bi-phase linear amplitude modulators. Standard unit designed to operate over –54°C to +95°C. Its small size and high-reliability make it ideal for use in demanding shipboard/airborne environmental conditions. Optional optimized performance is available over a narrower frequency range.

Kratos General Microwave Corp.
www.kratosmed.com

Amplified Switched Filter Bank

Lexatys' new three-channel amplified Switched Filter Bank has stopbands extending beyond 40 GHz to help eliminate undesired harmonics. With a compact size of 1.08 × 0.54 × 0.24 in. and paired with high speed switching between channels, the Filter Bank has a low profile with high impact. It features a solderless interconnect to help reusability within prototype assemblies to allow performance to be evaluated before being integrated into the design. This part is also compatible with the X-Microwave prototyping system.

Lexatys
www.lexatys.com

Broadband 6 to 18 GHz, 3-Way Power Divider

MECA's 3-way Wilkinson power divider has been optimized for excellent performance covering; 6 to 18 (P3S-12.000) with specifications such as isolation of 20 dB min/25 dB typical, VSWR 1.4:1 max, 0.7 dB max insertion loss and amplitude balance of 0.4 dB max all in a compact package of 1 × 1.5 × 0.4 in. Made in the U.S. with 36 month warranty.

MECA Electronics Inc.
www.e-MECA.com

Bus Couplers

MilesTek's RoHS compliant MIL-STD-1553B bus couplers can be used in mil/aero and ground vehicle applications. To address the growing demand for RoHS compliant products, MilesTek stocks a wide range of MIL-STD-1553B box style bus couplers with 1-8 stub options and models with single, double or no bus jacks. These bus couplers feature a transformer ratio of 1.41:1 with stub resistor values of 59 Ω, 2 W, 1 percent. These new bus couplers are in-stock and available for same-day shipping.

MilesTek
www.milestek.com

Broadband Resistors

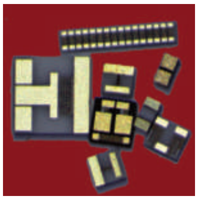

PPI broadband resistors are specifically designed to operate at frequencies up to 67 GHz. With special microwave laser-trimming used to ensure a tight tolerance at high frequencies, these broadband resistors are wire bondable, solderable and can be used in a flip-chip configuration. Applications include optical transceiver modules, broadband receiver, TOSA/ROSA, broadband test equipment, low noise amplifiers and MMIC amplifiers.

Passive Plus Inc.
www.passiveplus.com

Frequency Dividers

VENDORVIEW

Pasternack has launched a new line of frequency divider modules that cover broadband frequencies from 0.1 to 20 GHz. A comprehensive selection of 28 different models is offered with a variety of fixed divide-by-ratios from 2 to 40. These prescalers are ideal for use in phase locked loop (PLL) and frequency synthesizer circuit designs, as well as test instrumentation. Typical applications include use in aerospace and defense, SATCOM, VSAT, test & measurement equipment and point-to-point radio networks.

Pasternack
www.pasternack.com

Absorptive Switch

VENDORVIEW

PMI Model No. P4T-0R1G20G-80-T-SFF is a single pole, four throw, absorptive switch

operating over the frequency range of 0.1 to 20 GHz. It has a max insertion loss of 5 dB and a min isolation of 80 dB. This model is outfitted with SMA female connectors in a housing that measures 1.25 × 1.25 × 0.7 in.

Planar Monolithics Industries Inc.
www.pmi-rf.com

New**Products**

HEMP Tested RF Surge Protection Devices

PolyPhaser has released an innovative line of RF surge protection devices engineered and tested to protect equipment from high-altitude electromagnetic pulse (HEMP) and high-level RF weapons. The PolyPhaser HEMP tested product family includes solutions that protect sensitive equipment from intentional electromagnetic interference (IEMI) as specified by the Department of Homeland Security.

PolyPhaser
www.polyphaser.com

4 Channel Down-Converter

VENDOR**VIEW**

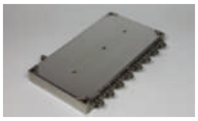

RFE's new cost-effective solution for block translating a 28 to 40 GHz RF signals down into the 6 to 18 GHz range with a single band giving extended frequency coverage to many existing systems. Four phased matched channels present identical channel-to-channel performance for various instrumentation and/or military applications. The down-converter features an internal low phase noise high side fixed LO and the option to accept an external phase reference. Each channel includes an activity threshold detector, all in a ruggedized compact housing.

RFE Inc.
www.rfe-mw.com

SMT Circulators

VENDOR**VIEW**

RFMW announced design and sales support for a robust lead circulator from Skyworks Ireland. The SKYFR-001692 is offered in a 10 mm diameter package measuring 7 mm in height. Designed for wireless infrastructure and power amplifier applications, this circulator operates over the frequency range of 3400 to 3600 MHz. Operating temperature range is –40°C to +105°C, making it ideal for 5G massive MIMO and small cell applications. Accommodates automated SMT placement for ease of use.

RFMW
www.rfmw.com

High-Power 18 GHz SPDT Switch

RLC Electronics announced the addition of a high-power 18 GHz SPDT switch with N connectors to its product capabilities. The switch can handle

1000 W at 100 MHz, 200 W at 4 GHz and 125 W at 18 GHz, and provides high-reliability, long life and excellent electrical performance characteristics over the frequency range (including high isolation). Options on the switch include operating mode (failsafe or latching) and coil voltage (12 or 28 VDC), as well as indicator circuitry and a TTL Driver.

RLC Electronics
www.rlcelectronics.com

Temperature Variable Attenuators

VENDORVIEW

Smiths Interconnect Thermopad® temperature variable attenuators are a totally passive, easy to implement solution for gain compensation designed specifically for demanding high-reliability applications. The Thermopad® can be used in place of a standard chip attenuator to combine level setting or buffering and temperature compensation in a single chip design. This will reduce component count, increase reliability and lower costs. Applications include power amplifiers, mixers, MMIC amplifiers, directional couplers and diode detectors.

Smiths Interconnect
www.smithsinterconnect.com

15 dB 2 to 18 GHz Coupler

Werbel Microwave model C-1182-dB is available as 10, 15, 20 and 30 dB models covering the full 2 to 18 GHz band with typical 0.5 dB frequency sensitivity. Typical directionality is 17 dB and typical VSWR is 1.2:1. Designed conservatively to handle 20 W input power.

Werbel Microwave
www.werbelmicrowave.com

CABLES & CONNECTORS

Johnson™ 2.92 mm Connector Series

Cinch Connectivity Solutions announced an extension to its Johnson 2.92 mm series coax connectors, with the addition of solder end launch/straddle mount jacks. The new connectors provide additional board option thicknesses of 0.016, 0.042, 0.062 and 0.093 in. The Johnson 2.92 mm end launch/straddle mount series offers a low VSWR of 1.25 up to 26.5 GHz and 1.5 max from 26.5 to 40 GHz, also utilizing air dielectric and support bead for higher cutoff frequency that enable for advanced frequency performance and signal integrity.

Cinch Connectivity Solutions
www.belfuse.com/cinch

Coaxial Adapter Mates 1.85 mm-F to 2.92 mm-F Connectors

VENDORVIEW

Mini-Circuits' 185F-KF+ is a coaxial 1.85 mm-F to 2.92 mm-F adapter, supporting a wide range of applications from DC to 40 GHz. This model provides 1.05:1 VSWR and 0.13 dB insertion loss with flat response over its full frequency range. The unit features rugged, passivated stainless steel construction and measures 0.82 in. in length.

Mini-Circuits
www.minicircuits.com

Coaxial Adapter

Model SCT-DF1F-UB is a SMPM (GPPO) female to 1 mm female coaxial adapter that covers the frequency range of DC to 65 GHz. This coaxial adapter offers efficient transitioning between the coaxial connectors with a high return loss and typical insertion loss of 1 dB. The impedance of the adapter is 50 Ω. Other configurations are available under different model numbers.

SAGE Millimeter
www.sagemillimeter.com

SEMICONDUCTORS

E-Series SiC MOSFETs

Richardson RFPD Inc. announced the availability and full design support capabilities for a robust family of SiC semiconductor devices from Wolfspeed, a Cree Company. The E-Series line of SiC MOSFETs represents the industry's first automotive-qualified, PPAP-capable and humidity-resistant MOSFETs. The E-Series MOSFETs are optimized for use in EV battery chargers and high voltage DC/DC converters for on-board automotive power conversion systems, off-board charging, solar inverters and other outdoor applications.

Richardson RFPD Inc.
www.richardsonrfpd.com

AMPLIFIERS

Tactical Booster Amplifiers

Maintaining clear, dependable communications is essential to the successful completion of missions—and often saves lives. Forces around the globe rely on lightweight AR Modular RF tactical booster amplifiers for long-range communications and connectivity in even the most extreme conditions. With available man-pack, vehicle-mounted and airborne models, AR Modular RF's line of

New**Products**

battle tested tactical booster amplifiers supports uninterrupted communication on the ground, at sea and in the air.
AR Modular RF
www.arww-modularrf.com

Solid-State Power Amplifier Module

COMTECH PST introduced its latest addition to its GaN solid-state power amplifier product line. Comtech's latest development continues to expand on its integrated RF GaN power amplifier designs by offering a small form factor (SFF) module. Consistent with its planned technology development roadmap, Comtech proudly introduces the latest in GaN-based 6 to 18 GHz RF amplifier for TWT/MPM Replacement. This highly integrated design is ideal for use in communication, EW and radar transmitter systems, where space, cooling and power are limited.
Comtech PST
www.comtechpst.com

Pulse Amplifier

VENDORVIEW

Exodus Advanced Communications' Pulse Amp (2 to 4 GHz; 2, 4 and 8 KW Pulse) series is designed for Lab Pulse/HIRF Mil-Std 461/464 test applications. Other frequency ranges and power levels available. The unit can produce different power levels based on configuration implementation. The design provides excellent band flatness, reliable robust performance with outstanding pulse fidelity. Rack integrated for ease of application integration.
Exodus Advanced Communications
www.exoduscomm.com

Front-End Modules

VENDORVIEW

Skyworks introduced the SKY65725-11 and the SKY65728-11, shielded GPS low-noise amplifier front-end modules (FEM) for mobile applications such as smartphones and tablets. Both devices feature high linearity, excellent gain and superior noise figure to enable design flexibility and high levels of integration. Pre-filters provide the low in-band insertion loss and excellent rejections of the cellular, PCS and WLAN frequency bands. The SKY65725-11 is ideal for GPS/GNSS/BDS receivers while the SKY65728-11 works well for GPS L5 applications.
Skyworks Solutions Inc.
www.skyworksinc.com

Low Noise Amplifier

Model ALN3325-41-3525 is a low-cost, 2.92 mm connectorized low noise amplifier (LNA) module offering 35 dB linear gain and 2.5 dB noise figure over the entire Ka-Band frequency range from 26.5 to 40 GHz with excellent gain flatness and input/output return loss. The unit has built in voltage regulator and reverse polarity protection circuitry. It operates with a single DC power supply voltage from +10 to +15 V. The package size of the amplifier is 1.5 × 0.85 × 0.375 in.
Wenteq Microwave
www.wenteq.com

SOURCES

High Performance Oscillators

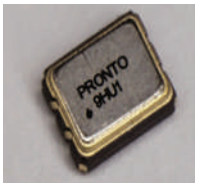

Pletronics presents the new PRONTO® oscillator series offering a 2 × 1.6 mm package. The PRONTO® series state-of-the-art design is able to provide any frequency with lead times in days not weeks. The small form and footprint of the 2 × 1.6 mm with endless frequency options up to 200 MHz and superior jitter performance makes this an ideal device to service all application phases from board design to production volumes. The PRONTO® series

UNITED STATES POSTAL SERVICE — Statement of Ownership, Management, and Circulation (All Periodicals Publications Except Requester Publications)

1. Publication Title: Microwave Journal	2. Publication Number: 3 9 6 - 2 5 0	3. Filing Date: September 30, 2019
4. Issue Frequency: Monthly	5. Number of Issues Published Annually: 12	6. Annual Subscription Price: Domestic: $120.00 Foreign: $200.00
7. Complete Mailing Address of Known Office of Publication (Not printer) (Street, city, county, state, and ZIP+4®): HORIZON HOUSE PUBLICATIONS, INC. 685 Canton Street Norwood, MA 02062-2610		Contact Person: Barbara Walsh Telephone: 781-769-9750 x2025

8. Complete Mailing Address of Headquarters or General Business Office of Publisher (Not printer)

same as above

9. Full Names and Complete Mailing Addresses of Publisher, Editor, and Managing Editor (Do not leave blank)

Publisher (Name and complete mailing address)

Carl S. Sheffres, Horizon House Publications, Inc., 685 Canton Street, Norwood, MA 02062-2610

Editor (Name and complete mailing address)

Patrick Hindle, Horizon House Publications, Inc., 685 Canton Street, Norwood, MA 02062-2610

Managing Editor (Name and complete mailing address)

Jennifer DiMarco, Horizon House Publications, Inc., 685 Canton Street, Norwood, MA 02062-2610

10. Owner (Do not leave blank. If the publication is owned by a corporation, give the name and address of the corporation immediately followed by the names and addresses of all stockholders owning or holding 1 percent or more of the total amount of stock. If not owned by a corporation, give the names and addresses of the individual owners. If owned by a partnership or other unincorporated firm, give its name and address as well as those of each individual owner. If the publication is published by a nonprofit organization, give its name and address.)

Full Name	Complete Mailing Address
Horizon House Publications, Inc.	685 Canton Street, Norwood, MA 02062-2610
William M. Bazzy, CEO	" " " " " " "
Ivar A. Bazzy, President	" " " " " " "
Jared M. Bazzy, Vice President	" " " " " " "
Joan B. Egan, EVP	" " " " " " "

11. Known Bondholders, Mortgagees, and Other Security Holders Owning or Holding 1 Percent or More of Total Amount of Bonds, Mortgages, or Other Securities. If none, check box ✓ None

Full Name	Complete Mailing Address

12. Tax Status (For completion by nonprofit organizations authorized to mail at special rates) (Check one)
The purpose, function, and nonprofit status of this organization and the exempt status for federal income tax purposes:
☑ Has Not Changed During Preceding 12 Months
☐ Has Changed During Preceding 12 Months (Publisher must submit explanation of change with this statement)

13. Publication Title: Microwave Journal	14. Issue Date for Circulation Data Below: YTD September 30, 2019	
15. Extent and Nature of Circulation: 50K	Average No. Copies Each Issue During Preceding 12 Months	No. Copies of Single Issue Published Nearest to Filing Date
a. Total Number of Copies (Net press run)	35,826	31,951
b. Paid Circulation (By Mail and Outside the Mail) (1) Mailed Outside-County Paid Subscriptions Stated on PS Form 3541. (Include paid distribution above nominal rate, advertiser's proof copies, and ex change copies)	26,843	22,156
(2) Mailed In-County Paid Subscriptions Stated on PS Form 3541 (include paid distribution above nominal rate, advertiser's proof copies and exchange copies)	0	0
(3) Paid Distribution Outside the Mails Including Sales Through Dealers and Carriers, Street Vendors, Counter Sales, and Other Paid Distribution Outside USPS®	5,748	6,767
(4) Paid Distribution by Other Classes of Mail Through the USPS (e.g. First-Class Mail®)	0	0
c. Total Paid Distribution (Sum of 15b(1), (2), (3), and (4))	32,591	28,923
d. Free or Nominal Rate Distribution (By Mail and Outside the Mail) (1) Free or Nominal Rate Outside-Country Copies included on PS Form 3541	635	620
(2) Free or Nominal Rate In-Country Copies Included on PS Form 3541	0	0
(3) Paid Distribution Outside the Mails Including Sales Through Dealers and Carriers, Street Vendors, Counter Sales, and Other Paid Distribution Outside USPS®	0	0
(4) Free or Nominal Rate Distribution Outside the Mail (Carriers or other means)	2,536	2,324
e. Total Free or Nominal Rate Distribution (Sum of 15d (1), (2), (3) and (4))	3,171	2,944
f. Total Distribution (Sum of 15c and 15 e)	35,762	31,867
g. Copies not Distributed (See Instructions to Publishers #4 (page #3))	65	84
h. Total (Sum of 15f and g)	35,826	31,951
i. Percent Paid (15c divided by 15f times 100)	91.13%	90.76%

16. Publication of Statement of Ownership
✓ If the publication is a general publication, publication of this statement is required. Will be printed in the November, 2019 issue of this publication. ☐ Publication not required.

17. Signature and Title of Editor, Publisher, Business Manager, or Owner: Carl S. Sheffres, Publisher — Date: September 30, 2019

I certify that all information furnished on this form is true and complete. I understand that anyone who furnishes false or misleading information on this form or who omits material or information requested on the form may be subject to criminal sanctions (including fines and imprisonment) and/or civil sanctions (including civil penalties).

PS Form 3526, September 2007 (Page 2 of 3)

demonstrates outstanding performance in applications, such as 5G, IoT and digital communications.

Pletronics Inc.
www.pletronics.com

Low Noise VCO

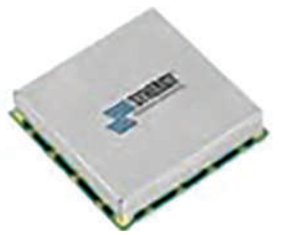

The DCRO240270-5 is an optimized bandwidth VCO covering a frequency range of 2400 to 2700 MHz in 12 V of tuning voltage. This device operates with +5 V bias voltage and a current draw of only 23 mA max. Other specifications include min output power of +3 dBm, typical tuning sensitivity of 28 to 38 MHz/V and typical harmonic suppression of 23 dB. The typical phase noise performance is –103 and –123 dBc/Hz at 10 and 100 kHz offsets.

Synergy Microwave Corp.
www.synergymwave.com

SOFTWARE

Microwave Global Model™

VENDORVIEW

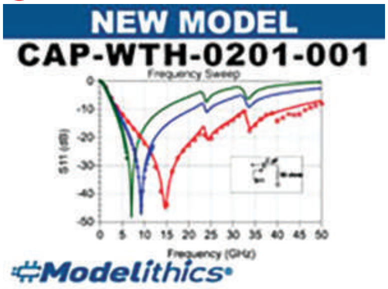

Modelithics has introduced a new equivalent circuit-based scalable Microwave Global Model for Würth Elektronik WCAP-CSRF 0201 surface mount chip capacitor family. The model is validated up to 50 GHz and features substrate, pad and part value scaling over the full range of the surface mount chip capacitor series, 0.2 to 33 pF. Würth Elektronik is a Sponsoring MVP and is sponsoring free 90-day trials of all available Modelithics models for Würth Elektronik parts by request and with approval.

Modelithics
www.Modelithics.com

TEST & MEASUREMENT

Analyzer Calibration Extender

Kaelus has released new functionality for the Analyzer Calibration Extender (ACE). It now supports the Range-to-Fault (RTF) module used for locating PIM and return loss faults in RF infrastructure. ACE allows customers to self-calibrate their Kaelus PIM instruments in the field. Reducing down-time of calibration to less than one hour, ACE extends the calibration due date by 12 months.

Kaelus
www.kaelus.com

MICRO-ADS

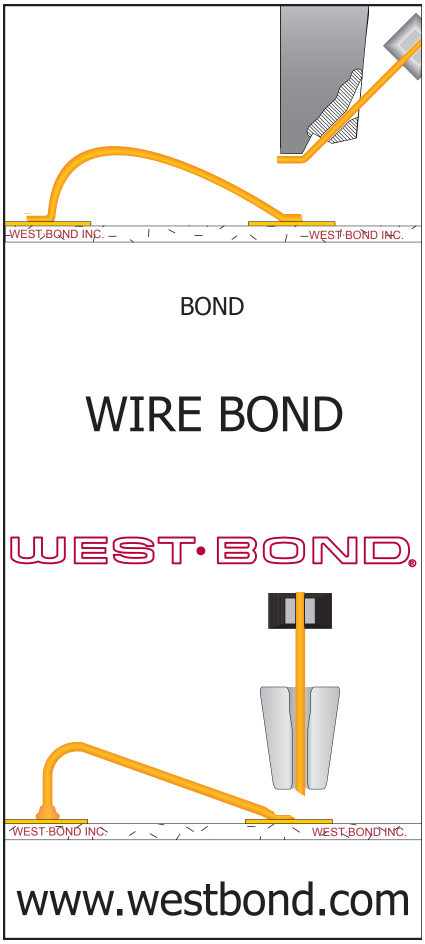

WEST BOND INC.
BOND
WIRE BOND
WEST·BOND
www.westbond.com

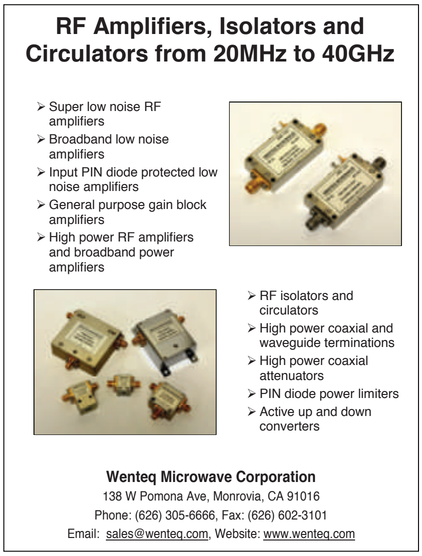

RF Amplifiers, Isolators and Circulators from 20MHz to 40GHz
Super low noise RF amplifiers
Broadband low noise amplifiers
Input PIN diode protected low noise amplifiers
General purpose gain block amplifiers
High power RF amplifiers and broadband power amplifiers
RF isolators and circulators
High power coaxial and waveguide terminations
High power coaxial attenuators
PIN diode power limiters
Active up and down converters
Wenteq Microwave Corporation
138 W Pomona Ave, Monrovia, CA 91016
Phone: (626) 305-6666, Fax: (626) 602-3101
Email: sales@wenteq.com, Website: www.wenteq.com

REVOLUTIONARY HERMETIC SMP CONNECTORS
These SMPs meet the requirements of MIL-STD-348, but utilize unique housing interface features, which significantly improves reliability and production assembly yields. Proprietary techniques are used to independently control plating thickness on pin and housing.
For use with Aluminum, Kovar and other package materials
SHP
SPECIAL HERMETIC PRODUCTS, INC.
PO BOX 269 – WILTON – NH – 03086
(603) 654-2002 – Fax (603) 654-2533
E-mail: sales@shp-seals.com
Web: www.shp-seals.com

Find Reps, Engineers and Used Equipment.
Post your listing on the MWJ classified section.
Microwave Journal
Classified
Help Wanted
Executives
www.mwjournal.com/classifieds

Waveguide and Coaxial Switches
We offer Switches for any application; HI-REL, MILITARY, COMMERCIAL
From design to delivery, all under one roof.
Offering the Finest in Microwave Switches Since 1974.
The only bright spot to go!!
Sector Microwave Ind., Inc.
(631) 242-2300 Phone (631) 242-8158 Fax
www.SectorMicrowave.com

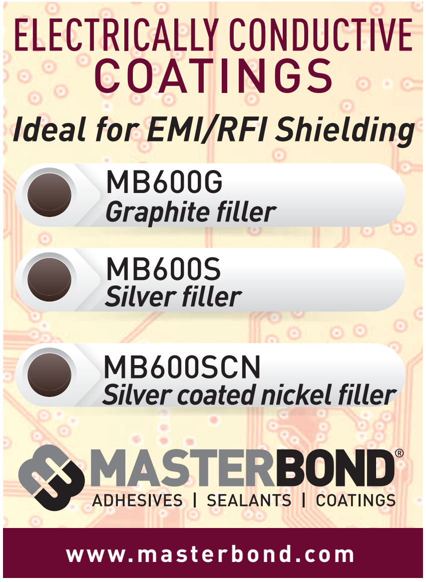

ELECTRICALLY CONDUCTIVE COATINGS
Ideal for EMI/RFI Shielding
MB600G Graphite filler
MB600S Silver filler
MB600SCN Silver coated nickel filler
MASTERBOND
ADHESIVES | SEALANTS | COATINGS
www.masterbond.com

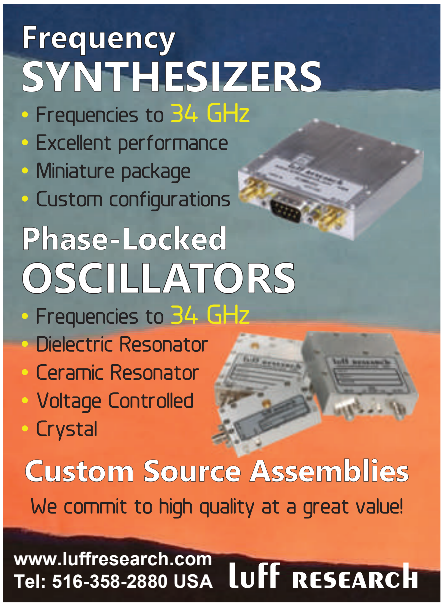

Frequency SYNTHESIZERS
Frequencies to 34 GHz
Excellent performance
Miniature package
Custom configurations
Phase-Locked OSCILLATORS
Frequencies to 34 GHz
Dielectric Resonator
Ceramic Resonator
Voltage Controlled
Crystal
Custom Source Assemblies
We commit to high quality at a great value!
www.luffresearch.com
Tel: 516-358-2880 USA
luff RESEARCH

ES MICROWAVE LLC.
Since 1985 we have offered our custom design filters and sub-assemblies in combline, interdigital and suspended-substrate technologies.
Broadband
Suspended-Substrate
Filters, Diplexers, Triplexers, Quadruplexers, Quintuplexers, Sextuplexers...
DC-40 GHz Filters
Multiplexers &
Switch Filter Banks
ES Microwave, LLC
8031 Cessna Avenue, Gaithersburg, MD 20879
P: 301-519-9407 F: 301-519-9418
www.esmicrowave.com

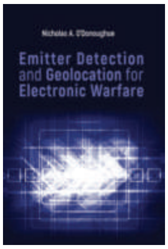

Emitter Detection and Geolocation for Electronic Warfare

Nicholas O'Donoughue

This comprehensive resource provides theoretical formulation for detecting and geolocating non-cooperative emitters. Implementation of geolocation algorithms are discussed, as well as performance prediction of a hypothetical passive location system for systems analysis or vulnerability calculation. Comparison of novel direction finding and geolocation algorithms to classical forms are also included. Rooted in statistical signal processing and array processing theory, this book also provides an overview of the application of novel detection and estimation algorithms to real-world problems in electronic warfare (EW).

The book is divided into three parts: detection, angle of arrival estimation and geolocation. Each section begins with an introductory chapter covering the relevant signal processing theory (either detection or estimation), then provides a series of chapters covering specific methods to achieve the desired end-product. MATLAB® code is provided to assist readers with relevant probability and statistics, RF propagation, atmospheric absorption and noise, giving readers an understanding of the implementation of the algorithms in the book, as well as developing new approaches to solving problems. Packed with problem sets and examples, this book strikes a balance between introductory texts and reference manuals, making it useful for novice as well as advanced practitioners.

To order this book, contact:

Artech House
www.artechhouse.com
Email: artech@artechhouse.com
US 800-225-9977
UK +44 (0)20 70596 8750

ISBN: 978-1-63081-564-6
348 pages

$139/£119

Use code ODO25 to receive 25% discount on this title! (expires 12/31/2019)

AdvertisingIndex

Sales Representatives

Microwave Journal

Eastern and Central Time Zones
Michael Hallman
Associate Publisher
(NJ, Mid-Atlantic, Southeast, Midwest, TX)
4 Valley View Court
Middletown, MD 21769
Tel: (301) 371-8830
FAX: (301) 371-8832
mhallman@mwjournal.com

Jaime Leger
Northeast Reg. Sales Mgr.
(New England, New York, Eastern Canada)
685 Canton Street
Norwood, MA 02062
Tel: (781) 619-1942
FAX: (781) 769-5037
jleger@mwjournal.com

Pacific and Mountain Time Zones
Brian Landy
Western Reg. Sales Mgr.
(CA, AZ, OR, WA, ID, NV, UT, NM, CO, WY, MT, ND, SD, NE & Western Canada)
144 Segre Place
Santa Cruz, CA 95060
Tel: (831) 426-4143
FAX: (831) 515-5444
blandy@mwjournal.com

International Sales
Richard Vaughan
International Sales Manager
16 Sussex Street
London SW1V 4RW, England
Tel: +44 207 596 8742
FAX: +44 207 596 8749
rvaughan@horizonhouse.co.uk

Germany, Austria, and Switzerland (German-speaking)
WMS.Werbe- und Media Service
Brigitte Beranek
Gerhart-Hauptmann-Street 33,
D-72574 Bad Urach
Germany
Tel: +49 7125 407 31 18
FAX: +49 7125 407 31 08
bberanek@horizonhouse.com

France
Gaston Traboulsi
Tel: 44 207 596 8742
gtraboulsi@horizonhouse.com

Korea
Young-Seoh Chinn
JES MEDIA, INC.
F801, MisahausD EL Tower
35 Jojeongdae-Ro
Hanam City, Gyeonggi-Do
12918 Korea
Tel: +82 2 481-3411
FAX: +82 2 481-3414
yschinn@horizonhouse.com

China
Shenzhen
Michael Tsui
ACT International
Tel: 86-755-25988571
FAX: 86-755-25988567
michaelt@actintl.com.hk

Shanghai
Linda Li
ACT International
Tel: 86-021-62511200
lindal@actintl.com.hk

Beijing
Cecily Bian
ACT International
Tel: +86 135 5262 1310
cecilyb@actintl.com.hk

Hong Kong, Taiwan, Singapore
Mark Mak
ACT International
Tel: 852-28386298
markm@actintl.com.hk

Japan
Katsuhiro Ishii
Ace Media Service Inc.
12-6, 4-Chome,
Nishiiko, Adachi-Ku
Tokyo 121-0824, Japan
Tel: +81 3 5691 3335
FAX: +81 3 5691 3336
amskatsu@dream.com

Ed Kiessling • Traffic Manager • 685 Canton Street, Norwood, MA 02062 • Tel: (781) 619-1963 FAX: (781) 769-6178 • ekiessling@mwjournal.com

MMIC FIXED EQUALIZERS

DC to 20 GHz

- Absorptive
- 2x2mm QFN and Bare Die

DC to 6 GHz

Model	Slope, (dB)
EQY-0-63+	0
EQY-1-63+	1.2
EQY-2-63+	2.1
EQY-3-63+	3.2
EQY-4-63+	4.2
EQY-5-63+	5.0
EQY-6-63+	6.5
EQY-8-63+	8.2
EQY-10-63+	10.2

DC to 20 GHz

Model	Slope, (dB)
EQY-0-24+	0
EQY-2-24+	2.1
EQY-3-24+	3.1
EQY-5-24+	5.1
EQY-6-24+	6.3
EQY-8-24+	8.3
EQY-10-24+	10.2
EQY-12-24+	12

CELEBRATING 50 YEARS Mini-Circuits®

www.minicircuits.com P.O. Box 350166, Brooklyn, NY 11235-0003 (718) 934-4500 sales@minicircuits.com 610 RevOrig__P

Keysight's Atlanta Software Design Center: Improving Workflows with Software Platform

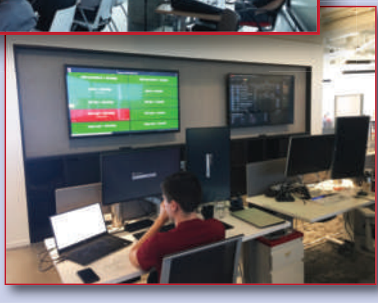

With the increasing complexity of the industry's test & measurement (T&M) needs, Keysight recognized that single function T&M products cannot fully assess system-level performance. The industry needs "smarter" T&M solutions that integrate multiple instruments with software, with the ability to measure system parameters and simulate system performance, whether it is a radar barraged by noise jamming or a mmWave 5G smartphone in an urban canyon connecting to a massive MIMO base station. To address this challenge, Keysight moved to strengthen its software competency. In 2016, it announced plans to form a stand-alone software design center in Atlanta, a start-up with a software-centric, agile culture.

For a company headquartered in Santa Rosa, whose roots are in Palo Alto, starting a new venture across the country in Atlanta, far from the corporate center, may seem risky. Yet the choice was intentional. Steve Chen, who moved from Santa Rosa to lead the initiative, says isolation and independence were important in choosing the location. "We needed to circumvent the corporate immune system," he quips, explaining that many large companies try to kill new ventures falling outside the mainstream business and culture. Another constraint on the location was proximity to an excellent university, as Keysight planned to recruit two-thirds of the new staff from college, the other third with industry experience. Georgia Tech has an excellent reputation, strong ties to Keysight and a corporate innovation center to assist new ventures. More broadly, Atlanta has a tech community of software engineers supporting a growing number of companies working in cloud management and "big data" applications.

Chen and a handful of Keysight employees recruited some 50 to the center during the first year, and the team now exceeds 70. To support planned growth, the design center moved mid-summer to the 19th floor of a 21-story office tower across the street from Georgia Tech, offering expansive views of the city and enough space to house over 200.

The mission of Keysight's software design center is to develop a common software platform—Chen compares it to a modular chassis—which Keysight's businesses use to develop more comprehensive T&M solutions and get to market faster. Branded PathWave, the software is the foundation of Keysight's ambitious strategy to integrate design, test, measurement and analysis across the life cycle of a customer's products, from development through manufacturing. PathWave combines design simulation and layout, instrument control and test routines into a comprehensive workflow with an integrated data base. An open development environment, PathWave works with third-party software and hardware, enabling users to set up test routines for their unique environments. The platform includes tools for analyzing equipment status and usage, so companies can monitor the health and availability of their test systems, improving efficiency and the return on investment in T&M.

As a part of PathWave, the Atlanta team is developing a cloud-based edition to increase scalability, availability and parallel processing of large data sets. They are also helping Keysight move into nascent markets such as electric vehicles, working on battery management, vehicle connectivity and security.

In just three years, the Atlanta Software Design Center has created a high-performance team with an unique software culture, recognized as one of the top places to work in Atlanta by *The Atlanta Journal-Constitution*. Helping customers improve their workflows is the maximum value Keysight can provide, and the Atlanta team is integral to Keysight's strategy to do that—building a "PathWave" to Keysight's goal of becoming a solutions company.

https://jobs.keysight.com/atl/#section-keysight-software-design-center

WERLATONE®

500 - 8000 MHz COUPLERS, COMBINERS, & HYBRIDS

In-Phase & Hybrid Designs ✦ ***Mismatch Tolerant***® Designs ✦ Lowest Loss & Smallest Size

Directional Couplers

Model	Type	Frequency (MHz)	Power (W CW)	Coupling (dB)	Insertion Loss (dB)	Mounting Style	Size (inches)
C8000	Bi	600-6000	100	30	0.40	SMA-Female	1.8 x 1.0 x 0.56
C10799	Dual	700-6000	100	40	0.20	N-Female	2.0 x 2.0 x 1.06
C10117	Dual	700-6000	250	40	0.20	N-Female	2.0 x 2.0 x 1.06
C10526	Dual	700-6000	300	40	0.20	N Female	2.0 x 2.0 x 1.06
C10364	Dual	700-6000	500	50	0.20	7/16-Female	2.15 x 2.0 x 1.36
C10614	Dual	700-6000	500	60	0.20	7/16-Female	2.15 x 2.0 x 1.36
C10996	Dual	700-6000	700	50	0.20	7/16-Female	2.15 x 2.0 x 1.36
C11555	Dual	700-6000	1,000	50	0.20	7/16-Female	2.15 x 2.0 x 1.36
C10695	Dual	700-6500	500	50	0.20	7/16-Female	2.15 x 2.0 x 1.36

0° (In-Phase) Combiners/Dividers

Model	Type	Frequency (MHz)	Power (W CW)	Isolation (dB)	Insertion Loss (dB)	Mounting Style	Size (inches)
D11911	2-Way	600-6000	100	15	0.60	N-F / SMA-F	2.00 x 2.0 x 1.00
D11959	2-Way	600-6000	100	Non-Isolated	0.40	N-F / SMA-F	2.00 x 2.0 x 1.00
D11958	4-Way	600-6000	100	18 (PI*)	0.60	N-F / SMA-F	4.00 x 2.0 x 1.00
D11149	4-Way	700-6000	300	Non-Isolated	0.60	N-Female	4.35 x 3.9 x 1.15
D11832	2-Way	700-6000	500	Non-Isolated	0.60	7/16-Female	5.50 x 2.4 x 1.06
D10803	2-Way	700-6500	300	Non-Isolated	0.60	N-Female	5.50 x 2.4 x 1.06

(PI*) references Partial Isolation

90° Hybrid Couplers

Model	Type	Frequency (MHz)	Power (W CW)	Amp. Bal. (±dB)	Insertion Loss (dB)	Mounting Style	Size (inches)
QH11687	90°	500-6000	150	0.7	0.75	SMT	1.28 x 1.08 x 0.13
QH11443	90°	600-6000	150	0.8	0.70	SMT	1.30 x 1.30 x 0.13
QH10756	90°	700-6000	100	0.6	0.55	SMT	0.74 x 0.45 x 0.09
QH10541	90°	700-6000	150	0.6	0.50	SMT	0.86 x 0.66 x 0.09
QH10827	90°	1000-7500	100	0.7	0.65	SMT	0.86 x 0.61 x 0.09
QH10828	90°	1000-8000	100	0.7	0.90	SMT	0.65 x 0.50 x 0.07

Werlatone, Inc. 17 Jon Barrett Road Patterson, NY 12563 T 845-278-2220 sales@werlatone.com www.werlatone.com